KfK 4163
November 1986

GANTRAS
A System of Codes for the Solution of the Multigroup Transport Equation with a Rigorous Treatment of Anisotropic Neutron Scattering

Plane and Spherical Geometry

A. Schwenk-Ferrero
Institut für Neutronenphysik und Reaktortechnik
Projekt Kernfusion

Kernforschungszentrum Karlsruhe

KERNFORSCHUNGSZENTRUM KARLSRUHE

Institut für Neutronenphysik und Reaktortechnik
Projekt Kernfusion

KfK 4163

GANTRAS
A System of Codes for the Solution of the Multigroup Transport Equation with a Rigorous Treatment of Anisotropic Neutron Scattering.
Plane and Spherical Geometry

Aleksandra Schwenk-Ferrero

Kernforschungszentrum Karlsruhe GmbH, Karlsruhe

Kernforschungszentrum Karlsruhe GmbH
Postfach 3640, 7500 Karlsruhe 1

ISSN 0303-4003

Abstract

GANTRAS is a system of codes for neutron transport calculations in which the anisotropy of elastic and inelastic (including (n,n'x)-reactions) scattering is fully taken into account. This is achieved by employing a rigorous method, so-called I*-method, to represent the scattering term of the transport equation and with the use of double-differential cross-sections for the description of the emission of secondary neutrons. The I*-method was incorporated into the conventional transport code ONETRAN. The ONETRAN subroutines were modified for the new purpose. An implementation of the updated version ANTRA1 was accomplished for plane and spherical geometry. ANTRA1 was included in GANTRAS and linked to another modules which prepare angle-dependent transfer matrices.

The GANTRAS code consists of three modules:

1. The CROMIX code which calculates the macroscopic transfer matrices for mixtures on the base of microscopic nuclide-dependent data.

2. The ATP code which generates discretized angular transfer probabilities (i.e. discretizes the I*-function).

3. The ANTRA1 code to perform S_N transport calculations in one-dimensional plane and spherical geometries.

This structure of GANTRAS allows to accommodate the system to various transport problems.

GANTRAS - Ein Programmsystem zur Lösung der Multigruppen-Neutronentransportgleichung mit direkter Behandlung der Anisotropie der Neutronenstreuung. Ebene und sphärische Geometrie

---

Zusammenfassung

GANTRAS ist ein Programmsystem, mit dem Neutronentransportrechnungen unter vollständiger Berücksichtigung der Anisotropie der elastischen und inelastischen Neutronenstreuung (einschließlich (n,n'x)-Reaktionen) durchgeführt werden können. Dies wird durch Verwendung eines direkten Verfahrens zur Darstellung der Streuterme in der Transportgleichung, des sogenannten I*-Verfahrens, unter Benutzung doppelt-differentieller Wirkungsquerschnitte erreicht. Das I*-Verfahren wurde in das konventionelle Neutronen-Transportprogramm ONETRAN eingebaut. Die ONETRAN-zugehörigen Unterprogramme wurden zu diesem Zweck entsprechend verändert. Die neue Version ANTRA1 wurde für eindimensionale Rechnungen in ebener und sphärischer Geometrie fertiggestellt. ANTRA1 wurde im Rahmen des Programmsystems GANTRAS eingesetzt und mit anderen Moduln, die die Verarbeitung von winkelabhängigen Streumatrizen durchführen, gekoppelt.

Das ganze Programmsystem besteht aus drei Moduln:

1. Das Programm CROMIX zur Berechnung makroskopischer Streumatrizen für Materialmischungen unter Benutzung der mikroskopischen materialabhängigen Daten.

2. Das Programm ATP zur Erzeugung der diskretisierten Winkel-Übergangswahrscheinlichkeiten (d. h. zur Diskretisierung der I*-Funktion).

3. Das Transportprogramm ANTRA1 zur Durchführung von eindimensionalen S_N-Rechnungen.

Durch diesen modularen Aufbau kann GANTRAS leicht an unterschiedliche Problemstellungen angepaßt werden.

Table of Contents

Table of Contents (continued)

List of Figures

List of Tables

List of Examples

Code Abstract

1. Programme Identification: GANTRAS - General Anisotropic Transport System

2. Computers: The code was developed on Siemens 7890, it can be implemented on IBM/3081 or IBM/3090.

3. Function: GANTRAS (in a present version) solves numerically the one-dimensional multigroup transport equation in plane and spherical geometries with a rigorous treatment of the anisotropy of neutron scattering for elastic, inelastic and (n,n'x)-reactions.

   An expansion of the scattering kernel into Legendre polynomial series (i.e. P_1-method) usually used in standard neutron transport codes is avoided here. Instead the I*-method, introduced by Takahashi et al. /2/, to perform an integration over direction variable in the scattering term, is applied.

   An I*-P_1 hybrid method, i.e. a rigorous representation or P_1-expansion approximation of the group scattering term is also allowed in subsequent coarse-mesh intervals, provided in each zone, assigned to a coarse-mesh, the corresponding scattering matrices (P_1 or angular representation) are supplied.

   Regular, inhomogeneous and homogeneous (k_{eff} and eigenvalue searches) problems subject to vacuum, reflective, periodic, white, albedo or inhomogeneous boundary flux conditions are solved.

4. Method of Solution: The I*-method is used for a formulation of the group scattering source and it is incorporated into ONETRAN /13/ code.

   ONETRAN was extended and modified for a new purpose, a new version, called ANTRA1 - Anisotropic Transport in 1-Dimension is included in GANTRAS as a transport module.

   ANTRA1 retains all major ONETRAN features.
   The discrete ordinates approximation for the angular variable is used with the diamond (central) difference approximation for the angular

extrapolation in curve-linear geometries. A linear discontinuous finite element representation for the angular flux in each spatial mesh cell is applied. Negative fluxes can be eliminated by a local set-to-zero and correcting algorithm. Standard dual iteration strategy is employed. Inner (within group) iteration cycles are accelerated by system rebalance, coarse-mesh rebalance, or Chebyshev acceleration. Outer iterations are accelerated by coarse mesh rebalance.

The I*-method is based on the use of double differential cross-sections (DDX) for describing the emission of neutrons in a nuclear reaction, therefore in the transport calculation angular-dependent transfer matrices had to be introduced.

The mixing operations for these transfer matrices are performed prior to the transport calculations with the aid of the CROMIX code. The discretization and tabulation of the I*-function is done by the ATP code.

Both the CROMIX and the ATP are included in the system.

5. Restrictions: GANTRAS is established as a KAPROS /14/ module. Data transmission and allocation of the necessary computer storage is managed by KAPROS routines. Variable dimensioning is used so that any combination of problem parameters leading to a container array of length less than MAXCOR can be accommodated. MAXCOR on IBM computers with their large storage capacity reaches up to 7000 K.

6. Running Time: The computational time required is problem dependent and therefore, in general, cannot be easily assessed.

   An inhomogeneous problem in spherical geometry (with 14 MeV volume neutron source, situated in the first coarse-mesh interval), characterized by 25 energy groups, 2 coarse-mesh intervals (of 5 cm and 10 cm external radius, respectively) and 10 fine-mesh intervals requires, in

S_8 approximation, 2.39 sec CPU time when run with ONETRAN in the P_3-representation of the transfer matrices and 3.17 sec CPU time when run with ANTRA1.

The same problem, but with 2 coarse-mesh intervals of 5 cm and 25 cm external radius, respectively needs 8.60 sec CPU time when computed by ONETRAN and 6.93 sec CPU time when computed with ANTRA1.
However, in order to handle more correctly strongly anisotropic scattering in the ONETRAN code higher orders of anisotropy are required what increases execution times, in this case ANTRA1 (with e.g. S_{20}-segmentation) is expected to bring significant gains of computing times.

A 25-group, 45-interval mesh, S_8 k_{eff} calculations for a critical uranium sphere resulted in 3 outer iterations, 430 inner iterations and 11.83 CPU time with ONETRAN (in P_3 approximation), and 3 outer iterations, 427 inner iterations and 31.79 sec CPU time with ANTRA1.

Sample tests were performed on the Siemens 7890 computer.

7. Unusual Features of the Programme:

Original ONETRAN-features

Provision is made for creation of standard interface output files for S_N constants, inhomogeneous sources, angle-dependent fluxes. Standard interface input files for S_N constants, cross-sections, and total or angular fluxes may be read. Some transfer operations are localized in subroutines REED and RITE (in versions suitable for use on IBM computers). Flexible edit options including restart capabilities are provided.

New features

Additionally new interface input files (in a form of KAPROS Data Blocks) are used. Scattering matrices in the angular representation and discretized angular transfer probability tables (e.g. discretized I*-function) may be read from these files. Transfer operations are managed by KAPROS subroutines and by newly developed service subroutines RITEF, REEDF.

8. Machine Requirements: Seven interface units (use of interface units is optional), five output units, and two system input/output units are required.

9. Related Programs: GANTRAS may be used to prepare initial conditions to the TIMEX code, a time dependent kinetic version of ONETRAN.

10. Programming Language: FORTRAN IV

11. Material Available: Source list, test problems, results of executed problems and the documentation are available from the Kernforschungszentrum Karlsruhe.

I. Introduction

The distribution of neutrons in space and energy is determined by the neutron transport equation which is the linearized form of the Boltzmann equation. In this equation, the total information about the scattering process is contained in the transfer scattering cross-section (i.e. scattering kernel). This is the double-differential cross-section that depends on energy and direction of both the incident and outgoing neutrons. Thus to handle on a computer the double-differential cross-sections in a pointwise form for subsequent use by a neutron transport code, an unacceptably large storage area is needed. Additionally, in the neutron transport codes employing the exact kernel methods, the angular fluxes must be retained what extends the necessary storage even more.

For computational purposes it was found advantageous to:

(1) represent the angular dependence of the scattering kernel in terms of Legendre polynomial expansion

(2) discretize the relevant energy range (from 0.001 eV to about 15 MeV) into energy groups and to process the pointwise data from evaluated nuclear data files into a multigroup form.

The groupwise cross-sections are stored in libraries, suitably formatted for further use by the general-purpose computer codes, solving the transport equation by the multigroup procedure.

In neutronic studies of fission reactors, it became customary to truncate the Legendre expansion series after a finite number of terms. The approximation, introduced in this way was proven to give sufficiently accurate results for the anisotropic neutron transport in fission reactors, in which only elastic and level inelastic scattering are of primary importance.

However, the straightforward application of methods and nuclear data suitable for fission reactors to the neutronics of fusion reactors causes some difficulties. The energy of neutrons in a (d,t) fusion reaction is 14 MeV.

This energy is significantly higher than the energy of neutrons from nuclear fission reactions. At such high neutron energies, the neutron scattering becomes strongly anisotropic (in general forward peaked in the laboratory system), especially for light nuclei (e.g. Li^6, Li^7, Be), which one has to deal with in fusion reactor blanket.

Moreover, some threshold reactions of minor significance in fission reactors (i.e. inelastic scattering with continuum excitation, (n,2n), (n,3n) etc.) were treated only approximately. In fission reactor blanket these reactions however play a dominant role.

To take account of the strong anisotropy in the frame of the Legendre polynomial representation would mean to carry on many terms of the series in the calculations. Premature truncation of the expansion has severe consequences. It introduces unphysical oscillations, negative transfer probabilities and finally negative values of the angular neutron flux. This decreases the accuracy of the total neutron flux, which is one of the important neutronic features in the fusion reactor blanket /1/.

Mispredicted total flux together with an uncertainty in the tritium production cross-section for both lithium isotopes prevents the correct estimation of a very important critical parameter, the tritium breeding ratio. Furthermore, other significant parameters in the thermal and mechanical design of a fusion reactor, e.g. the power density in the first wall, in the blanket, in the shielding materials and in the superconductive magnets, can be correctly calculated, provided the total neutron flux (and the gamma spectrum) as well as the kerma factors are accurately known.

Therefore, it has been recommended for fusion neutronic study to develop an improved calculational method for handling correctly the anisotropic scattering of neutrons in all neutron-emitting reactions (i.e. elastic and inelastic scattering, (n,2n), (n,3n), etc.) that could be implemented in existing neutron transport codes.

Since the storage limitations are no more a hindrance in available modern computers, this new method should:

(a) avoid the traditional expansion of the scattering kernel into a series of Legendre polynomials (in terms of the scattering angle).

(b) be suitable for direct use in a discrete ordinates formulation of the multigroup transport equation and give accurate numerical results.

(c) use double differential cross-sections for the description of the emission of secondary neutrons, since these data contain all physical information on the scattering process.

Such a technique, proposed by Takahashi and Rusch /2/, called the I*-method, has been successfully used here in conjunction with the modified S_N transport code ONETRAN, implemented at the Karlsruhe Nuclear Research Center. On the basis of the I*-method and the ONETRAN code, a system of computer codes, called GANTRAS has been recently developed. The new system in a present version solves numerically the multigroup form of the Boltzmann equation, in one-dimensional plane and spherical geometry (with a rigorous treatment of the anisotropic neutron scattering).

The transport module of GANTRAS, the ANTRA1 code, provides a significant advance over presently available discrete ordinate transport codes (e.g. ONETRAN, ANISN). ANTRA1 retains all major features of the ONETRAN code. Additionally, the ANTRA1 user is given a choice between the rigorous I*-method or/and Legendre polynomial expansion (of appropriate order) for the representation of the scattering source term, within one calculational run. This can be done according to requirements and the availability of nuclear data for particular materials (e.g. double or single differential cross-sections).

In the next sections of this report the theoretical basis of all the methods and approximations used in GANTRAS is presented. Section III contains a description of the code and computational algorithm. Section IV gives the rule for the user to specify input data. First numerical results are shown in Section V.

II. Theory

1. The Neutron Transport Equation

The time-independent Boltzmann equation for neutron transport, which determines the distribution of neutrons in space and energy is written:

$$\vec{\Omega}\cdot\nabla\psi(\vec{r},E,\vec{\Omega}) + \Sigma_t(\vec{r},E)\psi(\vec{r},E,\vec{\Omega}) =$$

$$\int_{4\pi}\int_{0}^{\infty}\Sigma_s(\vec{r},E'\to E,\vec{\Omega}'\to\vec{\Omega})\psi(\vec{r},E',\vec{\Omega}')dE'd\vec{\Omega}' +$$

$$\frac{1}{4\pi}\int_{4\pi}\int_{0}^{\infty}\chi(\vec{r},E'\to E)\nu\Sigma_f(\vec{r},E')\psi(\vec{r},E',\vec{\Omega}')dE'd\vec{\Omega}' + S(\vec{r},E,\vec{\Omega}) \qquad (1)$$

where

$\psi(\vec{r},E,\vec{\Omega})$	angular neutron flux (neutrons/length^2/unit energy/solid angle)
E	neutron energy
$\vec{r}$	position vector
$\vec{\Omega}$	unit vector in the direction of the neutron motion
$\Sigma_t(\vec{r},E)$	total macroscopic cross-section
$\Sigma_s(E'\to E,\vec{\Omega}'\to\vec{\Omega})$	scattering kernel, i.e. double differential neutron transfer cross-section (elastic and inelastic scattering, (n,2n), (n,3n), etc.) which transfers neutrons of energy E' and direction $\vec{\Omega}'$ into the energy interval dE about E and into the direction interval $d\vec{\Omega}$ about $\vec{\Omega}$
$\Sigma_f(\vec{r},E')$	macroscopic fission cross-section
$\chi(\vec{r},E'\to E)$	fraction of neutrons, released at $\vec{r}$ with energy in the range dE about E from fission in dE' about E'
ν	mean number of fission neutrons emitted isotropically ($\frac{1}{4\pi}$) per fission
$S(\vec{r},E,\vec{\Omega})$	external neutron source, which emits neutrons with energy E, at position $\vec{r}$ in direction $\vec{\Omega}$

The integrodifferential form of the Boltzmann equation (Eq. (1)) is based

on a local neutron balance at $(\vec{r},E,\vec{\Omega})$ i.e. within each infinitesimal element of volume direction and energy $d\vec{r}dEd\vec{\Omega}$. It states that the total derivative of the time-independent neutron flux $\psi(\vec{r},E,\vec{\Omega})$ in the direction $\vec{\Omega}$ (streaming term), which accounts for neutron losses due to leakage, equals to the rate at which neutrons are emitted or scattered into the phase space element $d\vec{r}dEd\vec{\Omega}$, represented by the right hand side of Eq. (1) (the source term), less the rate of removal due to absorption and scattering process (second term of the left hand side).

In general, there are three contributions to the source term: the scattering source, the fission source and the external source.
The scattering source term, together with the fission source term, which are linear functions of the neutron flux, are referred to as homogeneous term, whereas the external source (independent on the neutron flux) is referred to as an inhomogeneous term.

The total macroscopic cross-section and the double-differential scattering cross-section characterize the interactions of neutrons with the nuclei of the matter. If we take into consideration only media, whose properties are invariant under rotation the scattering kernel Σ_s depends on $\vec{\Omega}'$ and $\vec{\Omega}$ only through their product $\vec{\Omega}\cdot\vec{\Omega}'$.

In conventional calculational approach it became customary to expand Σ_s into a series of Legendre polynomials (in terms of the scattering angle $\vec{\Omega}\cdot\vec{\Omega}'$)

$$\Sigma_s(\vec{r},E'\to E,\vec{\Omega}'\to\vec{\Omega}) = \frac{1}{2\pi}\Sigma_s(\vec{r},E'\to E,\vec{\Omega}\cdot\vec{\Omega}') =$$

$$= \sum_{l=0}^{\infty}\frac{2l+1}{4\pi}\Sigma_s^l(\vec{r},E',E)P_l(\vec{\Omega}\cdot\vec{\Omega}') \qquad (2)$$

In practice, however, it is necessary to terminate the series of Eq. (2) after a finite number of terms and to specify coefficients $\Sigma_s^l(\vec{r},E',E)$ in order to perform the summation. This procedure leads to the following representation of the scattering kernel:

$$\Sigma_s(r,E'\to E,\vec{\Omega}'\to\vec{\Omega}) = \sum_{l=1}^{L}\frac{2l+1}{4\pi}\Sigma_s^l(\vec{r},E',E)P_l(\vec{\Omega}\cdot\vec{\Omega}') \qquad (3)$$

The coefficients $\Sigma_s^l(\vec{r},E',E)$ are derived in the Appendix.

In order to handle the anisotropy in an adequate manner in Eq. (3), the number of retained terms, i.e. L, called order (or degree) of anisotropy must be consistent to real anisotropy present in the system.

2. Approximate Representation of the Source Term by Means of Truncated Spherical Harmonics Expansion

Further approximations refer to the source term of the transport equation (1), namely,

$$q_s(\vec{r},E,\vec{\Omega}) = \int_0^\infty \int_{4\pi} \Sigma_s(\vec{r},E'\to E,\vec{\Omega}'\to\vec{\Omega})\psi(\vec{r},E',\vec{\Omega}')d\vec{\Omega}'dE' =$$

$$= \int_0^\infty \int_{4\pi} \Sigma_s(\vec{r},E'\to E,\vec{\Omega}\cdot\vec{\Omega}')\psi(\vec{r},E',\vec{\Omega}')d\vec{\Omega}'dE' \qquad (4)$$

In the following we restrict our attention to one-dimensional geometries. In one-dimensional plane and spherical geometry the angular neutron flux is azimuthally symmetrical. Thus the directional dependence of the angular flux can be specified by only one variable, direction cosine $\mu = \cos\Theta$, where in plane geometry Θ is chosen to be the angle between $\hat{e}_x$-axis and the direction $\vec{\Omega}$ (see Fig. 1) and in spherical geometry Θ is the angle between $\vec{\Omega}$ and the $\hat{e}_r$-axis (see Fig. 2).

The integral over the direction variable in Eq. (4) (i.e. over μ',ϕ') can be simplified by inserting the Legendre polynomial representation of the scattering kernel from Eq. (3) and then, with the aid of the addition theorem for Legendre polynomials, by expressing $P_l(\vec{\Omega}\cdot\vec{\Omega}')$ in terms of associated polynomials $P_l^m(\mu)$, $P_l^m(\mu')$:

$$P_l(\vec{\Omega}\cdot\vec{\Omega}') = P_l(\mu)P_l(\mu') + 2\sum_{m=1}^{l}\frac{(l-m)!}{(l+m)!}P_l^m(\mu)P_l^m(\mu')\cos m(\phi-\phi')$$

where μ',μ are direction cosines and ϕ',ϕ are azimuthal angles, specifying the directions $\vec{\Omega}'$ and $\vec{\Omega}$, respectively.

Upon integration over the azimuthal angle ϕ' the scattering term may be written in spherical geometry as

$$q_s(r,E,\mu) = \int_0^\infty dE' \sum_{l=0}^{L} \frac{2l+1}{2} \Sigma_s^l(r,E',E) P_l(\mu) \int_{-1}^{1} d\mu' P_l(\mu') \psi(r,E',\mu') \tag{5}$$

The angular integrals on the right hand side of Eq. (5) are now just the coefficients

$$\Phi_l(r,E') = \int_{-1}^{1} \frac{d\mu'}{2} P_l(\mu') \psi(r,E',\mu') \tag{6}$$

that result from expanding the angular flux into a series of Legendre polynomials.

$$\psi(r,E,\mu) = \sum_{l=0}^{\infty} (2l+1) P_l(\mu) \Phi_l(r,E) \tag{6a}$$

Finally the expression for the scattering source takes the form

$$q_s(r,E,\mu) = \int_0^\infty dE' \sum_{l=0}^{L} (2l+1) \Sigma_s^l(r,E',E) P_l(\mu) \Phi_l(r,E') \tag{7}$$

Consequently, the scattering source moments have the simple form

$$q_s^l(r,E) = \int_0^\infty dE' \Sigma_s^l(r,E',E) \Phi_l(r,E') \tag{7a}$$

Above equations hold for one-dimensional plane geometry where the variable r has to be replaced by x.

To derive the formula representing the scattering source in one-dimensional cylindrical geometry, the angular coordinate system is oriented as depicted in Fig. 3.

The angular flux at point $\vec{r}$ depends on one spatial coordinate r, since we are dealing with one-dimensional geometry and both angular coordinates (ξ,ϕ).

Eq. (4) takes the form

$$q_s(r,E,\vec{\Omega}) = \frac{1}{2\pi}\int_0^{\infty}\int_{-1}^{1}\int_0^{2\pi}\Sigma_s(r,E',E,\xi_0)\psi(r,E',\xi',\phi')d\phi'd\xi'dE' \qquad (8)$$

where now

ξ',ξ are the direction cosines and ϕ',ϕ are the azimuthal angles, specifying the directions $\vec{\Omega}'$ and $\vec{\Omega}$, respectively,

$$\xi_0 = \vec{\Omega}\cdot\vec{\Omega}'$$

The cosine of the scattering angle, expressed in (ξ,ϕ)-coordinates becomes

$$\xi_0 = \xi'\xi - (1-\xi^2)^{1/2}(1-\xi'^2)^{1/2}\cos(\phi-\phi') \qquad (9)$$

According to addition theorem of Legendre polynomials:

$$P_l(\xi_0) = P_l(\xi)P_l(\xi') + 2\sum_{m=1}^{l}\frac{(l-m)!}{(l+m)!}P_l^m(\xi)P_l^m(\xi')\cos(m(\phi-\phi')) \qquad (10)$$

We get

$$q_s(r,E,\xi,\phi) = \int_0^{\infty}dE'\sum_{l=0}^{L}\frac{2l+1}{4\pi}\Sigma_s^l(r,E',E)\Big[P_l(\xi)\int_{-1}^{1}d\xi'\int_0^{2\pi}d\phi'P_l(\xi')\psi(r,E',\xi',\phi') +$$

$$+ 2\sum_{m=1}^{l}\frac{(l-m)!}{(l+m)!}P_l^m(\xi)\int_{-1}^{1}d\xi'\int_0^{2\pi}d\phi'P_l^m(\xi')\cos(m(\phi-\phi'))\psi(r,E',\xi',\phi')\Big] \qquad (11)$$

By using the geometrically imposed symmetry on the angular flux in ϕ, what allows to eliminate the expansion terms add in ϕ we obtain

$$q_s(r,E,\xi,\phi) = \int_0^{\infty}dE'\sum_{l=0}^{L}\frac{2l+1}{2\pi}\Sigma_s^l(r,E',E)\sum_{m=0}^{l}R_l^m(\xi,\phi)\int_{-1}^{1}d\xi'\int_0^{2\pi}d\phi'R_l^m(\xi',\phi')\psi(r,E',\xi',\phi'$$

(12)

The functions $R_l^m(\xi,\phi)$ are defined by

$$R_l^m(\xi,\phi) = \left[\frac{(2-\delta_{m,o})(l-m)!}{(l+m)!}\right]^{1/2}P_l^m(\xi)\cos m\phi \qquad (13)$$

Furthermore, R_l^m constitute an orthogonal set of functions:

$$\int_1^1 d\xi \int_0^{2\pi} d\phi R_l^m(\xi,\phi) R_n^k(\xi,\phi) = \frac{2\pi}{2l+1} \delta_{l,n} \delta_{m,k} \tag{14}$$

It is possible therefore to expand the angular flux in a series of R_l^m

$$\psi(r,E,\xi,\phi) = \sum_{m=0}^{\infty} (2l+1) \sum_{k=0}^{m} R_m^k(\xi,\phi) \Phi_m^k(r,E) \tag{15}$$

with

$$\Phi_m^k(r,E) = \frac{1}{4\pi} \int_{-1}^{1} \int_0^{2\pi} R_m^k(\xi,\phi) \psi(r,E,\xi,\phi) d\phi d\xi \tag{16}$$

Hence, equation (12) may be written

$$q_s(r,E,\xi,\phi) = \int_0^{\infty} dE' \sum_{l=0}^{L} (2l+1) \Sigma_s^l(r,E',E) \sum_{m=0}^{l} R_l^m(\xi,\phi) \Phi_l^m(r,E') \tag{17}$$

and the angular moments of the scattering source can be expressed in a simple form

$$q_{s,l}^m(r,E) = \int_0^{\infty} dE' \Sigma_s^l(r,E',E) \Phi_l^m(r,E') \tag{17a}$$

The number of flux moments involved in Eq. (17) is $(L+2)^2/4$, since the flux moments with (l-m) odd vanish due to the symmetry of the angular flux in ξ.

If the external source is not isotropic, it can also be expanded into a series of Legendre polynomials or R_l^m-functions (according to geometry) and then truncated after K-terms.

Finally, we arrive at an approximate representation for the entire source term:

(a) in spherical and plane geometry

$$q(r,E,\mu) = \int_0^\infty dE' \sum_{l=0}^{L} (2l+1)\Sigma_s^l(r,E',E)P_l(\mu)\Phi_l(r,E') + \int_0^\infty dE'\nu\Sigma_f(r,E')\chi(E'\to E)\Phi_0(r,E') + \sum_{k=0}^{K}(2k+1)P_k(\mu)S_k(r,E) \tag{18a}$$

(b) in cylindrical geometry

$$q(r,E,\xi,\phi) = \int_0^\infty dE' \sum_{l=0}^{L} (2l+1)\Sigma_s^l(r,E',E) \sum_{m=0}^{l} R_l^m(\xi,\phi)\Phi_l^m(r,E') + \int_0^\infty dE'\nu\Sigma_f(r,E')\chi(E'\to E)\Phi_0^0(r,E') + \sum_{k=0}^{K}(2k+1) \sum_{i=0}^{k} R_k^i(\xi,\phi)S_k^i(r,E) \tag{18b}$$

Representations of the source term, given by Eqs. (18a) and (18b) are conventionally used in most numerical procedures for the solution of the neutron transport equation. However, in practical applications, in which fast neutrons and/or anisotropic neutron sources must be taken into consideration, the proper choice of the order of truncation L and K is one of the main problems.

By an early truncation of the series expansion a great portion of information may be lost /3/. Since the Legendre polynomial expansion converges slowly, in case the exact cross-section exhibits strong anisotropy to reconstruct the scattering kernel correctly high-order expansions are needed. In consequence high order Legendre coefficients must be accurately evaluated. This is generally a difficult numerical task. For high neutron energies the angular distributions in the center-of-mass system are already highly anisotropic. Also for light nuclei even if the scattering is isotropic in the center-of-mass system, the angular distribution becomes strongly forward peaked in the laboratory system.

Moreover, it is not the cross-section alone, that determines up to which order the Legendre coefficients in Eq. (5) or Eq. (11) have to be regarded. The scattering source includes the product of both the angular flux and the cross-section moments and therefore it also depends on the behaviour of the angular flux at which term the series expansion can be truncated.

Due to premature truncation, the scattering source can exhibit nonphysical fluctuations and became even negative in some angular ranges, which is in turn reflected in the calculated (e.q. by iterational scheme) angular fluxes. On the other hand to carry on many expansion terms means to cope with difficulties related to computational tools, so often a compromise between accuracy and computational time must be made.

Therefore in order to take account of the detailed angular dependence of the transfer cross-section in calculating the scattering source it is more reasonable to derive an improved representation.
Several methods have been already developed /2/, /4/, /5/. The one adopted here, introduced by Takahashi et al. /2/, is called the I*-method.

3. Rigorous Representation of the Scattering Source Term by the I*-Method

The I*-method is based on the simple idea to introduce the true physical scattering angle in the laboratory system, denoted by μ^*, into the scattering kernel instead of the purely geometrical scattering angle μ_o (as it is given by Eq. (9) as a function of μ,μ',ϕ,ϕ').

To simplify the notation in foregoing equations, the direction variable $\vec{\Omega}$ will be represented by (μ,ϕ) angular coordinates. In cylindrical geometry, however, it is the most convenient to describe the scattering process in respect to $\hat{e}_z$-axis (see Figs. (3) and (4)) and therefore in this case a coordinate μ has to be replaced by ξ.

By putting

$$\Sigma_s(r,E'\to E,\mu_o) = \int_{-1}^{1} \Sigma_s(r,E',E,\mu^*)\delta(\mu_o-\mu^*)d\mu^* \qquad (19)$$

where

$\mu^* = \mu_L(E',E)$ is the true physical scattering angle in the laboratory system fixed by the energy of the incident and outgoing neutron

$\Sigma_s(r,E',E,\mu^*)$ is the double-differential scattering cross-section

and

δ is the Dirac-delta function

into equation (4) the following expression for the scattering term is obtained

$$q_s(r,E,\mu,\phi) = \frac{1}{2\pi}\int_0^\infty dE' \int_{-1}^{1}\int_{-1}^{1} \Sigma_s(r,E',E,\mu^*)\left[\int_0^{2\pi}\delta(\mu_o-\mu^*)\psi(r,E',\mu',\phi')d\phi'\right]d\mu^* d\mu'$$

$$= \int_0^\infty dE' \int_{-1}^{1}\int_{\beta_1^*}^{\beta_2^*} \Sigma_s(r,E',E,\mu^*)\left[I^*(\mu,\mu',\mu^*)\psi(r,E',\mu',\phi'(\mu,\phi,\mu',\mu^*))\right]d\mu^* d\mu' \qquad (20)$$

where

the limits of the restricted μ^*-range (because in Eq. (9) $|\cos(\phi-\phi')| \leq 1$), are given by

$$\beta_1^* = \mu'\mu - \sqrt{1-\mu^2}\sqrt{1-\mu'^2}$$

$$\beta_2^* = \mu'\mu + \sqrt{1-\mu^2}\sqrt{1-\mu'^2} \qquad (20a)$$

the I^* is defined by

$$I^*(\mu,\mu',\mu^*)\psi(r,E',\mu',\phi'(\mu,\phi,\mu',\mu^*)) = \frac{1}{2\pi}\int_0^{2\pi}\delta(\mu_o-\mu^*)\psi(r,E',\mu',\phi')d\phi' \qquad (20b)$$

and the possible ϕ' values (see Fig. (4)) can be determined from Eq. (9) for $|\mu| \neq 1$ and $|\mu'| \neq 1$

$$\phi'(\mu,\phi,\mu',\mu^*) = \phi + \arccos\left\{\frac{\mu^*-\mu'\mu}{\sqrt{1-\mu^2}\ \sqrt{1-\mu'^2}}\right\} = \phi+\Delta\phi(\mu,\mu',\mu^*) \qquad (20c)$$

If the angular flux ψ is independent of ϕ (spherical and plane geometry) then

$$I^*(\mu,\mu',\mu^*) = \frac{1}{2\pi}\int_0^{2\pi} \delta(\mu_0-\mu^*)d\phi' \qquad (21)$$

can be calculated analytically.

According to the values of three arguments μ, μ' and μ^* we get:

1. For $|\mu| \neq 1$, $|\mu'| \neq 1$ and $|\mu^*| \neq 1$

$$I^*(\mu,\mu',\mu^*) = \begin{cases} \dfrac{1}{\pi\sqrt{1-\mu^2-\mu'^2-\mu^{*2}-2\mu\mu'\mu^*}}, & \text{if } \beta_1^* \leq \mu^* \leq \beta_2^* \\ 0, & \text{otherwise} \end{cases} \qquad (22a)$$

2. For $|\mu| = 1$ or $|\mu'| = 1$ or $|\mu^*| = 1$ it is found that

$$I^*(\mu,\mu',\mu^*) = \begin{cases} \delta(\mu\mu'-\mu^*), & \text{if } |\mu| = 1 \text{ or } |\mu'| = 1 \\ \delta(\mu-\mu'\mu^*), & \text{if } |\mu^*| = 1 \end{cases} \qquad (22b)$$

The representative examples of the I^*-function are shown in Figs. 5a - 5d. For given μ' and μ the azimuthal angle shift $\Delta\phi$ is fixed, since the cosine of the scattering angle is fixed by the scattering law (i.e. physically), μ^* is identical to μ_0, therefore there is only one incident vector $\vec{\Omega}'$ corresponding to the outgoing $\vec{\Omega}$.

The physical meaning of the I^*-function can be described (in reference to Fig. 4) as follows.
After scattering through the angle $\cos^{-1}\mu^*$, the direction vector $\vec{\Omega}$ of the outgoing neutron forms a cone around the direction vector $\vec{\Omega}'$ of the incoming neutron, since the neutron scattering is independent on the azimuthal angle. In case of $\vec{\Omega}'$ symmetry this cone rotates around the axis of symmetry ($\hat{e}_r$ or $\hat{e}_z$ according to geometry). All outgoing vectors are distributed on this

curved surface. Inside the cone with the opening angle Θ_1 and outside the cone with the opening angle Θ_2 there are no outgoing vectors. The region between Θ_1 and Θ_2 is the geometrically allowed region.

The I*-function can be interpreted as:

(a) the probability distribution function of the outgoing vectors.
That means: for $\mu^* = \text{const}$ i.e. for a given scattering process with μ' and μ^* given, $\vec{\Omega}$ is distributed on this curved surface with the probability $I^*(\mu,\mu',\mu^*)$.

(b) the probability that a neutron incident at angle $\cos^{-1}\mu'$ will appear at the outgoing angle $\cos^{-1}\mu$ upon being scattered through an angle $\cos^{-1}\mu^* = \Theta^*$.
That means: if μ' and μ are fixed then the incoming vector $\vec{\Omega}'$ and outgoing $\vec{\Omega}$ (determined by only one coordinate) may rotate around the axis of symmetry. There is a number of possibilities for the scattering angle Θ^*, in a purely geometrical sense (Θ_1^*, Θ_2^* are the limits of the geometrically allowed Θ^*-region, β_1^*, β_2^* of μ^*-range respectively). I* gives the probability for each of these possibilities. Scattering kinematics determines these angles Θ^* which are physically attainable.

If the geometry imposes azimuthal symmetry on the angular flux an important simplification to Eq. (20) can be made.

$$q_s(r,E,\mu) = \int_0^\infty dE' \int_{-1}^{1} \left[\int_{\beta_1^*}^{\beta_2^*} \Sigma_s(r,E',E,\mu^*) I^*(\mu,\mu',\mu^*) d\mu^* \right] \psi(r,E',\mu') d\mu' \tag{23}$$

In this case the transfer cross-section can be expressed in a form

$$\Sigma_s(r,E'\to E,\vec{\Omega}\cdot\vec{\Omega}') = \int_{\beta_1^*}^{\beta_2^*} \Sigma_s(r,E',E,\mu^*) I^*(\mu,\mu',\mu^*) d\mu^* \tag{24}$$

It is essential to note that all physical aspects underlying the I*-method are contained in Eq. (24). It states that the transfer cross-section $\Sigma_s(r,E'\to E,\vec{\Omega}\cdot\vec{\Omega}')$ which transfers neutrons from energy E' to energy E and

simultaneously from direction $\vec{\Omega}'$ to $\vec{\Omega}$ is obtained by summing up for fixed μ' and μ the weighted contributions $\Sigma_s(r,E',E,\mu^*)$ from all possible scattering angles μ^*.

For a trivial problem when the angular distribution of secondary neutrons is assumed to be isotropic, inserting

$$\Sigma_s(r,E'\to E,\mu^*) = \frac{1}{2}\,\Sigma_{iso}(r,E',E)$$

into Eq. (23) we find that

$$q_s(r,E,\mu) = \frac{1}{2}\int_0^\infty dE'\Sigma_{iso}(r,E',E)\int_{-1}^{1}\left[\int_{\beta_1^*}^{\beta_2^*} I^*(\mu,\mu',\mu^*)d\mu^*\right]\psi(r,E',\mu')d\mu' \tag{25}$$

The integral over μ^* in Eq. (25) is just a normalization condition for the I^*-function, it can be analytically evaluated

$$\int_{\beta_1^*}^{\beta_2^*} I^*(\mu,\mu',\mu^*) = 1$$

Hence,

$$q_s(r,E,\mu) = \int_0^\infty dE'\Sigma_{iso}(r,E',E)\Phi_0^0(r,E') \tag{26}$$

where

$$\Phi_0^0(r,E') = \int_{-1}^{1}\psi(r,E',\mu')\frac{d\mu'}{2} \quad \text{is the total flux.}$$

The total macroscopic double differential cross-section $\Sigma_s(r,E',E,\mu^*)$ contains all physical information of the scattering process. It comprises a sum of cross-sections for various types of neutron scattering: elastic, level inelastic, inelastic with continuum excitation and reactions designated as (n,2n) or (n,3n) that result in the emission of more than one neutron.

Since for elastic and discrete level inelastic scattering the energy-angle coupling is explicitly known, the double differential cross-sections can easily be reconstructed from the angular neutron distributions, taking into account scattering kinematics. An accurate description of the secondary neutrons resulting from (n,n'continuum), (n,2n) and further many particle reactions requires the use of energy- and angle-correlated distributions i.e. full double-differential data.

4. Incorporation of the I*-Method into the Discrete Ordinates Formulation of the Multigroup Transport Equation

4.1 Multigroup Equations

The multigroup form of the Boltzmann equation is of interest in most methods for solving neutron transport problems. The first step to the development of the multigroup procedure is to divide a relevant energy range into a finite number of discrete energy groups. By integrating the energy-dependent transport equation over the group intervals i.e. $E_{g+1} \leq E \leq E_g$ $(g=1,2,\ldots,G)$ and by substituting all integrals over the energy variable by sums

$$\int_0^\infty dE = \sum_{g=1}^{G} \int_{E_{g+1}}^{E_g} dE \tag{27}$$

a system of G coupled integrodifferential equations is obtained

$$\vec{\Omega}\cdot\nabla\psi_g(r,\vec{\Omega}) + \Sigma_{t,g}(r)\psi_g(r,\vec{\Omega}) =$$

$$\sum_{g'=1}^{G} \int_{4\pi} \Sigma_{s,g'\to g}(r,\vec{\Omega}\cdot\vec{\Omega}')\psi_{g'}(r,\vec{\Omega}')d\vec{\Omega}' + \tag{28}$$

$$+ \frac{1}{4\pi} \sum_{g'=1}^{G} \int_{4\pi} \chi(r,g'\to g)\nu\Sigma_{f,g'}(r)\psi_{g'}(r,\vec{\Omega}')d\vec{\Omega}' + S_g(r,\vec{\Omega}),\ g=1,\ldots,G$$

for the group angular fluxes, defined as

$$\psi_g(r,\vec{\Omega}) = \int_{E_{g+1}}^{E_g} \psi(r,E,\vec{\Omega})dE \tag{29}$$

with the corresponding group cross-sections

$$\Sigma_{t,g}(r,\vec{\Omega}) = \frac{\int_{E_{g+1}}^{E_g} \Sigma_t(r,E)\psi(r,E,\vec{\Omega})dE}{\int_{E_{g+1}}^{E_g} \psi(r,E,\vec{\Omega})dE} \tag{30}$$

$$\Sigma_{s,g'\to g}(r,\vec{\Omega}\cdot\vec{\Omega}') = \frac{\int_{E_{g+1}}^{E_g}\int_{E_{g'+1}}^{E_{g'}} \Sigma_s(r,E'\to E,\vec{\Omega}\cdot\vec{\Omega}')\psi(r,E',\vec{\Omega}')dE'dE}{\int_{E_{g'+1}}^{E_{g'}} \psi(r,E',\vec{\Omega}')dE'} \tag{31}$$

$$\Sigma_{f,g'}(r,\vec{\Omega}') = \frac{\int_{E_{g'+1}}^{E_{g'}} \Sigma_f(r,E')\psi(r,E',\vec{\Omega}')dE'}{\int_{E_{g'+1}}^{E_{g'}} \psi(r,E',\vec{\Omega}')dE'} \tag{32}$$

$\chi(r,g'\to g)$ is the fraction of neutrons produced in the g-th group due to fission in group g' and

$$S_g(r,\vec{\Omega}) = \int_{E_{g+1}}^{E_g} S(r,E,\vec{\Omega})dE \tag{33}$$

By using the angular flux as a weighting function in Eqs. (30) - (32), the total group cross-section (Eq. (30)) becomes angular dependent. To eliminate this undesired angular dependence an approximation has to be made. Usually it is assumed that within each energy group the angular flux can be approximated as a product of a known function of energy $\phi(r,E)$ and the angular dependent part $g(\vec{\Omega})$:

$$\psi(r,E,\vec{\Omega}) = \phi(r,E)g(\vec{\Omega}) \qquad E_{g+1} \leq E \leq E_g \tag{34}$$

From this postulate of separability it follows that $\Sigma_{t,g}$ and $\Sigma_{f,g}$ become angle independent and $\Sigma_{s,g'\to g}$ is, as it was before, a function only of the scattering angle $\vec{\Omega}\cdot\vec{\Omega}'$.

Inserting equation (34) into (30) - (32) we get

$$\Sigma_{t,g}(r) = \frac{\int_{E_{g+1}}^{E_g} \Sigma_t(r,E)\phi(r,E)dE}{\int_{E_{g+1}}^{E_g} \phi(r,E)dE} \tag{30a}$$

$$\Sigma_{s,g'\to g}(r,\vec{\Omega}\cdot\vec{\Omega}') = \frac{\int_{E_{g+1}}^{E_g}\int_{E_{g'+1}}^{E_{g'}} \Sigma_s(r,E'\to E,\vec{\Omega}\cdot\vec{\Omega}')\phi(r,E')dE'dE}{\int_{E_{g'+1}}^{E_{g'}} \phi(r,E')dE'} \tag{31a}$$

$$\Sigma_{f,g'}(r) = \frac{\int_{E_{g'+1}}^{E_{g'}} \Sigma_f(r,E')\phi(r,E')dE'}{\int_{E_{g'+1}}^{E_{g'}} \phi(r,E')dE'} \tag{32a}$$

so that the group cross-sections can be evaluated after estimating the weighting function $\phi(r,E)$. The spatial dependence of the flux $\phi(r,E)$ can be treated by introducing the spatial zones, in which $\phi(r,E)$ is varying only weakly with r and thus can be replaced by spatial average. If there is a strong spatial dependence of $\phi(r,E)$ it is necessary to use zone-dependent group cross-sections.

The second, alternative multigroup approximation avoids the assumption of flux separability in defining cross-sections. Instead, it allows to use more realistic weighting of the multigroup cross-sections.

The multigroup procedure is, in this case, applied to another form of the transport equation in which the scattering term had already been expanded in a Legendre series /5/.
It leads, accomplished by the consistent P_N approximation or the extended transport approximation, to improved definitions of the multigroup cross-sections.

Before multigroup transport calculations can be performed the multigroup cross-sections (Eq. (30a) - (32a)) must be evaluated. The processing of energy- and angle-dependent transfer cross-sections as given by (31a) necessitates an establishment of a new calculational scheme.

The group-averaged and angle-segmented microscopic transfer cross-sections are calculated as follows /6/:

$$\sigma_{nem,g'\to g}(\mu_m^*) = \frac{\int_{E_{g'+1}}^{E_{g'}} \phi(r,E') \int_{E_{g+1}}^{E_g} \int_{\Delta\mu_m^*} \sigma_{nem}(E',E,\mu^*)\,d\mu^*\,dE\,dE'}{\int_{\Delta\mu_m^*} \int_{E_{g'+1}}^{E_{g'}} \phi(r,E')\,dE'} \qquad (35)$$

where

$\sigma_{nem}(E',E,\mu^*)$ is the total double-differential cross-section, containing all physical information on the scattering processes.

$\Delta\mu_m^*$ is a width of m-th angular segment (in the segmentation imposed on [-1,1] interval)

It is convenient to split $\sigma_{nem}(E',E,\mu^*)$ into two parts:

(i) a low energy part σ_{nem}^{discr} including elastic and discrete level inelastic scattering

(ii) a high energy part σ_{nem}^{cont} including inelastic neutron scattering to the continuum and all (n,n'x) reactions.

To calculate the first type (i.e. (i)) the conventional (single-differential) angular distributions, contained in all nuclear data files, in connection with scattering kinematics can be used.
On the basis of the GROUPR-module of the NJOY-System /9/ the processing module SDXDDX /10/ was developed which calculates $\sigma^{discr}_{nem,g'\to g}(\mu^*_m)$ according to Eq. (35).

To calculate the second type (i.e. (ii)) (many particle reactions) angular- and energy-distributions of the scattering process have to be known.
Full double-differential data, i.e. angle and energy correlated distributions, are available on the European Fusion File EFF. The newly developed code GROUPIE /10/ based on the ECN/Petten code GROUPXS /17/ processes $\sigma^{cont}_{nem,g'\to g}(\mu^*_m)$ from double-differential cross-sections.

In both modules, GROUPIE and SDXDDX, a Legendre representation of the data in the center-of-mass system (as given on the files) is used but in the transformation to the laboratory system the Legendre representation is avoided. The angular segmentation of the data is done in a consistent manner to the angular segmentation in the S_N-procedure used in ANTRA1.

4.2 Discrete Ordinates Equations in Plane, Spherical and Cylindrical Geometries

The discrete ordinates method is a general and dominant technique used for the solution of the multigroup transport equations. The essential basis of this method is that the angular distribution of the neutron flux is evaluated only in a finite number of discrete directions and the spatial dependence is treated by introducing discrete space meshes.

The new problems encountered in the development of the method are:
(1) the proper choice of the particular discrete directions (i.e. S_N quadrature)
(2) the approximation of the integrals over the direction variable
(3) the approximation of the derivatives of the neutron angular flux with respect to the components of $\vec{\Omega}$ appearing in the transport equations in curved geometries and

(4) accurate and stable discretization scheme of the neutron flux in the spatial variable.

4.2.1 Approximations for the Angular Variable

The quadrature set $\{\vec{\Omega}_m, w_m, m=1,N, N \text{ even}\}$ of N angular directions $\vec{\Omega}_m$ and corresponding weights w_m must be selected so that it does not introduce an undesired directional bias. This is usually achieved by requiring that the set $S_N = \{\vec{\Omega}_m=(\mu_m,\phi_m), m=1,N\}$ be invariant for the main symmetries of the geometries. The associated weights w_m must obey the same symmetries and be positive. They may be determined so as to preserve moment conditions involving the angular integral by associating an area on a unit sphere about each $\vec{\Omega}_m$. The S_N-set is used to define a quadrature formula on a unit sphere of direction. Applying this quadrature formula, the integral term of the transport equation simplifies to a linear combination of the angular fluxes

$$\psi_m(r) = \psi_g(r,\vec{\Omega}_m) \tag{36}$$

with w_m as coefficients.

The S_N approximation to the multigroup transport equation consists of a system of differential equations

$$\vec{\Omega}\cdot\nabla\psi_g(r,\vec{\Omega}) + \Sigma_{t,g}(r)\psi_g(r,\vec{\Omega}) = q_g(r,\vec{\Omega}) \qquad \vec{\Omega}\in S_N\ , \tag{37}$$

coupled through the source term, which is now approximated as

$$q_g(r,\vec{\Omega}) = \sum_{g'=1}^{G} \int_{S_N} \Sigma_{s,g'\to g}(r,\vec{\Omega}\cdot\vec{\Omega}')\psi_{g'}(r,\vec{\Omega}')d\vec{\Omega}' +$$

$$+ \frac{1}{4\pi} \sum_{g'=1}^{G} \chi(r,g'\to g)\nu\Sigma_{f,g'}(r) \int_{S_N} \psi_{g'}(r,\vec{\Omega}')d\vec{\Omega}' + S_g(r,\vec{\Omega}) \tag{38}$$

where the integral over S_N stands for the weighted sum over the directions from S_N-set.

In the scattering source representation with the exact kernel, given by formula (20) the cosine of the scattering angle μ^* and the direction cosine μ' are employed as integration variables instead of (μ',ϕ').

Before the numerical integration is carried out, it must be considered that the direction variable $\vec{\Omega}$ had already been discretized by the S_N-quadrature set (conventionally used in the angular discretization of the multigroup equation). The unit vectors representing the discrete directions Ω'_m lie on a sphere on μ'-latitudes in positions determined by the azimuthal angles ϕ'_m. Thus the numerical integration over μ' variable in Eq. (20) must be done using a quadrature on the interval $[-1,1]$ consistent with S_N quadrature, while for the integration over the scattering angle μ^* e.g. a trapezoidal rule or Simpson's rule can be applied. After the transformation of integration variables from (μ',ϕ') to (μ',μ^*) μ' remains unaltered but the possible ϕ' values (calculated by Eq. (20c)) differ from those given by the S_N-set (see Figs. (6), (7b)) i.e. from these in which the angular flux is calculated. Therefore the use of (μ',μ^*) mesh at which the scattering source is evaluated in addition to (μ,ϕ) mesh, at which the angular flux is evaluated involves a serious drawback. This requires in the discrete ordinates solution that the angular flux at the points $(\mu',\phi'(\mu,\phi,\mu',\mu^*))$ be determined between the iterations by interpolation of the angular flux given at the points of (μ,ϕ) mesh (identical to (μ',ϕ') mesh) in order to perform the integration.

Moreover, the quantities I^* and ϕ' must be discretized. This represents no additional problem and can be done before the actual discrete ordinates solution.

The discretization of the I^*-function is performed using following averaging formula /2/:

$$I^*(m,m',m^*) = \int_{\Delta\mu_m} \int_{\Delta\mu'_{m'}} \int_{\Delta\mu^*_{m^*}} I^*(\mu,\mu',\mu^*)d\mu^*d\mu'd\mu/(\Delta\mu^*_{m^*}\cdot\Delta\mu'_{m'}\cdot\Delta\mu_m) \tag{39}$$

Equation (39) can be simplified by inserting an analytical form of I^*, given by Eq. (22a) and integrating over $\Delta\mu^*_{m^*}$. Thus, we obtain

$$I^*(m,m',m^*) = \frac{\int_{\Delta\mu_m}\int_{\Delta\mu'_{m'}} \left[\arcsin y_{m^*+1/2}(\mu,\mu') - \arcsin y_{m^*-1/2}(\mu,\mu')\right] d\mu' d\mu}{\pi \cdot \Delta\mu^*_{m^*} \Delta\mu'_{m'} \Delta\mu_m} \tag{40}$$

with

$$y_{m^*\pm1/2}(\mu,\mu') = \frac{\mu^*_{m^*\pm1/2} - \mu'\mu}{\sqrt{1-\mu^2}\sqrt{1-\mu'^2}} \quad \text{for } \beta^*_1 \le \mu^*_{m^*\pm1/2} \le \beta^*_2 \tag{41a}$$

$$y_{m^*-1/2}(\mu,\mu') = -1 \quad \text{for } \mu^*_{m^*-1/2} < \beta^*_1 < \mu^*_{m^*+1/2} < \beta^*_2 \tag{41b}$$

$$y_{m^*+1/2}(\mu,\mu') = 1 \quad \text{for } \beta^*_1 < \mu^*_{m-1/2} < \beta^*_2 < \mu^*_{m+1/2} \tag{41c}$$

$$y_{m^*\pm1/2}(\mu,\mu') = 0 \quad \text{for } \mu^*_{m+1/2} < \beta^*_1 \text{ or } \beta^*_2 < \mu^*_{m-1/2} \tag{41d}$$

The matrix containing the discretized angular transfer probability is normalized according to the condition

$$\sum_{m^*_1}^{m^*_2} I^*(m,m',m^*) w_{m^*} = 1 \tag{42}$$

where m^*_1 and m^*_2 correspond to β^*_1 and β^*_2, w_{m^*} are weights associated with the μ^*-segmentation.

For a fixed triplet $(\mu_m, \mu'_{m'}, \mu^*_{m^*})$ the $\phi'(m,m',m^*)$ values may be obtained using

$$\phi'(m,m',m^*) = \phi_m + \arccos \frac{\mu^*_{m^*} - \mu_m \mu'_{m'}}{\sqrt{1-\mu_m^2}\sqrt{1-\mu'^2_{m'}}} \tag{43}$$

Resulting from Eqs. (20), (35), (39), (43) discretization formula for a scattering term has the form

$$q^g_s(r,\mu_m,\phi_m) = \tag{44}$$

$$= \sum_{g'=1}^{G} \sum_{m'} \left(\sum_{m^*} \Sigma_{s,g'\to g}(r,m^*) I^*(m,m',m^*) \cdot \psi_{g'}(r,\mu'_{m'},\phi'(m,m',m^*)) \cdot w_{m^*} \right) w_{m'}$$

In the following, when it does not lead to misunderstanding group indices will be omitted for the sake of notation simplicity.

An application of the discrete ordinate method to multigroup transport equation in one-dimensional plane geometry causes no difficulties.

For a standard plane geometry, the direction of neutron travel is specified in terms of direction cosines only, and these do not change as the neutron travels along the straight line. Consequently, no angular derivatives appear in the streaming operator $\vec{\Omega}\cdot\nabla$.

The discrete ordinate solution to Eq. (28) is achieved by determining the S_N set on an interval $\mu \in [-1,1]$. The quadrature points and associated quadrature weights are ordered as in Fig. 7a.

The quadrature weights w are normalized so that $\sum_{m=1}^{N} w_m = 1$ (analogous to the scale factor 1/2 in Eq. (6)). The (angular) cell-centered angular flux (Eq. (36)) is assumed to be given by

$$\psi_m(x) = \psi(x,\mu_m) \tag{45}$$

The angles are chosen so that the ordinates may be used directly to evaluate accurately the flux moments by a quadrature formula:

$$\Phi_l(x) = \sum_{m=1}^{N} w_m P_l(\mu_m)\psi_m(x) \tag{46}$$

If the appropriate form of the streaming term $\vec{\Omega}\cdot\nabla\psi$ is taken from Table I, then the discrete ordinate approximation to Eq. (28) (i.e. Eq. (37)) reduces to

$$\mu_m \frac{\partial\psi_m(x)}{\partial x} + \Sigma_t(x)\psi_m(x) = q_m(x) \tag{47}$$

with the scattering source obtained by applying the compatible quadrature approximations to the integral term:

(a) in the Legendre polynomial representation

$$q^g_{s,m}(x) = \sum_{l=0}^{L}(2l+1)\sum_{g'=1}^{G}\Sigma^l_{s,g'\to g}(x)P_l(\mu_m)\Phi_{g',l}(x) \qquad (48a)$$

(b) in the rigorous I*-representation

$$q^g_{s,m}(x) = \sum_{g'=1}^{G}\sum_{m'=1}^{N}\Big(\sum_{m^*=m_1^*}^{m_2^*}\Sigma_{s,g'\to g}(x,m^*)I^*(m,m',m^*)w_{m^*}\Big)\psi_{g',m'}(x)w_{m'} \qquad (48b)$$

In cylindrical and spherical geometries special care must be taken to ensure neutron conservation when constructing a discrete ordinate approximation to the transport equation. In these geometries, the direction vector $\vec{\Omega}$ is described in a local system of coordinates that depend on a spatial position. Since the direction variables continuously change for a streaming neutron, extra terms involving derivatives with respect to the angular variable appear in the streaming operator $\vec{\Omega}\cdot\nabla$, hence, the straightforward discretization may result in a nonconservative scheme. To avoid this, the numerical approximation must be applied to the proper (i.e. conservative) form of the transport equation. To derive this conservative form, the streaming operator $\vec{\Omega}\cdot\nabla$ must be expressed in terms of the local system of ordinates. The explicit conservative form of the curve-linear streaming term in one-dimensional cylindrical and spherical geometries is depicted in Table I. From the appropriate form of $\vec{\Omega}\cdot\nabla$ (Table I), the multigroup transport equation in 1-d cylindrical geometry becomes:

$$\mu\frac{\partial(r\psi_g)}{\partial r} - \frac{\partial(\eta\psi_g)}{\partial\phi} + r\Sigma_{t,g}(r)\psi_g(r,\vec{\Omega}) = rq_g(r,\vec{\Omega}) \qquad (49)$$

Cylindrical geometry is complicated by the fact that even in one spatial dimension two angular coordinates are needed.

To discretize the direction variable $\vec{\Omega}$, Gaussian quadratures are applied which provide a very desirable quadrature set for wide classes of problems.

The angular domain of a quadrant of a unit sphere is discretized into a set of N quadrature points (μ_m,η_m) and associated quadrature weights normalized

by $\sum_{m=1}^{N} w_m = 1$. The arrangement of these quadrature points is illustrated in Fig.7b for the S_6 quadrature.

The angular cell-centered (in angle) flux is assumed to be given by

$$\psi_m(r) = \psi(r,\mu_m,\eta_m) \tag{50}$$

and the angular flux moments (see Eq. (16)) are approximated now by

$$\Phi_l^n(r) = \sum_{m=1}^{N} w_m R_l^n(\xi_m,\phi_m)\psi_m(\xi_m,\phi_m) \tag{51}$$

where both ξ_m and ϕ_m may be determined from

$$\mu_m = (1-\xi_m^2)^{1/2}\cos\phi_m \quad \text{and} \quad \eta_m = (1-\xi_m^2)^{1/2}\sin\phi_m$$

Denoting $\psi_{m-1/2}(r)$ and $\psi_{m+1/2}(r)$ the angular cell edge fluxes on the same ξ-level we can write the discrete ordinate approximation (Eq. (37)) as

$$\mu_m \frac{\partial(r\psi_m(r))}{\partial r} + \frac{\alpha_{m+1/2}}{w_m}\psi_{m+1/2}(r) - \frac{\alpha_{m-1/2}}{w_m}\psi_{m-1/2}(r) +$$

$$+ r\Sigma_t(r)\psi_m(r) = rq_m(r) \tag{52}$$

where

$\alpha_{m+1/2}$, $\alpha_{m-1/2}$ are the angular differencing coefficients introduced to take account of the angular redistribution effect.

It can be shown /12/ that these coefficients must satisfy

$$\alpha_{m+1/2} = \alpha_{m-1/2} - \mu_m w_m \qquad m=1,N \tag{53}$$

with the requirement from neutron conservation that the first $\alpha_{1/2}$ coefficient and the last $\alpha_{N+1/2}$ coefficient must vanish.

Thus equation (53) is just a recursive relationship which uniquely determines all the $\alpha_{m+1/2}$ in terms of the selected quadrature set.

The scattering term is represented by means of:

(a) truncated series of Legendre polynomials as

$$q^g_{s,m}(r) = q^g_s(r,\xi_m,\phi_m) = \sum_{l=0}^{L}(2l+1)\sum_{g'=1}^{G}\Sigma^l_{s,g'\to g}(r)\sum_{n=0}^{l}R^n_l(\xi_m,\phi_m)\Phi^n_{g',l}(r) \tag{54a}$$

(b) the I*-function as

$$q^g_{s,m}(r) = q^g_s\ (r,\xi_m,\phi_m) = \tag{54b}$$

$$\sum_{g'=1}^{G}\sum_{m'=1}^{N'}\left[\sum_{m^*=m_1^*}^{m_2^*}\Sigma_{s,g'\to g}(r,m^*)I^*(m,m',m^*)\psi_{g'}(r,\xi'_{m'},\phi'(m,m',m^*))w_{m^*}\right]w_{m'}$$

To develop the discrete ordinates equations in spherical geometry we proceed in an analogous manner to that used for plane geometry. Equation (37) is evaluated for the same S_N set as in the plane geometry case. With the explicit form of the streaming operator taken from Table 1 we get

$$\mu_m\frac{\partial(r^2\psi_m(r))}{\partial r} + \left[\frac{\beta_{m+1/2}}{w_m}\psi_{m+1/2}(r) - \frac{\beta_{m-1/2}}{w_m}\psi_{m-1/2}(r)\right]r +$$

$$+ r^2\Sigma_t(r)\psi_m(r) = r^2q_m(r) \tag{55}$$

The angular differencing coefficients β obey the recursion relation

$$\beta_{m+1/2} = \beta_{m-1/2} - 2w_m\mu_m \qquad m=1,N$$

$$\beta_{1/2} = \beta_{N+1/2} = 0 \tag{56}$$

The scattering source has the same form as that of Eqs. (48a), (48b) if we replace the spatial variable x by r.

To solve the discrete ordinates transport equations, Eqs. (52) and (55) in curved geometries for three unknown functions the cell-centered angular flux $\psi_m(r)$ and mesh cell edge fluxes $\psi_{m+1/2}(r)$ and $\psi_{m-1/2}(r)$ it is necessary to add auxiliary relationships.

Since, in general we have 2N+1 functions, but only N equations, the diamond difference assumption (in angle) is made

$$\psi_m(r) = \frac{1}{2}\left[\psi_{m-1/2}(r) + \psi_{m+1/2}(r)\right] \qquad (57)$$

to relate the edge and cell-centered fluxes. The $\psi_{m-1/2}(r)$ edge flux is assumed to be known from the previous angular mesh cell computation and imposing continuity on the angular mesh cell boundaries. Eq. (57) solved for $\psi_{m+1/2}$ derives N additional relationships.
Thus in each angular mesh cell the number of unknown functions in Eqs. (52) and (55) has been reduced to one, i.e. $\psi_m(r)$.

Moreover, additional supplementary equations are needed for boundary conditions of the angular dependence of the angular flux, i.e. $\psi_{1/2}(r)$. These equations are constructed by considering the special directions along which the local neutron direction coordinates do not change with streaming.
For spherical geometry, this special direction is the radially inward direction $\mu = -1$ (see Fig.7a). For cylindrical geometry, these special directions correspond to coordinates directed towards the cylindrical axis, $\mu = 0$, $\phi = 180^o$ as illustrated in Fig. 7b.

4.2.2 Discretization of the Spatial Variable

A spatial discretization scheme for the multigroup discrete-ordinates transport equation included in ONETRAN /13/ and ANTRA1 (the 1-d transport module of GANTRAS code) is based on linear discontinuous (LD) finite element scheme.

To discretize the spatial variable the spatial grid with IT mesh points is introduced. The cross-sections are taken piecewise constant and may change

their values only at half mesh points $r_{i\pm1/2}$.

In the LD method the flux is assumed to be approximated by a piecewise linear function with discontinuities at the spatial mesh cell edges, as indicated in Fig. 8. The flux on the mesh cell boundary is assumed to be the limit of the angular flux as the boundary is approached from the direction in which neutrons are streaming. In the spatial mesh i the flux is depicted by:

$$\psi(r) = \frac{1}{\Delta r_i}\left[(r_{i+1/2} - r)\psi_{i-1/2} + (r - r_{i-1/2})\psi_{i+1/2}\right] \qquad (58)$$

where $\Delta r_i = r_{i+1/2} - r_{i-1/2}$ and $\psi_{i-1/2}$ and $\psi_{i+1/2}$ are the unknown discrete ordinates fluxes on the left and right boundaries respectively.

The computed source (which uses ψ values from the previous iteration), is taken also to be piecewise linear

$$q(r) = \frac{1}{\Delta r_i}\left[(r_{i+1/2}-r)q_{i-1/2} + (r - r_{i-1/2})q_{i+1/2}\right] \qquad (59)$$

For the angular mesh cell, a continuity is imposed on the mesh cell edges and the diamond difference relation is assumed:

$$\psi_{m+1/2} = 2\left[\frac{1}{2}(\psi_{i+1/2} - \psi_{i-1/2})\right] - \psi_{m-1/2} \qquad (60)$$

The arrangement of the angular flux node points in a single mesh cell i is illustrated in Fig. 9.

With the above assumptions inserted therein, the discrete ordinates equations Eqs. (47), (52) and (55) in the (i,m)th mesh cell becomes respectively /13/:

in plane geometry

$$\frac{\mu_m}{\Delta x_i}\frac{d}{dr}\left[(x_{i+1/2} - x)\psi_{i-1/2} + (x - x_{i-1/2})\psi_{i+1/2}\right]$$
$$+ \frac{\sigma}{\Delta x_i}\left[(x_{i+1/2} - x)\psi_{i-1/2} + (x - x_{i-1/2})\psi_{i+1/2}\right]$$
$$\simeq \frac{1}{\Delta x_i}\left[(x_{i+1/2} - x)q_{i-1/2} + (x - x_{i-1/2})q_{i+1/2}\right] \qquad (61a)$$

in cylindrical geometry

$$\frac{\mu_m}{\Delta r_i}\frac{d}{dr}\left[r(r_{i+1/2}-r)\psi_{i-1/2}+r(r-r_{i-1/2})\psi_{i+1/2}\right]$$

$$+\frac{\alpha_{m+1/2}}{w_m}\left[\psi_{i+1/2}+\psi_{i-1/2}-\psi_{m-1/2}\right]-\frac{\alpha_{m-1/2}}{w_m}\psi_{m-1/2}$$

$$+\frac{\sigma}{\Delta r_i}\left[r(r_{i+1/2}-r)\psi_{i-1/2}+r(r-r_{i-1/2})\psi_{i+1/2}\right]$$

$$\simeq\frac{1}{\Delta r_i}\left[r(r_{i+1/2}-r)q_{i-1/2}+r(r-r_{i-1/2})q_{i+1/2}\right] \qquad (61b)$$

and in spherical geometry

$$\frac{\mu_m}{\Delta r_i}\frac{d}{dr}\left[r^2(r_{i+1/2}-r)\psi_{i-1/2}+r^2(r-r_{i-1/2})\psi_{i+1/2}\right]$$

$$+\frac{\alpha_{m+1/2}}{w_m}\left[\psi_{i+1/2}+\psi_{i-1/2}-\psi_{m-1/2}\right]2r-\frac{\alpha_{m-1/2}}{w_m}\psi_{m-1/2}\,2r$$

$$+\frac{\sigma}{\Delta r_i}\left[r^2(r_{i+1/2}-r)\psi_{i-1/2}+r^2(r-r_{i-1/2})\psi_{i+1/2}\right]$$

$$\simeq\frac{1}{\Delta r_i}\left[r^2(r_{i+1/2}-r)q_{i-1/2}+r^2(r-r_{i-1/2})q_{i+1/2}\right], \qquad (61c)$$

$$\text{for}\quad r\varepsilon(r_{i-1/2},\, r_{i+1/2})\ .$$

In the spherical geometry (Eq. (61c)), the relation

$$\beta_{m\pm1/2}=2\alpha_{m\pm1/2}$$

has been used. The new curvature coefficients α satisfy the recursion relation of Eq. (53). To determine the two unknown fluxes per cell, $\psi_{i-1/2}$ and $\psi_{i+1/2}$ in Eqs. (61), two equations are required per cell. These are obtained by integrating Eqs. (61) over the mesh cell width (i.e. Δx_i or Δr_i) to remove the spatial derivative, successively using 1 and $(x-x_{i-1/2})$ or $(r-r_{i-1/2})$ as weights for the integration in case of rightward-directed

sweeps ($\mu > 0$), and 1 and ($x_{i+1/2} - x$) or ($r_{i+1/2} - r$) in case of leftward-directed sweeps. The results are:

$$\begin{bmatrix} \Delta A_i \frac{\alpha_{m+1/2}}{w_m} + \sigma V_{i-1/2} & \mu A_{i+1/2} + \Delta A_i \frac{\alpha_{m+1/2}}{w_m} + \sigma V_{i+1/2} \\ \mu z_3 + z_5 \frac{\alpha_{m+1/2}}{w_m} + \sigma z_1 & \mu z_4 + z_5 \frac{\alpha_{m+1/2}}{w_m} + \sigma z_2 \end{bmatrix} \begin{Bmatrix} \psi_{i-1/2} \\ \psi_{i+1/2} \end{Bmatrix}$$

$$= \begin{Bmatrix} q_{i+1/2} V_{i-1/2} + q_{i+1/2} V_{i+1/2} + \Delta A_i \frac{\alpha}{w_m} \psi_{m-1/2} + \mu A_{i-1/2} \psi_b \\ q_{i-1/2} z_1 + q_{i+1/2} z_2 + z_3 \frac{\alpha}{w_m} \psi_{m-1/2} \end{Bmatrix}, \quad \mu > 0, \tag{62a}$$

and

$$\begin{bmatrix} -\mu A_{i-1/2} + \Delta A_i \frac{\alpha_{m+1/2}}{w_m} + \sigma V_{i-1/2} & \Delta A_i \frac{\alpha_{m+1/2}}{w_m} + \sigma V_{i+1/2} \\ \mu z_8 + z_{10} \frac{\alpha_{m+1/2}}{w_m} + \sigma z_6 & \mu z_9 + z_{10} \frac{\alpha_{m+1/2}}{w_m} + \sigma z_7 \end{bmatrix} \begin{Bmatrix} \psi_{i-1/2} \\ \psi_{i+1/2} \end{Bmatrix}$$

$$= \begin{Bmatrix} q_{i-1/2} V_{i-1/2} + q_{i+1/2} V_{i+1/2} + \Delta A_i \frac{\alpha}{w_m} \psi_{m-1/2} - \mu A_{i+1/2} \psi_b \\ q_{i-1/2} z_6 + q_{i+1/2} z_7 + z_{10} \frac{\alpha}{w_m} \psi_{m-1/2} \end{Bmatrix}, \quad \mu < 0. \tag{62b}$$

Here $\alpha = \alpha_{m-1/2} + \alpha_{m+1/2}$

ψ_b is the angular flux on the boundary of the previous mesh cell as indicated in Fig. 9 and the remaining symbols are defined in Table II.

Supplementary equations in spherical and cylindrical geometry are derived considering special directions - m along which there is no angular redistribution, i.e.

$$\psi_{m+1/2} = \psi_{m-1/2} = \frac{1}{2} (\psi_{i+1/2} - \psi_{i-1/2}) \tag{63}$$

Since $\alpha_{m-1/2} = 0$, then $\frac{\alpha_{m+1/2}}{w_m} = -\mu_m$ and

$$\frac{\alpha_{m+1/2}}{w_m} \psi_{m+1/2} = -\frac{1}{2} \mu_m(\psi_{i-1/2} + \psi_{i+1/2}) \tag{64}$$

Equation (64) replaces the curvature terms in Eqs. (61b) and (61c). Integrating over the mesh cell width with the weighting functions 1 and $(r_{i+1/2} - r)$ the following system of equations for the mesh cell edge fluxes is obtained

$$\begin{bmatrix} -\frac{1}{2}\mu(A_{i-1/2} + A_{i+1/2}) + \sigma V_{i-1/2} & -\frac{1}{2}\mu\,\Delta A_i + \sigma V_{i+1/2} \\ \mu(z_8 - \frac{1}{2} z_{10}) + \sigma z_6 & \mu(z_9 - \frac{1}{2} z_{10}) + \sigma z_7 \end{bmatrix} \begin{Bmatrix} \psi_{i+1/2} \\ \psi_{i+1/2} \end{Bmatrix}$$

$$= \begin{Bmatrix} q_{i-1/2} V_{i-1/2} + q_{i+1/2} V_{i+1/2} - \mu A_{i+1/2} \psi_b \\ q_{i+1/2} z_6 + q_{i+1/2} z_7 \end{Bmatrix} \tag{65}$$

The basic algebraic equation actually solved by ANTRA1 is one of Eqs. (61) according to the specified geometry.

The main steps of the algorithm used to implement Eqs. (61) are described in detail in Ref. (13). The boundary conditions, sweep of the space-angle mesh, negative flux fix up, iterative technique, acceleration schemes and convergence test remain unaltered in the ANTRA1 code.

TABLE I

Conservation Forms of the Streaming Operator $\vec{\Omega}\cdot\nabla\psi$ in One-Dimensional Geometries

Geometry	Dependence of ψ	Definition of Variables	$\vec{\Omega}\cdot\nabla\psi$
Plane	$\psi(x,\mu)$	$\mu = \hat{e}_x\cdot\vec{\Omega}$	$\mu\,\frac{\partial\psi}{\partial x}$
Cylindrical	$\psi(r,\mu,\eta)$	$\mu = \hat{e}_r\cdot\vec{\Omega}$ $\xi = \hat{e}_z\cdot\vec{\Omega}$ $\eta = (1-\xi^2)^{1/2}\sin\phi$ $\mu = (1-\xi^2)^{1/2}\cos\phi$	$\frac{\mu}{r}\frac{\partial r\psi}{\partial r} - \frac{1}{r}\frac{\partial\eta\psi}{\partial\phi}$
Spherical	$\psi(r,\mu)$	$\mu = \hat{e}_r\cdot\vec{\Omega}$	$\frac{\mu}{r^2}\frac{\partial(r^2\psi)}{\partial r} + \frac{1}{r}\frac{\partial\left[(1-\mu^2)\psi\right]}{\partial\mu}$

TABLE II

TABLE OF GEOMETRIC FUNCTIONS

Notation: $r_+ = r_{i+1/2}$, $r_- = r_{i-1/2}$

The i subscript is omitted from all quantities

Quantity	Plane*) Geometry	Cylindrical Geometry	Spherical Geometry
Δr	$r_+ - r_-$	$r_+ - r_-$	$r_+ - r_-$
A_-	1	$2\pi r_-$	$4\pi r_-^2$
A_+	2	$2\pi r_+$	$4\pi r_+^2$
ΔA	0	$A_+ - A_-$	$A_+ - A_-$
V_-	$\frac{1}{2}\Delta r$	$\frac{\pi}{3}\Delta r(r_+ + 2r_-)$	$\frac{\pi}{3}\Delta r(r_+^2 + 2r_+r_- + 3r_-^2)$
V_+	$\frac{1}{2}\Delta r$	$\frac{\pi}{3}\Delta r(2r_+ + r_-)$	$\frac{\pi}{3}\Delta r(3r_+^2 + 2r_+r_- + r_-^2)$
z_1	$10\Delta r$	$5(r_+ + r_-)\Delta r$	$(3r_+^2 + 4r_+r_- + 3r_-^2)\Delta r$
z_2	$20\Delta r$	$5(3r_+ + r_-)\Delta r$	$(12r_+^2 + 6r_+r_- + 2r_-^2)\Delta r$
z_3	-30	$-10(r_+ + 2r_-)$	$-5(r_+^2 + 2r_+r_- + 3r_-^2)$
z_4	+30	$10(4r_+ - r_-)$	$5(9r_+^2 - 2r_+r_- - r_-^2)$
z_5	0	$30\Delta r$	$20(2r_+ + r_-)\Delta r$
z_6	$20\Delta r$	$5(r_+ + 3r_-)\Delta r$	$(2r_+^2 + 6r_+r_- + 12r_-^2)\Delta r$
z_7	$10\Delta r$	$5(r_+ + r_-)\Delta r$	$(3r_+^2 + 4r_+r_- + 3r_-^2)\Delta r$
z_8	-30	$10(r_+ - 4r_-)$	$5(r_+^2 + 2r_+r_- - 9r_-^2)$
z_9	+30	$10(2r_+ + r_-)$	$5(3r_+^2 + 2r_+r_- + r_-^2)$
z_{10}	0	$30\Delta r$	$20(r_+ + 2r_-)\Delta r$

*) variable x was replaced by r to simplify a notation

III. GANTRAS Programme Structure

On the basis of the mathematical methods and approximations introduced in the previous section, a general transport code system GANTRAS was developed, which treats the anisotropy of neutron scattering in a rigorous way.

1. Overall Programme Flow

GANTRAS consists of a set of modules that solve different numerical tasks. In the first step, the processing codes SDXDDX and GROUPIE are used to produce microscopic group-averaged and angle-segmented (3-dimensional) transfer matrices for given nuclides, starting from ENDF/B or EFF evaluated data files.

Then the nuclide-dependent transfer matrices are mixed by the CROMIX code to form the macroscopic transfer matrices for each mixture needed in the transport calculation.

Additionally, the transfer probability function I* is discretized by the ATP code and tabulated in a form suitable to be used directly in the evaluation of group scattering source in the transport module ANTRA1.

The resulting interface files, the transfer and the storage of data are managed by the KAPROS-System /14/. The files are stored as KAPROS Data Blocks. They create a supplementary set of input data needed to perform transport calculations with the ANTRA1 code.

The internal organisation of the GANTRAS and the transfer of data within the system is shown in Fig. 10.

2. Role and Function of the Programme Modules

It has been already stated that most of the data required by ANTRA1 is transfered to the code from the data files, created by the associated codes CROMIX and ATP.

2.1 The CROMIX Code. Files Assignment and Internal Arrangement

The main function of CROMIX is to perform mixing operations on microscopic nuclide-dependent 3-dimensional transfer matrices to form macroscopic transfer matrices for mixtures. The flow diagram of CROMIX is illustrated in Fig. 11. The CROMIX program accepts data from a binary ISODDX file. An interface input of cross-sections from ISODDX is managed by the DDXPRE subroutine.

The ISODDX is a nuclide (isotope)-ordered, multigroup library of angle-segmented data. Each nuclide (isotope) is identified by a name of eight (two times REAL*4) alphanumeric characters written as a separate record. A full set of data for a single nuclide consists of IGM records, each for one sink-energy group g. A record for a particular sink-group g of length IHM*MMST constitutes a block of energy- and angle-dependent cross-sections, of IHM rows and MMST columns (MMST denotes the number of angle segments). The row position of the transfer cross-section is specified relative to the total cross-section σ_t (row IHT) and the within group scattering cross-section $\sigma_{g\to g}$ (row IHS). This arrangement is based on the data arrangement prescribed in ONETRAN suitably extended to include angular segments.

The representation of the cross-section block, presented in Table III is assumed.

TABLE III. Cross-Section Type. Sink-Group g.

Row \ Column	1	2	. . .	MMST
.				
.				
.				
IHT-2	σ_a	0	. . .	0
IHT-1	$\nu\sigma_f$	0	. . .	0
IHT	σ_t	0	. . .	0
IHT+1	$\sigma^s_{g+N\to g,1}$	$\sigma^s_{g+N\to g,2}$	. . .	$\sigma^s_{g+N\to g,MMST}$
.	.	.		.
.	.	.		.
IHM .	.	.		.
IHS-2	$\sigma^s_{g+2\to g,1}$	$\sigma^s_{g+2\to g,2}$	. . .	$\sigma^s_{g+2\to g,MMST}$
IHS-1	$\sigma^s_{g+1\to g,1}$	$\sigma^s_{g+1\to g,2}$	. . .	$\sigma^s_{g+1\to g,MMST}$
IHS	$\sigma^s_{g\to g,1}$	$\sigma^s_{g\to g,2}$	. . .	$\sigma^s_{g\to g,MMST}$
IHS+1	$\sigma^s_{g-1\to g,1}$	$\sigma^s_{g-1\to g,2}$	. . .	$\sigma^s_{g-1\to g,MMST}$
IHS+2	$\sigma^s_{g-2\to g,1}$	$\sigma^s_{g-2\to g,2}$	. . .	$\sigma^s_{g-2\to g,MMST}$
.	.	.	.	.
.	.	.	.	.
.	.	.	.	.
IHS+M	$\sigma^s_{g-M\to g,1}$	$\sigma^s_{g-M\to g,2}$	. . .	$\sigma^s_{g-M\to g,MMST}$

In this format, as usual group g+1 corresponds to a lower energy than group g. The symbol $\sigma^s_{g'\to g,m}$ (g'=g-M,...,g+N,m=1,MMST) denotes the transfer cross-section from group g' to group g through the m-th segment of the laboratory scattering angle. The format allows N groups for upscattering and M-groups for downscattering. All the cross-section blocks must have the same values for IHM, IHS, IHT and MMST. The fission cross-section, σ_f, times the mean number of neutrons per fission, ν, must be located in row IHT-1 column 1, and the absorption cross-section, σ_a, must be entered in row IHT-2, column 1.

As in ONETRAN, the user is free to enter cross-sections at the top of the format, in column 1. These extra cross-sections are used for reaction-rate computations in the flux edits. The block of cross-sections represented in a matrix form in Table III is stored in ISODDX as a sequence of IHM vectors of MMST elements (i.e. rowwise).

The CROMIX code must be provided with the number of mixtures and for a particular mixture: the number of nuclides composing it, nuclide identifiers (in the ISODDX library) and nuclide densities.

The last two input data are stored in the REAL*4 vector MIXCOM and the REAL*4 array MIXDEN, respectively. They are used in the subroutine MIXDDX performing mixing-operations to manipulate cross-section blocks.

MIXCOM length is twice as long as the number of different nuclides specified for all mixtures, MIXDEN depends on the mixture number and the nuclide number, and contains the particle density of a nuclide for every mixture containing this nuclide.

CROMIX is supplied with cross-section data from the ISODDX library. The ISODDX is searched sequentially and is rewound to the beginning after each successful "read in" of a full data set for a particular nuclide.

Microscopic cross-sections read from ISODDX are transferred to the named (direct access) data block 'MIXDDX_INPUT____' for further use by the MIXDDX subroutine. The alphanumeric nuclide identifiers are not written on this working file. The operational scheme of the mixing program MIXDDX is shown in Fig. 12.

Finally, the CROMIX yields the macroscopic transfer matrices prepared for the use by the transport module. These data are stored on the named (direct-access) KAPROS file 'GANTRAS_DDX_____'.

'GANTRAS_DDX_____' is a sink-group-ordered file. It consists of IGM records, each for one sink-group g data. Each record has a length MTDDX×IHM×MMST (MTDDX denotes the number of mixtures) and contains the block of macroscopic cross-sections for absorption, fission, total, within group scattering and down-scattering from successive groups of energy higher than that con-

sidered in the record (see Table III). This block is repeated for each material (i.e. mixture). Mixtures are identified by numbers, describing their position in a library. The structure of the data file 'GANTRAS_DDX____' is depicted in Table IV.

TABLE IV. The Internal Arrangement of the 'GANTRAS_DDX____' Data Block.

Record No	Content
1	MTDDX - number of mixtures
2	Sink-energy group g=1: macroscopic transfer cross-sections for mixture 1 (in a form presented in Table III) . . . macroscopic transfer cross-sections for mixture MTDDX (in a form presented in Table III)
3	Sink-energy group g=2: macroscopic transfer cross-sections for mixture 1 (in a form presented in Table III) . . . macroscopic transfer cross-sections for mixture MTDDX (in a form presented in Table III)
. . .	. . .
IGM+1	Sink-energy group IGM: macroscopic transfer cross-sections for mixture 1 (in a form presented in Table III) . . . macroscopic transfer cross-sections for mixture MTDDX (in a form presented in Table III)

TABLE V. CROMIX. Files Assignment.

Unit No	Name of the Variable	Comments
4	ISODDX	nuclide-ordered microscopic multigroup and angle-segmented cross-sections (binary file)
5	INP	input unit
6	IOUT	output unit

KAPROS Data Blocks:

'GANTRAS_DDX_____'

and 'GANTRAS_DATP_____'

are stored permanently in a user-managed KAPROS archive, located on unit 12. Files assignment in CROMIX is shown in Table V.

2.2 The ATP Code. Discretization of the Generalized Transfer Probability Function

The ATP code generates a three-dimensional matrix, containing the generalized angular transfer probabilities. A discretization of the I*-function is done following the averaging formula given by Eq. (40) and associated conditions i.e. Eqs. (41a), (41b), (41c), (41d).

Prior to the discretization of the I*-function over each angular mesh cell $\Delta\mu_m$, $\Delta\mu'_{m'}$, $\Delta\mu^*_{m^*}$, a proper segmentation must be specified for the μ-, μ'-μ^*-range, respectively.

A common μ_m- and μ'_m-set for both $\mu', \mu \in [-1,1]$ is determined by the quadrature set S_N chosen in the transport calculations, whereas the μ^*-range must be segmented in a way identical to that used to process double-differential data.

The integration over $\Delta\mu_m$ and $\Delta\mu'_{m'}$ in Eq. (40) must be performed numerically. For this purpose /2/, each angular mesh cell $\Delta\mu_m$ and $\Delta\mu'_{m'}$ is divided into KMAX intervals, $\Delta\mu_{m,k}$, $\Delta\mu'_{m',k'}$, respectively. With a subinterval mesh sufficiently fine (e.g. a value of 30 assigned to KMAX for S_8 quadrature), the I^*-function on the intervals $\Delta\mu_{m,k}$, $\Delta\mu'_{m',k'}$ can be assumed constant. Hence the integral over $\Delta\mu_{m,k}$ and $\Delta\mu'_{m',k'}$ can be evaluated by multiplying a point value of the integrated function i.e.

$$\left[\arcsin y_{m^*+1/2}(\mu_{m,k},\mu'_{m',k'}) - \arcsin y_{m^*-1/2}(\mu_{m,k},\mu_{m',k'})\right]$$

by the subinterval widths. In this procedure the conditions (41a), (41b), (41c) and (41d) must be taken into account.

Consequently, the integral in Eq. (40) may be approximated by

$$I^*(m,m',m^*) \times \Delta\mu_m \times \Delta\mu'_{m'} \times \Delta\mu^*_{m^*} =$$

$$= \frac{1}{\pi} \sum_{k'} \sum_{k} \left[\arcsin y_{m^*+1/2}(\mu_{m,k},\mu'_{m',k'}) - \arcsin y_{m^*-1/2}(\mu_{m,k},\mu_{m',k'})\right] \times$$

$$\times w_{m,k} \times w_{m',k'} \qquad (66)$$

where

$$y_{m^*\pm1/2}(\mu_{m,k},\mu'_{m',k'}) = \frac{\mu^*_{m^*\pm1/2} - \mu_{m,k}\cdot\mu_{m',k'}}{\sqrt{1-\mu^2_{m,k}}\ \sqrt{1-\mu'^2_{m',k'}}} \quad \text{for } \beta^*_1 \le \mu^*_{m\pm1/2} \le \beta^*_2 \qquad (67a)$$

$$y_{m^*-1/2}(\mu_{m,k},\mu'_{m',k'}) = -1 \quad \text{for } \mu^*_{m^*-1/2} < \beta^*_1 < \mu^*_{m^*+1/2} < \beta^*_2 \qquad (67b)$$

$$y_{m^*+1/2}(\mu_{m,k},\mu'_{m',k'}) = 1 \quad \text{for } \beta^*_1 < \mu^*_{m-1/2} < \beta^*_2 < \mu^*_{m+1/2} \qquad (67c)$$

$$y_{m^*\pm1/2}(\mu_{m,k},\mu'_{m',k'}) = 0 \quad \text{for } \mu^*_{m+1/2} < \beta^*_1 \text{ or } \beta^*_2 < \mu^*_{m-1/2} \qquad (67d)$$

$$\left.\begin{aligned} \beta^*_1 = \beta^*_1(\mu_{m,k},\mu'_{m',k'}) &= \mu_{m,k}\mu_{m',k'} - \sqrt{1-\mu^2_{m,k}}\ \sqrt{1-\mu'^2_{m',k'}} \\ \beta^*_2 = \beta^*_2(\mu_{m,k},\mu'_{m',k'}) &= \mu_{m,k}\mu_{m',k'} + \sqrt{1-\mu^2_{m,k}}\ \sqrt{1-\mu'^2_{m',k'}} \end{aligned}\right\} \qquad (68)$$

and

$$\left.\begin{aligned} 2w_{m,k} &= \Delta\mu_{m,k} \\ 2w_{m',k'} &= \Delta\mu'_{m',k'} \end{aligned}\right\} \qquad (69)$$

A discretized form of the I*-function for two representative cases of the S_8 and S_{20} quadratures is shown in Fig. 13 and Fig. 14, respectively.

Alternatively, equation (39) was evaluated with the aid of the QB01AD subroutine from the Harwell Subroutine Library /15/ in order to perform the three-dimensional integration.

The QB01AD routine allows the user to choose either Chebyshev fitting or Simpson's rule or Gauss integration for each dimension of the integral. An agreement was achieved between the results obtained by applying QB01AD and that from the ATP code.

The matrix I*(m,m',m*) was normalized, according to Eq. (42):

$$\sum_{m^*=m_1^*}^{m_2^*} I^*(m,m',m^*)w_{m^*} = 1 \qquad (70)$$

Here w_{m^*} denote the quadrature weights associated to the $\mu^*_{m^*}$-set. The quantities m_1^*, m_2^*, corresponding to β_1^*, β_2^*, are calculated for each pair of segments $\Delta\mu_m$, $\Delta\mu'_{m'}$. They specify the number of nonzero elements of the I*-matrix (i.e. that part $\left[\left[I^*(m^*,m',m);\ m^*=m_1,m_2\right]m',m=1,N\right]$ which is different from zero).

The matrices MS1(N,N), MS2(N,N) are stored on a named direct-access KAPROS data block 'GANTRAS_DATP____' together with a vector W(MMST), which contains the weights w_{m^*}.

The angular transfer probability table I*(m*,m',m) is also transferred to 'GANTRAS_DATP____' and located after MS1, MS2 and W. A flow chart for ATP and the accompanying subroutine INIATP is shown in Fig. 15.

The discretized angular transfer probabilities from Fig. 13 and Fig. 14 are plotted, after renormalization in Figs. 16 and 17, respectively.

In the present version of the module preparing the interface file 'GANTRAS_DATP____' the discretization of the phase shift in azimuthal angle $\Delta\phi$ (Eq. (20c)) is not included, since these data are not required as an input data to the transport code, operating in one-dimensional spherical or plane geometry.

In both modules: CROMIX and ATP all data fields are dynamically dimensioned through the KAPROS subroutines KSPUTP/KSGETP /14/.

2.3 The Transport Code ANTRA1

The transport module ANTRA1 - ANisotropic TRAnsport in 1-dimension, based on the ONETRAN program /13/, solves (in the present version) the one-dimensional multigroup transport equation in plane and spherical geometries.

ANTRA1, similar to ONETRAN, treats regular, inhomogeneous and homogeneous (k_{eff} and eigenvalue searches) problems subject to vacuum, reflective, periodic, white, albedo or inhomogeneous flux boundary conditions.

The angle-dependent generalized anisotropic inhomogeneous sources are permitted. A rigorous representation of anisotropic neutron scattering is implemented. This has been achieved by employing the I*-method in the formulation of the group scattering term. This procedure uses multigroup, angle-segmented (i.e. three-dimensional) scattering matrices and a generalized angular transfer probabilities.

Moreover, ANTRA1 has a further option, which allows the user to choose between the I*-method only or the combined I*/P_1-method, where either I* or Legendre expansion is used in subsequent coarse mesh intervals, depending on the cross-section type available.

The new nonexpanded form of the scattering kernel was incorporated into a standard S_N code framework, what necessitated many modifications in the ONETRAN subroutines.

The discrete ordinates (S_N) approximation for the angular variable the diamond (central) difference approximation for the angular extrapolation (in spherical geometry) is used.

A new numerical scheme to evaluate the integral in the direction variable involved in the scattering term (expressed in terms of the I*-function) was implemented. A linear discontinuous finite element representation for the angular flux in each spatial mesh is applied.

The methods of solution enumerated above were described in detail in the previous sections.

Negative fluxes due to interpolations in space and angle are eliminated by a local "set-to-zero and correct" algorithm. Standard inner (within group) iteration cycles are accelerated by system rebalance, coarse mesh rebalance or Chebyshev acceleration. Outer iteration cycles are accelerated by coarse mesh rebalance.

A schematic flow chart of ANTRA1 is shown in Fig. 17. All main sub-routines are ONETRAN subroutines, these whose names are underlined were updated for the new purpose.

2.3.1 Relation of Newly Introduced Programme Variables and Programme Mnemonics

A list of the relations between problem variable symbols introduced in the presentation of the theoretical basis of GANTRAS and program variable names is given in Table VI.

The notation previously applied in ONETRAN was fully preserved here. To all variables commonly used by ONETRAN and ANTRA1 the same names are assigned. For this reason the variable N (defined as S_N order) is denoted in Table VI by MM, since in 1-dimensional plane and spherical geometries we are dealing with, both N and MM have the same value and meaning.

TABLE VI. Relation of New Problem Variables to Program Mnemonics

Program Mnemonics	Subroutine	Problem Variable	Refer to
MS1(MM,MM)	SOURCE	m_1^*	Eq. (70)
	INNER		
MS2(MM,MM)	GREBAL	m_2^*	
DATP(MMST,MM,MM)	SOURCE,INNER GREBAL	$I^*(m,m',m^*)$	Eq. (39)
W1(MMST)	SOURCE,INNER GREBAL	w_{m^*}	Eqs. (48b) and (54b)
DDX(MMST,IHM,MTDDX)	INITAL,INITF SOURCE,GREBAL	$\Sigma_a, \nu\Sigma_f, \Sigma_t,$ $\Sigma_{s,g'\to g}(r,m^*)$	Eqs. (48b), (54b)
DDXS(MMST,IT)	INITAL,INNER	$\Sigma_{s,g\to g}(r,m^*)$	Eqs. (48b), (54b)
CXT(IT)	INITAL,INITF,SOURCE	$\Sigma_{t,g}$	ONETRAN Manual /13/
CXA(IT)	INITAL,SUMS	$\Sigma_{a,g}$	
CXS(IT)	INITAL,INNER,SUMS	$\Sigma_{s,g}$	
AFLUX(MM,2,IT)	INITF,SOURCE REEDF,RITEF INNER,GREBAL	angular neutron flux $\psi_{i-1/2}, \psi_{i+1/2}$	Eqs. (62a), (62b)
AQ(MM,2,IT)	SOURCE,INNER,READQ	angular-dependent source $q_{i\pm1/2}$	Eq. (62a), (62b)
IDDX(IM)	INITAL,INITF,SOURCE INNER,GREBAL,EDIT	angular dependent cross-section identification number for each coarse-mesh interval	input data description

2.3.2 Description of ANTRA1 Subroutines. Specification of Introduced Modifications

SUBROUTINE MAIN

The control subroutine, MAIN initializes program parameters and calls successive routines, which read input, perform initialization, computation and finally print output.

The new named common block /DDXUNI/ was introduced in MAIN. It contains the symbolic names of input data files, additionally required by ANTRA1 (see TABLE VII).

TABLE VII. Contents of the Common Block /DDXUNI/

Unit No	Name of the Variable	KAPROS Data Block Name	Contents
36	NDDX	'GANTRAS_DDX_____'	Angle-segmented transfer matrices
37	NIDDX	'ANTRA1_____IDDX'	New material identification numbers for each coarse mesh interval
38	NDATP	'GANTRAS_DATP____'	Generalized angular transfer probabilities

The data files 36, 37 and 38 are handled as KAPROS data blocks. Two of them 'GANTRAS_DDX_____' and 'GANTRAS_DATP____' are permanently stored in a user initialized and managed archive, the third one 'ANTRA1_____IDDX' is defined by KSIOX cards in the KAPROS input. These data blocks are attached to the module ANTRA1 with the aid of READKØ code /18/, which is called as a subroutine by ANTRA1. Table VIII shows an updated input for the READKØ code. Updates refer to the input of READKØ conventionally prepared for ONETRA (a version of ONETRAN implemented in Karlsruhe Center) /19/.

TABLE VIII. Updated Input for READKØ Code

Unit No	Data Block Name	Index	Realization	File Length	Lengths of the Record
23	ANTRA1___EINGABE	1	1	10 000	0
21	ANTRA1 21	1	6	10 000	0
22	ANTRA1 22	1	6	10 000	0
18	ANTRA1 18	1	6	10 000	0
31	ANTRA1 31	1	6	10 000	0
30	ANTRA1 30	1	6	10 000	0
32	ANTRA1 32	1	6	10 000	0
33	ANTRA1 33	1	6	10 000	0
34	ANTRA1 34	1	6	10 000	0
15	ANTRA1 15	1	6	10 000	0
39	ANTRA1 39	1	6	10 000	0
36	GANTRAS_DDX____	1	1	10 000	0
37	ANTRA1_____IDDX	1	1	10 000	0
38	GANTRAS_DATP____	1	1	10 000	0

SUBROUTINE INPUT1

INPUT1 performs input functions. It reads header and control integer parameters, sets up a switch (ISWDDX) over I*-mode and the combined mode (P_1/I*) performs some checking of input data.

SUBROUTINE INPUT2

This subroutine calculates commonly used integers and reads problem-dependent arrays by calling various interface subroutines.

Since the number of actually read data is problem-dependent, it is convenient to store the data in one container-array A, dynamically dimensioned, located in the blank common block.
The length of A is determined internally after the number of cells required for any portion of the data has been computed. The computer core field occupied by A is suitably extended, using the KAPROS-subroutine KSPUTP.

Blocks of different data stored in array A are addressed by pointers. Pointers and problem input parameters are contained in array IA. In ANTRA1 the length of the vector IA has been increased (compared to ONETRAN). The elements from IA(298) to IA(400) are reserved for newly introduced variables. The contents of block IA and the definition of the variables is presented in Table IX. New problem-dependent data locations in the A-array are depicted in Table X.

TABLE IX. Contents of Common Block IA(298) - IA(400)

Position	Name	Pointer for Array or Definition of the Variable	Remarks
298	ISWDDX		Switch over I*-mode or combined mode (P_1/I^*)
299			
300	MMST		μ^*-S_N order
301			
302	MTDDX		Total numbers of materials, described
303			by angle dependent transfer matrices
304			
305			
306			
307			
308			
309			
310			
311			
312			
313			
314			
315	MMSQ	MM*MM	
316			
317	LNGDDX	IHM*MMST*MTDDX	Length of the angle-segmented transfer
318			matrix for fixed group g
319	LMS1	MS1(MM,MM)	Lower limit of segmented μ^*-range
320	LMS2	MS2(MM,MM)	Upper limit of segmented μ^*-range
321	LDATP	DATP(MMST,MM,MM)	Generalized angular transfer probabilities
322	LW1	W1(MMST)	Weights
323			
324	LDDX	DDX(MMST,MM,MM)	Angle-segmented transfer matrix for group g
325	LCXT	CXT(IT)	Total cross-section * density
326	LDDXS	DDXS(MMST,IT)	Self-scattering angular dependent
			cross-section * density
327	LCXA	CXA(IT)	Absorption cross-section * density
328	LCXS	CXS(IT)	Self-scatt.cross-sect.(integrated over angle)
329	LIDDX	IDDX(IM)	New material identification
330			numbers
331			
332			
333	LEAF	AFLUX(MM,2,IT)	Group angular flux
334	LAQ	AQ(MM,2,IT)	Angular-dependent source to a group g
335			
336			
337			
338	LNDATP	MMST*MMSQ	Length of angular transfer probability table
339			
340	LNAFL	MM*2*IT	Length of group angular flux array
341	LNAQ	MM*2*IT	Length of angular source to a group
342			
343			
344			
345			
346			
347			
348			
349			

TABLE X. COMMON-Array A, Problem-Dependent Data Locations

Starting Address	Lengths	Description
	INTRODUCED AFTER S_N-CONSTANTS BLOCK	
LMS1	MMSQ	MS1(MM,MM)
LMS2	MMSQ	MS2(MM,MM)
IDATP	LNDATP	DATP(MMST,MM,MM)
LW1	MMST	W1(MMST)
LDDX	LNGDDX	DDX(MMST,MM,MM)
LDDXS	MM*IT	DDXS(MMST,IT)
LCXS	IT	CXS(IT)
LCXT	IT	CXT(IT)
LCXA	IT	CXA(IT)
LIDDX	IM	IDDX(IM)
LEAF	LNAFL	AFLUX(MM,2,IT)
LAQ	LNAQ	AQ(MM,2,IT)
	INTRODUCED AS A FIRST LCM STORAGE BLOCK	
KSAQ	1*LNAQ	source to group array AQ(MM,2,IT) for repeated use in SUBROUTINE INNER

SUBROUTINE INITAL

INITAL performs mixing of single-differential cross-sections, modifies coarse-mesh boundaries for critical size calculations, calculates geometric functions by call of GEOFUN, initializes inhomogeneous source by call to INITQ and fission arrays by call to INITF, calculates macroscopic cross-section arrays, i.e. CT, CA, CS and/or CXT, CXA, CXS and stores CXT, CXA, CXS on the KAPROS data block 'STOT_SAB_SSSCATT' in a group order.

SUBROUTINE GEOFUN (unchanged)

This subroutine calculates various geometric functions on the coarse and fine mesh.

SUBROUTINE INITQ

Generates volume and surface integrals of inhomogeneous sources for rebalance, normalizes sources, stores boundary sources in boundary flux array.

SUBROUTINE INITF

Computes $\chi\nu\Sigma_f$ array for fission source and transposes for adjoint problems, calculates volume integral for fission source and normalizes fluxes.

SUBROUTINE MONITR (unchanged)

Prints résumé of convergence parameters, monitor line headings, and outer iteration monitor data.

SUBROUTINE OUTER

Performs a single outer iteration, contains the group loop. Transmits data for a particular energy group from KDB 'STOT_SAB_SSSCATT' to CXT,CXA,CXS. Calculates the source to the group by call to SOURCE, performs the inner iterations by call to INNER, stores angular flux in LCM, calculates group sums by call to SUMS.

SUBROUTINE SNCON (unchanged)

SNCON reads or generates S_N quadrature constants, calculates some indexing arrays and spherical harmonic polynomials.

SUBROUTINE IFINSN (unchanged)

Reads S_N constants from interface file ISNCON.

SUBROUTINE CSPREP (unchanged)

This subroutine is called only when ANTRA1 operates in the combined mode. CSPREP reads single differential cross-sections in standard LASL /13/ format, FIDO format, or from interface file by calling IFINXS, prints cross-sections, checks cross-sections and stores cross-sections in the array A.

SUBROUTINE IFINXS (unchanged)

Interface input of cross-sections from standard interface file ISOTXS.

SUBROUTINE READF

The function of subroutine READF is to read initial flux guesses from cards or a standard interface file by calling IFINF.

It initializes the angle-dependent flux and stores this flux in LCM.

SUBROUTINE READQ (unchanged)

Reads distributed and boundary sources from cards or a standard interface file by calling IFINQ.

SUBROUTINE IFINQ (unchanged)

Reads distributed and boundary sources from the standard interface file FIXSRC.

SUBROUTINE SOURCE

Calculates the source to the group from inhomogeneous sources, fissions in all groups and inscattering from other groups. Calculates total source for inner iteration rebalance.

Main modifications implemented in the subroutine SOURCE are shown (in a schematic manner) in Fig. 19.

SUBROUTINE INNER

Performs the inner iterations for a group. Adds the within-group scattering term to the source, performs sweeps over the space-angle mesh, solving the 2×2 system of equations for the edge angular fluxes, calculates rebalance flows and absorptions, performs rebalance or Chebyshev accelerations, and checks convergence of inner iterations.

Updates concern:

1. Computational scheme for the total source, evaluated in each iteration.
2. New representation of total sources.
3. Application of rebalance factors to angular fluxes.

The new branches, added to the existing algorithm in order to calculate within-group scattering sources (represented by a rigorous I*-method) for each inner iteration, are in principle identical to those presented in Fig. 19.

SUBROUTINE SETBC (unchanged)

Sets the angular flux boundary condition on either the left or right boundary. Called by INNER.

SUBROUTINE REBAL (unchanged)

Performs inversion of the tridiagonal matrix for group coarse-mesh rebalance factors. Called by INNER and GREBAL.

SUBROUTINE IFRITE (unchanged)

Writes the interface files SNCONS, FIXSRC, RTFLUX or ATFLUX, and RAFLUX or AAFLUX.

SUBROUTINE TIMEXF (unchanged)

Writes the angular flux file NTIMEX for the initial conditions to TIMEX code. Called by FINAL.

Service Routines

SUBROUTINE DUMPER (unchanged)

Reads or writes restart dump.

SUBROUTINE PRINTP

Prints input control integer and floating point variables.

SUBROUTINE MAPPER

Draws material map of system.

SUBROUTINE LOAD (unchanged)

KAPROS dependent data loader.

SUBROUTINE WRITE (unchanged)

Generalized output routine for printing 1-d, 2-d or 3-d arrays, either integer or floating point.

SUBROUTINE ERROR (unchanged)

Prints error messages and sets fatal error trigger.

SUBROUTINE REED / IBM-360 Version (unchanged)

Handles all binary reading operations (including end-of-file and rewind) and data transfers.

SUBROUTINE RITE / IBM-360 Version (unchanged)

Handles all binary writing operations (including end of file and rewind) and data transfers.

SUBROUTINE SUMS

Accumulates quantities in system balance table for each group. Renormalizes the fission source to the group and calculates λ for k_{eff} calculations.

SUBROUTINE GREBAL

Computes the fission source, normalizes the fission source and flux moments, computes group rebalance factors by call to REBAL and performs outer iteration accelerations. Applies rebalance factors to group angular fluxes.

SUBROUTINE NEWPAR (unchanged)

Computes new parameters for implicit eigenvalue search.

SUBROUTINE SUMMARY (unchanged)

Prints system balance table for each group and final iteration monitor line.

SUBROUTINE FINAL (unchanged)

Controls final edit output. Prints flux moments, angular flux and fission rates by a call of EDIT. Reads zone and point edit input. Allocates temporary storage for edits and performs zone and point edits by call to ZEDIT and PEDIT. Calls the PLOTTR routine, if specified. Writes the interface file output by call to IFRITE.

SUBROUTINE EDIT

Prints the scalar flux and components, the angular flux, and the fission rates.

SUBROUTINE ZEDIT (unchanged)

Calculates zone macroscopic activities, constituent activities, microscopic activities, and power densities.

SUBROUTINE PEDIT (unchanged)

Calculates pointwise microscopic activities.

Newly Developed Service Subroutines

SUBROUTINE RITEF

This subroutine transfers the whole content of group angular flux array AFLUX(MM,2,IT) to the flux storage field, located in the container array A, starting from address KAF.

Since in ONETRAN angular fluxes are stored in MM*IGM blocks, each of length LNAF=2*IT, for each group G LEAF=MM*2*IT elements of AFLUX must be transferred in MM portions of 2*IT elements, by subsequent calls of subroutine RITE.

SUBROUTINE REEADF

Subroutine RITEF transfers group angular flux values from the flux storage field in container-array A to the matrix AFLUX(MM,2,IT). This is realized by MM subsequent calls of subroutine REED.

Summarizing, an incorporation of the I*-method in multilevel algorithm of the ONETRAN code is accomplished by making the following main modifications in computation of the group scattering term:

1. In the ONETRAN code

SUBROUTINE INNER	Total group scattering source for one inner iteration: $q_s^g(\mu,r) = \sum_{l=0}^{L} P_l(\mu)\{q_{s,l}^g(r) + \Sigma_{s,g\to g}^l(r)\Phi_{g,l}^p(r)\}$ (71)
	Angular flux moments: $\Phi_{q,l}(r) = \sum_{\mu'} \psi_g(r,\mu')P_l(\mu')w_{\mu'}$ (72)
SUBROUTINE SOURCE	An effective inscattering group source (to the g-th group), independent of inner iteration: $q_{s,l}^g(r) = \sum_{g'\neq g} \Sigma_{s,g'\to g}^l \Phi_{g',l}(r)$ (73)

where

$\Sigma_{s,g\to g}^l(r)\Phi_{g,l}^p(r)$ in Eq. (71) is the self-scattering (within one energy group) source depending upon the flux from previous inner iterations (denoted by p superscript),

independent variables r,μ',μ have been already discretized i.e.

$r = r_{i\pm1/2}$, $\mu',\mu \in S_N$

2. In the ANTRA1 code

SUBROUTINE INNER	The total group scattering source for inner iterations: $q_s^g(r,\mu) = q_s'^g(r,\mu) + \sum_{\mu'} \sum_{\mu^*} \Sigma_{s,g\to g}(\mu^*) I^*(\mu,\mu',\mu^*)$ $w_{\mu^*}\psi_g^p(r,\mu')w_{\mu'}$ (73)
SUBROUTINE SOURCE	An effective inscattering group source (to the g-th group), independent of inner iteration: $q_s'^g(r,\mu) = \sum_{g'\neq g} \sum_{\mu'} \sum_{\mu^*} \Sigma_{s,g'\to g}(\mu^*) I^*(\mu,\mu',\mu^*) w_{\mu^*}\psi_{g'}(r,\mu')w_{\mu'}$ (74)

where

$\sum_{\mu'} \sum_{\mu^*} \Sigma_{s,g\to g}(\mu^*) I^*(\mu,\mu',\mu^*) w_{\mu^*}\psi_g^p(r,\mu')w_{\mu'}$ in Eq. (73) is the self-scattering group source depending upon the angular flux from previous inner iteration (denoted by p superscript),

$r = r_{i\pm1/2}$, $\mu',\mu \in S_N$, μ^* is discretized; $\mu^* \in \{\mu_1^*,\ldots,\mu^*_{MMST}\}$

IV. A Guide for User Application

1. Data Input Rules. Description of Input Data.

Three GANTRAS modules CROMIX, ATP and ANTRA1 are implemented as KAPROS program modules.

The input data are comprised in External KAPROS Data Blocks /14/ (KDB) specified by KSIOX-card, and connected to the module under KAPROS control. In account of this, besides the standard input description, additional information (required by KAPROS input data rules) will be given here for the user's convenience.

1.1 The CROMIX Code

The input data for CROMIX are contained in the KAPROS Input Data Block 'MIXDDX_EINGABE__'. The data set consists of:

Position of the Item in KDB	Name of Variable	Comments
CONTROL INTEGERS (unformatted) - - - - - - - - - - - - - - - - - - LINE 1		
1	MMST	Number of angle segments (i.e. angular mesh intervals) in μ^*-range
2	IHM	Total number of rows in angular-dependent 3-d transfer matrix (see Table III)
3	IGM	Number of energy groups
CONTROL INTEGERS (unformatted) - - - - - - - - - - - - - - - - - - LINE 2		
1	MTDDX	Total number of material (mixtures)

for each mixture:

CONTROL INTEGERS (unformatted) - LINE 3

1	MS	Number of components

for each component (nuclide):

- LINE 4

1	NNAME	Eight-character nuclide name (2xREAL*4) This name identifies a nuclide in a multigroup library, containing angle-segmented transfer cross-sections.
2	NDEN	Nuclide atomic density (real variable)

Remarks:

1) LINE 4 must be repeated MS times thereby specifying MS nuclides.
2) LINE 3 and LINE 4 (MS times) must be repeated MTDDX times, thereby specifying MTDDX mixtures.

KAPROS cards used:

(1) *KSIOX DBN=ATP_EINGABE_____,TYP=CARD,PMN=PRDUM

(precedes line 1) to assign numerical data to KDB 'ATP EINGABE_____'

(2) *KSIOX DBN=GANTRAS_DDX_____,TYP=ARCO,SPEC=FT12xxxx

to store permanently the generated macroscopic library (i.e. KDB 'GANTRAS_DDX_____') in a user KAPROS archive.

1.2 The ATP Code

The input data for the ATP code are listed below.

CONTROL INTEGERS (unformatted) - LINE 1

Position of Item in KDB	Name of Variable	Comments
1	MMST	Number of discrete cell-centered values in the segmentation of the μ^*-range
2	ISN	Number of discrete cell-centered values in the segmentation of the μ,μ'-range

PROBLEM-DEPENDENT DATA (real unformatted)

Block Name and Dimension	Entries	Comments
AMU(ISN)	ISN	Cell-centered values of the discretized μ,μ'-range
AMUST(MMST)	MMST	Cell-centered values of the discretized μ^*-range

KAPROS cards used:

(1) *KSIOX DBN=ATP_EINGABE____,TYP=CARD,PMN=PRDUM

(precedes line 1) to assign numerical data to KDB 'ATP_EINGABE_____'

(2) *KSIOX DBN=GANTRAS_DATP____',TYP=ARCO,SPEC=_____

to store permanently the generated generalized angular transfer probability table in a user KAPROS archive.

1.3 The ANTRA1 Code

In the following text all the necessary changes of the ONETRAN input data needed in order to run successfully ANTRA1, are indicated.

The data are listed exactly in this order in which they enter the ONETRAN and the ANTRA1 code.

Since ANTRA1 is established as KAPROS module, although for user convenience the ONETRAN notation is preserved, some of the terms (e.g. "card") become meaningless in reference to the KAPROS data input rules.

1.3.1 Input of Control Numbers

Position of Item on Card	Name of Variable	Comments
CONTROL INTEGERS - CARD 1		
3	ISCT	ISCT=0 isotropic neutron scattering is assumed
		ISCT<0 { i) P_1-representation of the scattering kernel. |ISCT| is the order of Legendre expansion used.
		ii) rigorous representation of the scattering term by means of the I*-method. ISCT is used as "switch on". }
CONTROL INTEGERS - CARD 2		
1	MT	Total number of materials, i.e. number of conventional cross-section blocks (including anisotropic cross-sections) used in the program. This is the original ONETRAN option.
		If MT = 0 only materials characterized by angular-dependent cross-section blocks (see Table III) are used.

CONTROL INTEGERS - CARD 3

16	IANG	±1 store angular flux. IANG is negative for printing of the angular flux. The TIMEX angular flux file ITIMEX is written.

1.3.2 Problem-Dependent Data

Block Name and Dimension	Format	Entries	Comments
IDC(IM)	S(I)	IM	Cross-section identification numbers. These numbers assign a conventional cross-section block to each coarse mesh interval. These numbers must be: (a) flagged negative for an anisotropic scattering term to be computed in that coarse mesh interval by the conventional P_1-method. (b) set to zero for an anisotropic scattering term to be computed in that coarse mesh interval by the rigorous I*-method.

Additional new data, introduced in a form of KAPROS Data Block 'ANTRA1_____IDDX', are attached to the ANTRA1 module with the aid of the READKØ subroutine. The data must be specified as follows:

Block Name and Dimension	Format	Entries	Comments
IDDX(IM)	S(I)	IM	Angular-dependent cross-section block identification numbers. These numbers assign a block containing transfer cross-sections (see Table III) to each coarse mesh interval. These numbers must be: (a) positive for an anisotropic scattering term to be computed in that coarse mesh interval by the rigorous I*-method.

(b) set up to zero for an anisotropic scattering term to be computed in that coarse mesh interval by conventional P_1-method

They are described by KAPROS control card:
*KSIOX DBN=ANTRA1_____IDDX,IND=1,TYP=CARD,PMN=PRDUM

Two interface KDB from private user archive (on unit 12) are connected to ANTRA1 through the READKØ subroutine. They are assigned by two KAPROS control cards:

1) *KSIOX DBN=GANTRAS_DDX_____',IND=1,TYP=ARCI,SPEC=FT12xxxx
2) *KSIOX DBN=GANTRAS_DATP____',IND=1,TYP=ARCI,SPEC=FT12xxxx

Consequently, the input list for READKØ (i.e. KDB'INIT_KAPROS_READ') must be updated as indicated in Table VIII.

In Table XI some examples of updated input data specification are presented. For user convenience different data assignments are shown as well for the ONETRAN code as for two different options of the ANTRA1 code.

TABLE XI. Updated Input Data Specification in Various ANTRA1 Options in Comparison to Conventional ONETRAN Input

ONETRAN	ANTRA1	
	I*-MODE	COMBINED MODE-(P_L/I^*)
Isotropic case ISCT = 0 regardless of the sign of IDC	Isotropic case ISCT = 0 MT = 0 IDC = 0 IDDX > 0	Isotropic case ISCT = 0 MT ≠ 0 IDC ≥ 0 IDDX ≥ 0
Anisotropic case ISCT > 0 IDC < 0	Anisotropic case ISCT < 0 MT = 0 IDC ≡ 0 IDDX > 0	Anisotropic case ISCT < 0 MT ≠ 0 IDC ≤ 0 IDDX ≥ 0 |ISCT| serves as an expansion order of the scattering kernel

2. Technical Notes on the Implementation of GANTRAS

GANTRAS was implemented on the SIEMENS 7890 computer of the KARLSRUHE NUCLEAR RESEARCH CENTER. GANTRAS operates under KAPROS (Karlsruher Programm System) control. A user library, named GANTRAS (partition data set), containing all GANTRAS modules, including the source versions of the CROMIX, ATP and ANTRA1 codes has been created. For computations, a compiled (translated) version of ANTRA1 code was used stored as an object module.

ANTRA1 is based on the Karlsruhe version of ONETRAN converted to IBM-360 machine, i.e. the program ONETRA. The major change made in the conversion from ONETRAN to ONETRA is the treatment of pheripheral storage. The data normally stored in LCM (large core memory of CDC 7600), are stored here directly after the A-container array.
The CDC 7600 system routines in subroutines REED and RITE, respectively, are replaced by simple routines which move data to and from sections of the A array. It is thus possible to keep the LCM pointer structure of the code with no change in logics.
The main container-array A, located on a blank COMMON data block is dynamically dimensioned with the aid of the KAPROS routines KSGEP/KSPUTP. By utilizing the same technique, a dynamical allocation of all arrays used by CROMIX and ATP modules was also achieved.

The KSGET/KSPUT, KSGETP/KSPUTP and KSDD subroutines of KAPROS have been applied for transmission (between disc and the program) of data to be permanently stored on data files (either KDB or external files). The complete sets of sample problem input data are available from a user data library and they can be updated according to the needs. For job control language (JCL) statements of CROMIX and ATP (joint together), and ANTRA1 see Example 1, 2 and 3, respectively.

V. First Results and Conclusions

GANTRAS was fully numerically tested for the one-dimensional spherical and plane geometry options.

Two types of problems were considered and solved with the use of GANTRAS.

1. Inhomogeneous problem.

   A Be-spherical shell: 5 cm inner radius, 10 and 25 cm outer radius (i.e. 5 and 20 cm thickness, respectively), surrounding a 14 MeV neutron source distributed uniformly over the spatial extent of the source region (of 5 cm radius).

2. Homogeneous problem

   A critical uranium assembly was chosen to check k_{eff}-calculations.

The results were compared to that obtained from ONETRAN with $S_N P_0$ and $S_N P_3$, N = 8,20 order of approximations.

The cross-sections used by ONETRAN were taken from the coarse group library of the University of Wisconsin /16/, which is at present available for fusion applications. It is a combined library based on VITAMIN-C and MACKLIB-IV, that had been condensed from the original 171 neutron groups into 25 groups using a 1/E spectrum. The scattering matrices are represented in the P_3 approximation and have been condensed presumably with the 1/E spectrum. The group boundaries are given in Table XII.

Angular dependent transfer matrices were created from the above mentioned matrices in Legendre-representation, by summing up the three terms of the Legendre polynomial expansion. In this way, of course only the numerical tests of the newly developed programme can be performed. For the physical test of the procedure, the angular dependent transfer matrices have to be based on true double-differential cross-sections without using a Legendre representation (at least in the laboratory system). If present, such data are scarcely available, moreover, the processing codes for these data are just under development.

TABLE XII. UW 25 Group Structure /16/

Group Number	Upper Boundary
1	14.9 MeV
2	13.5
3	12.2
4	11.05
5	10.0
6	9.05
7	8.19
8	7.41
9	6.70
10	6.07
11	5.49
12	4.49
13	3.68
14	3.01
15	2.47
16	1.35
17	0.743
18	0.408
19	0.166
20	31.8 KeV
21	3.35
22	353. eV
23	37.3
24	3.93
25	0.415

The objective of the calculations based on inhomogeneous problem no.1 was to check the neutron multiplication of Be^9 since at present there is a clear preference to use in fusion reactor blanket beryllium as the neutron multiplier. The results from ONETRAN calculations (whose accuracy has been proven) with different order of P_1 and S_N approximations were compared to corresponding results of the calculations carried out by the aid of ANTRA1 in the same geometrical and material configuration but with various S_N approximations. Tables XIII, XIV and XV show the neutron leakage out of the system (L) and neutron multiplication (M) inside a spherical 5 cm and 20 cm thick Beryllium-shell, obtained with ONETRAN and ANTRA1, respectively.

For an isotropic problem, i.e. when the angular distribution of secondary neutrons in the laboratory system is assumed to be isotropic, the P_0-representation of the scattering term (see Eq. (5) with L=0) is equivalent to the rigorous I*-representation (see Eq. (26)). Therefore, in this case, a full agreement between compared quantities is to be expected. Observed differences which are practically negligible (on fourth decimal place) may be attributed to different numerical procedures applied in each code.

The comparisons between ONETRAN calculations performed with the scattering matrices in P_3-representation and adequate ANTRA1 calculations exhibits larger differences in achieved results. It can be seen that the angular mesh density (determined by S_N order) influences significantly the accuracy of ANTRA1 calculations. In fact, in reference to Fig. 13, it becomes clear that the diagram representing discretized angular transfer probabilities in S_8 approximation only roughly reproduces the true shape of the I*-function. For this reason the P_3S_8 ONETRAN results should be compared to S_{20} ANTRA1 results. The results of homogeneous problem no. 2 are presented in Table XVI.

In plane geometry option similar test calculations were performed and the results are in good agreement. Thus it may be concluded that GANTRAS is suitable to be used as a calculational tool for transport problems characterized by strongly anisotropic neutron scattering. The physical effect of the new cross-section data on calculated neutronic parameters which are of importance in fusion reactor blanket, can be studied, however, only when realistic double-differential cross-sections become available.

TABLE XIII. Multiplication (M) and leakage (L) for a beryllium shell of 5 cm thickness (with 5 cm inner and 10 cm outer radius), surrounding a 14 MeV neutron source, calculated by ONETRAN and ANTRA1 in S_8 approximation

	ONETRAN ($P_N S_8$)		GANTRAS ($I^* S_8$)	
	isotropic	anisotropic	isotropic	anisotropic
	P_0	P_3		
M	1.546	1.490	1.546	1.510
L	1.496	1.447	1.498	1.468

TABLE XIV. Multiplication (M) and leakage (L) for a beryllium shell of 5 cm thickness (5 cm inner and 10 cm outer radius), surrounding a 14 MeV neutron source, calculated by ONETRAN and ANTRA1 in S_{20} approximation

	ONETRAN ($P_3 S_{20}$)	GANTRAS ($I^* S_{20}$)
	anisotropic	anisotropic
	P_3	
M	1.482	1.488
L	1.440	1.446

TABLE XV. Multiplication (M) and leakage (L) for a beryllium shell of 20 cm thickness (with 5 cm inner and 25 cm outer radius), surrounding a 14 MeV neutron source, calculated by ONETRAN and ANTRA1 in S_8 approximation

	ONETRAN ($P_N S_8$)		GANTRAS ($I^* S_8$)	
	isotropic	anisotropic	isotropic	anisotropic
	P_0	P_3		
M	2.702	2.577	2.702	2.600
L	2.386	2.306	2.386	2.328

TABLE XVI. Critical uranium assembly. K-eff calculations

	ONETRAN ($P_N S_8$)		GANTRAS ($I^* S_8$)	
	isotropic	anisotropic	isotropic	anisotropic
	P_0	P_3		
k-eff	1.387	1.324	1.387	1.310

Example 1. JCL statements and sample input data for linked CROMIX and ATP codes.

```
//INR271Q JOB (____,___,_____),SCHWENK,REGION=1200K,NOTIFY=INR271,          JCL
//  MSGCLASS=H,TIME=(00,20)                                                 JCL
//*MAIN LINES=8                                                             JCL
//*FORMAT PR,DDNAME=,FORMS=E                                                JCL
// EXEC KSCLG                                                               JCL
//K.FT06F001 DD SYSOUT=*                                                   JCL
//K.FT42F001 DD SYSOUT=*                                                   JCL
//*************************************************************************** JCL
//**                        ISODDX - BINARY FILE                          ** JCL
//**  NUCLIDE-ORGANIZED MULTIGROUP ANGLE-SEGMENTED MICROSCOPIC DATA       ** JCL
//**                           LIBRARY                                    ** JCL
//*************************************************************************** JCL
//**                                                                        JCL
//K.FT04F001 DD DISP=SHR,DSN=INR271.ISODDX.FORT                            JCL
//K.FT15F001 DD DISP=SHR,DSN=INR271.GANTRAS.FORT(CROMIX)                   JCL
//**                                                                        JCL
//*************************************************************************** JCL
//**                        KSA5.GANTPER                                  ** JCL
//**              USER-MANEGED KAPROS ARCHIVE                             ** JCL
//*************************************************************************** JCL
//K.FT12F001 DD DISP=SHR,DSN=INR271.KSA5.GANTPER                           JCL
//K.SYSIN DD *                                                             JCL
*COMPILE H,UNIT=15                                                         JCL
*$*$                                                                       JCL
*LINK MAP,LIST                                                            JCL
 ENTRY CROMIX                                                             JCL
 NAME CROMIX                                                              JCL
*$*$                                                                       JCL
*KSIOX DBN=MIXDDX EINGABE   ,TYP=CARD,PMN=PRDUM                      I.CROMIX
*$ MMST IHM  IGM                                                     I.CROMIX
   8    30   25                                                      I.CROMIX
*$    NUMBER OF MIXTURES                                             I.CROMIX
 2                                                                   I.CROMIX
*$   MIXTURE ONE ;  VACUUM                                          I.CROMIX
*$   NUMBER OF NUCLIDES THAT COMPOSE MIXTURE ONE                    I.CROMIX
 1                                                                   I.CROMIX
*$ NUCLIDE NAME ' REAL*8 '    NUCLIDE DENSITY                       I.CROMIX
'BE-9     '  1.E-12                                                 I.CROMIX
*$   MIXTURE TWO ; BERYLLIUM                                        I.CROMIX
*$   NUMBER OF NUCLIDES THAT COMPOSE MIXTURE TWO                    I.CROMIX
 1                                                                   I.CROMIX
*$ NUCLIDE NAME ' REAL*8 '    NUCLIDE DENSITY                       I.CROMIX
'BE-9     '   0.117                                                 I.CROMIX
*$*$                                                                I.CROMIX
*KSIOX DBN=ATP EINGABE      ,TYP=CARD,PMN=PRDUM                        I.ATP
*$ MMST ISN                                                           I.ATP
    8   8                                                           I.ATP
*$ CELL-CENTERED POINTS OF THE ANGULAR MESH                          I.ATP
*$ MU  AND MU-PRIME                                                  I.ATP
 -9.602898E-01 -7.966665E-01 -5.255324E-01 -1.834347E-01             I.ATP
 1.834347E-01 5.255324E-01 7.966665E-01 9.602898E-01                 I.ATP
*$ MU-STAR                                                           I.ATP
 -9.602898E-01 -7.966665E-01 -5.255324E-01 -1.834347E-01             I.ATP
 1.834347E-01 5.255324E-01 7.966665E-01 9.602898E-01                 I.ATP
```

```
*$*$                                                                  I.ATP
*KSIOX DBN=GANTRAS DDX      ,IND=1,TYP=ARCO,SPEC=FT12A505          O.CROMIX
*KSIOX DBN=GANTRAS DATP     ,IND=1,TYP=ARCO,SPEC=FT12A506             O.ATP
*GO SM=CROMIX
```

Example 2. JCL statements and sample input data for the ANTRA1 code operating in the I*-mode.

```
//INR271C JOB (____,___,_____),SCHWENK,TIME=(00,30),REGION=3000K,          JCL
//  MSGCLASS=H,NOTIFY=INR271                                                JCL
//*MAIN LINES=5                                                             JCL
//*FORMAT PR,DDNAME=,FORMS=E                                                JCL
//*************************************************************************JCL
//*************     BE-SHELL OF 5 CM THICKNESS              **********      JCL
//*************     ANGLE-DEPENDENT TRANSFER MATRICES       **********      JCL
//*************     CREATED FROM CONVENTIONAL VITAMIN-C     **********      JCL
//*************     TRANSFER MATRICES IN P_L - REPRESENTATION**********
//*************************************************************************JCL
// EXEC KSCLG                                                               JCL
//K.FT12F001 DD DISP=SHR,DSN=INR271.KSA1.GANTPER                            JCL
//K.FT21F001 DD UNIT=SYSDA,SPACE=(TRK,(50,10)),                            JCL
//              DCB=(RECFM=VBS,LRECL=4080,BLKSIZE=4086)                     JCL
//K.FT22F001 DD UNIT=SYSDA,SPACE=(TRK,(50,10)),                            JCL
//              DCB=(RECFM=VBS,LRECL=4080,BLKSIZE=4086)                     JCL
//K.FT18F001 DD UNIT=SYSDA,SPACE=(TRK,(50,10)),                            JCL
//              DCB=(RECFM=FB,LRECL=80,BLKSIZE=4086)                        JCL
//K.FT31F001 DD UNIT=SYSDA,SPACE=(TRK,(50,10)),                            JCL
//              DCB=(RECFM=VBS,LRECL=4080,BLKSIZE=4086)                     JCL
//K.FT15F001 DD UNIT=SYSDA,SPACE=(TRK,(50,10)),                            JCL
//              DCB=(RECFM=VBS,LRECL=4080,BLKSIZE=4080)                     JCL
//K.FT30F001 DD UNIT=SYSDA,SPACE=(TRK,(50,10)),                            JCL
//              DCB=(RECFM=VBS,LRECL=4080,BLKSIZE=4086)                     JCL
//K.FT32F001 DD UNIT=SYSDA,SPACE=(TRK,(50,10)),                            JCL
//              DCB=(RECFM=VBS,LRECL=4080,BLKSIZE=4086)                     JCL
//K.FT33F001 DD UNIT=SYSDA,SPACE=(TRK,(50,10)),                            JCL
//              DCB=(RECFM=VBS,LRECL=4080,BLKSIZE=4086)                     JCL
//K.FT34F001 DD UNIT=SYSDA,SPACE=(TRK,(50,10)),                            JCL
//              DCB=(RECFM=VBS,LRECL=4080,BLKSIZE=4086)                     JCL
//K.FT15F001 DD UNIT=SYSDA,SPACE=(TRK,(50,10)),                            JCL
//              DCB=(RECFM=VBS,LRECL=4080,BLKSIZE=4086)                     JCL
//K.FT36F001 DD UNIT=SYSDA,SPACE=(TRK,(50,10)),                            JCL
//              DCB=(RECFM=VBS,LRECL=4080,BLKSIZE=4086)                     JCL
//K.FT37F001 DD UNIT=SYSDA,SPACE=(TRK,(50,10)),                            JCL
//              DCB=(RECFM=VBS,LRECL=4080,BLKSIZE=4086)                     JCL
//K.FT38F001 DD UNIT=SYSDA,SPACE=(TRK,(50,10)),                            JCL
//              DCB=(RECFM=VBS,LRECL=4080,BLKSIZE=4086)                     JCL
//K.FT39F001 DD UNIT=SYSDA,SPACE=(TRK,(50,10)),                            JCL
//              DCB=(RECFM=FB,LRECL=80,BLKSIZE=4086)                        JCL
//K.OBJA DD DISP=SHR,DSN=INR271.ANTRA1R.OBJ                                 JCL
//K.FT06F001 DD SYSOUT=*,DCB=(LRECL=133,BLKSIZE=133,RECFM=FB,BUFNO=1)       JCL
//K.KSSNAP DD SYSOUT=*                                                     JCL
//K.SYSIN DD *                                                             JCL
*LINK MAP,LIST                                                            JCL
 INCLUDE OBJA                                                             JCL
 ENTRY ANTRA1                                                             JCL
 NAME ANTRA1                                                              JCL
*$*$                                                                      JCL
*KSIOX DBN=INIT KAPROS READ,IND=1,TYP=CARD,PMN=KETT                   I.READK0
23 'ANTRA1   EINGABE' 1 1 10000 0                                     I.READK0
21 'ANTRA1         21' 1 6 10000 0                                    I.READK0
22 'ANTRA1         22' 1 6 10000 0                                    I.READK0
18 'ANTRA1         18' 1 6 10000 0                                    I.READK0
31 'ANTRA1         31' 1 6 10000 0                                    I.READK0
```

```
30 'ANTRA1         30' 1 6 10000 0                                    I.READKO
32 'ANTRA1         32' 1 6 10000 0                                    I.READKO
33 'ANTRA1         33' 1 6 10000 0                                    I.READKO
34 'ANTRA1         34' 1 6 10000 0                                    I.READKO
15 'ANTRA1         15' 1 6 10000 0                                    I.READKO
39 'ANTRA1         39' 1 6 10000 0                                    I.READKO
36 'GANTRAS DDX      ' 1 1 10000 0                                    I.READKO
37 'ANTRA1       IDDX' 1 1 10000 0                                    I.READKO
38 'GANTRAS DATP     ' 1 1 10000 0                                    I.READKO
*$*$                                                                  I.READKO
*KSIOX DBN=ANTRA1   EINGABE,IND=1,TYP=CARD,PMN=PRDUM                  I.ANTRA1
1                                                                     I.ANTRA1
' BE -SHELL ANTRA1 TEST 5/85  ISODDX1       25/S8/                    JOBTITLE
*$ &&&&&&&&&&&&&&&&&&&&&&&&&&&&&&&&&&&&&&&&&&&&&&&&&&&&&&&&&&&&&&&&&&&       C
*$ &&&&&&&&&&&    EPS=0.01  NO EDIT                 &&&&&&&&&&&&&&&&&&       C
*$ &&&&&&&&&&&    TEST BE-SHELL  ANTRA1  I  MODE    &&&&&&&&&&&&&&&&&&       C
*$ &&&&&&&&&&&&&&&&&&&&&&&&&&&&&&&&&&&&&&&&&&&&&&&&&&&&&&&&&&&&&&&&&&&       C
*$ CARD  1 DEMANDS THE FOLLOWING VARIABLES:                                  C
*$ ITH ISCT ISN IGM IM IBL IBR IEVT ISTART IQOPT IGEOM IQUAD
    0  -3    8  25   2  0   0   0      0     -4     3     1              CARD 1
*$ CARD  2 DEMANDS THE FOLLOWING VARIABLES:
*$ MT MTP MCR MS IHT IHS IHM IDEN IQAN IQL IQR IACC
   0   0   0  0   5   6   30   0    0   0   0   1                        CARD2
*$ CARD  3 DEMANDS THE FOLLOWING VARIABLES:
*$ OITM IITL IITM IFISS IPVT IEDOPT IPLOT I1I2I3I4I5I6 ITLIM IFO IANG
   10   100   150   1    0     0      0    1 0 2 0 3 1   0     0  -1     CARD 3
*$ CARD  4 DEMANDS THE FOLLOWING VARIABLES:
*$ EV EVM PV XLAL XLAH XLAX
  0.0  0. 0.  0.   0.   0.                                               CARD 4
*$ CARD  5 DEMANDS THE FOLLOWING VARIABLES:
*$ EPSI NORM POD NBUC 0 0
  1.0E-2 1.0  0.  0   0 0                                                CARD 5
*$ CARD  6 DEMANDS THE FOLLOWING VARIABLES:
*$ BHGT BWTH
   0.   0.                                                               CARD 6
*$ IHR(IM)  10  MESHPOINTS                                                   .
0 0  5  0 0  5                                                               .
3*3                                                                          .
*$ IUPS IDOWS NTRANS                                                         P
*$  0      0     0                                                           R
*$ INPUT SOURCES ( IQOPT=-4) UNIT SOURCE IN GROUP NR.1                       O
0 0 1.  1 24 0.           3*3                                                B
*$ INPUT SOURCE RADIAL DISTRIBUTION 2*IT ENTRIES (IT IS THE NUMBER           L
*$ OF FINE MESHES)                                                           E
1 10 1.  1  10 0.   3*3                                                      M
*$ RAD(IM+1)
0 0 0.  0 0  5.    0 0  10.                                                  D
3*3                                                                          E
*$ IDC(IM)                                                                   P
*$ VACUUM   BERYLLIUM                                                        E
*$    1        2                                                             N
0 0  0      0 0  0                                                           D
3*3                                                                          E
*$ FISSION FRACTIONS                                                         N
*$ HERE IFISS=1                                                              T
*$ IGM ENTRIES : SINGLE FISSION SPECTRUM
*$ CHI(IGM) S(E)                                                             D
 1  25  0.  3*3                                                              A
*$ GROUP VELOCITIES                                                          T
*$ USED ONLY IN TIME ABSORPTION CALCULATIONS                                 A
*$ VEL(IGM) S(E) IGM                                                         .
```

```
 1  25  0.  3*3                                                                .
*$*$                                                                          .
*KSIOX DBN=ANTRA1       IDDX,IND=1,TYP=CARD,PMN=PRDUM                      I.ANTRA1
*$ IDDX(IM)                                                                I.ANTRA1
*$ VACCUM    BERYLLIUM                                                     I.ANTRA1
*$    1           2                                                        I.ANTRA1
 1 2                                                                       I.ANTRA1
*$*$                                                                       I.ANTRA1
*$                                                                         I.ANTRA1
*KSIOX DBN=GANTRAS DDX     ,IND=1,TYP=ARCI,SPEC=FT12A001                   I.ANTRA1
*KSIOX DBN=GANTRAS DATP    ,IND=1,TYP=ARCI,SPEC=FT12A002                   I.ANTRA1
*GO SM=ANTRA1
/*
//
```

Example 3. JCL statements and sample input data for the ANTRA1 code operating in the combined mode (P_ℓ /I*).

```
//INR271L JOB (____,___,_____),SCHWENK,TIME=(00,30),REGION=3000K,          JCL
//  MSGCLASS=A,NOTIFY=INR271                                               JCL
//*MAIN LINES=5                                                            JCL
//*FORMAT PR,DDNAME=,FORMS=E                                               JCL
//*************************************************************************JCL
//************     BE-SHELL 5 CM-THICK ANTRA1 TEST          ********        JCL
//************     ANGLE-DEPENDENT TRANSFER MATRICES        ********        JCL
//************     GENERATED FROM WSCM025C  LIBRARY         ********        JCL
//************                                              ********        JCL
//*************************************************************************JCL
// EXEC KSCLG                                                              JCL
//K.FT01F001 DD DISP=SHR,DSN=INR487.KSDA.WSCM025C                          JCL
//K.FT09F001 DD DISP=SHR,DSN=INR909.KSDA.JBGRUC                            JCL
//K.FT10F001 DD DISP=SHR,DSN=INR909.GRSTAB                                 JCL
//K.FT11F001 DD DISP=SHR,DSN=INR487.F26TNEXT                               JCL
//*************************************************************************JCL
//**          INR271.KSA1.GANTPER                                  ***      JCL
//**      USER-MANAGED KAPROS ARCHIVE                              ***      JCL
//*************************************************************************JCL
//K.FT12F001 DD DISP=SHR,DSN=INR271.KSA1.GANTPER                           JCL
//K.FT21F001 DD UNIT=SYSDA,SPACE=(TRK,(50,10)),                            JCL
//              DCB=(RECFM=VBS,LRECL=4080,BLKSIZE=4086)                    JCL
//K.FT22F001 DD UNIT=SYSDA,SPACE=(TRK,(50,10)),                            JCL
//              DCB=(RECFM=VBS,LRECL=4080,BLKSIZE=4086)                    JCL
//K.FT18F001 DD UNIT=SYSDA,SPACE=(TRK,(50,10)),                            JCL
//              DCB=(RECFM=FB,LRECL=80,BLKSIZE=4086)                       JCL
//K.FT31F001 DD UNIT=SYSDA,SPACE=(TRK,(50,10)),                            JCL
//              DCB=(RECFM=VBS,LRECL=4080,BLKSIZE=4086)                    JCL
//K.FT15F001 DD UNIT=SYSDA,SPACE=(TRK,(50,10)),                            JCL
//              DCB=(RECFM=VBS,LRECL=4080,BLKSIZE=4086)                    JCL
//K.FT30F001 DD UNIT=SYSDA,SPACE=(TRK,(50,10)),                            JCL
//              DCB=(RECFM=VBS,LRECL=4080,BLKSIZE=4086)                    JCL
//K.FT32F001 DD UNIT=SYSDA,SPACE=(TRK,(50,10)),                            JCL
//              DCB=(RECFM=VBS,LRECL=4080,BLKSIZE=4086)                    JCL
//K.FT33F001 DD UNIT=SYSDA,SPACE=(TRK,(50,10)),                            JCL
//              DCB=(RECFM=VBS,LRECL=4080,BLKSIZE=4086)                    JCL
//K.FT34F001 DD UNIT=SYSDA,SPACE=(TRK,(50,10)),                            JCL
//              DCB=(RECFM=VBS,LRECL=4080,BLKSIZE=4086)                    JCL
//K.FT36F001 DD UNIT=SYSDA,SPACE=(TRK,(50,10)),                            JCL
//              DCB=(RECFM=VBS,LRECL=4080,BLKSIZE=4086)                    JCL
//K.FT37F001 DD UNIT=SYSDA,SPACE=(TRK,(50,10)),                            JCL
//              DCB=(RECFM=VBS,LRECL=4080,BLKSIZE=4086)                    JCL
//K.FT38F001 DD UNIT=SYSDA,SPACE=(TRK,(50,10)),                            JCL
//              DCB=(RECFM=VBS,LRECL=4080,BLKSIZE=4086)                    JCL
//K.FT39F001 DD UNIT=SYSDA,SPACE=(TRK,(50,10)),                            JCL
//              DCB=(RECFM=FB,LRECL=80,BLKSIZE=4086)                       JCL
//K.OBJA DD DISP=SHR,DSN=INR271.ANTRA1R.OBJ                                JCL
//K.FT06F001 DD SYSOUT=*,DCB=(LRECL=133,BLKSIZE=133,RECFM=FB,BUFNO=1)      JCL
//K.KSSNAP DD SYSOUT=*                                                     JCL
//K.SYSIN DD *                                                             JCL
*LINK MAP,LIST                                                            JCL
 INCLUDE OBJA                                                             JCL
 ENTRY ANTRA1                                                             JCL
 NAME ANTRA1                                                              JCL
*$*$                                                                      JCL
```

```
*KSIOX DBN=GRUCAL,TYP=CARD,PMN=PRGRUC                                          I.GRUCAL
'GRUCAL  '                                                                     I.GRUCAL
'VITAMINC' '          ' '          '  1  10  11                                I.GRUCAL
'MISCH   '                                                                     I.GRUCAL
2                                                                              I.GRUCAL
*$ MISCHUNG 1 : VAKUUM                                                         I.GRUCAL
1  '         ' 'U 235   ' 'U 235   '                                           I.GRUCAL
'BE  9   ' 800.0 1.00-12                                                       I.GRUCAL
*$ MISCHUNG 2 : BE                                                             I.GRUCAL
1  '         ' 'U 235   ' 'U 235   '                                           I.GRUCAL
'BE  9   ' 800.0 0.117                                                         I.GRUCAL
'TYP     '                                                                     I.GRUCAL
'ZUSATZ  ' 6                                                                   I.GRUCAL
'SN2N    ' 'SNTH3   '  'SNG     '  'SMT01    '                                 I.GRUCAL
'SMT02   '  'SMT03  '                                                          I.GRUCAL
*$ 'DRUCKWQ '                                                                  I.GRUCAL
*$ 1                                                                           I.GRUCAL
*$ '                ' 0  0                                                     I.GRUCAL
                                                                               I.GRUCAL
*$ 'SEKINPT '                                                                  I.GRUCAL
*$ 1  '      '                                                                 I.GRUCAL
*$ 15                                                                          I.GRUCAL
                                                                               I.GRUCAL
'GRUCEND '                                                                     I.GRUCAL
*$*$                                                                           I.GRUCAL
*KSIOX DBN=INIT KAPROS READ,IND=1,TYP=CARD,PMN=KETT                            I.READKO
23 'ANTRA1   EINGABE' 1 1 10000 0                                              I.READKO
21 'ANTRA1        21' 1 6 10000 0                                              I.READKO
22 'ANTRA1        22' 1 6 10000 0                                              I.READKO
18 'ANTRA1        18' 1 6 10000 0                                              I.READKO
31 'ANTRA1        31' 1 6 10000 0                                              I.READKO
30 'ANTRA1        30' 1 6 10000 0                                              I.READKO
32 'ANTRA1        32' 1 6 10000 0                                              I.READKO
33 'ANTRA1        33' 1 6 10000 0                                              I.READKO
34 'ANTRA1        34' 1 6 10000 0                                              I.READKO
15 'ANTRA1        15' 1 6 10000 0                                              I.READKO
39 'ANTRA1        39' 1 6 10000 0                                              I.READKO
36 'GANTRAS DDX     ' 1 1 10000 0                                              I.READKO
37 'ANTRA1      IDDX' 1 1 10000 0                                              I.READKO
38 'GANTRAS DATP    ' 1 1 10000 0                                              I.READKO
*$*$                                                                           I.READKO
*KSIOX DBN=ANTRA1   EINGABE,IND=1,TYP=CARD,PMN=PRDUM                           I.ANTRA1
1                                                                              I.ANTRA1
' BE -SHELL ANTRA1-MMTEST 5/85  ISODDX1      25/8/P0                         ' JOBTITLE
*$ &&&&&&&&&&&&&&&&&&&&&&&&&&&&&&&&&&&&&&&&&&&&&&&&&&&&&&&&&&&&&&&&&&&&&&&&         C
*$ &&&&&&&&&&&     EPS=0.01     NO   EDIT           &&&&&&&&&&&&&&&&&&         C
*$ &&&&&&&&&&&     TEST BE-SHELL  ANTRA1            &&&&&&&&&&&&&&&&&&         C
*$ &&&&&&&&&&&     COMBINED-MODE                    &&&&&&&&&&&&&&&&&&         C
*$ &&&&&&&&&&&&&&&&&&&&&&&&&&&&&&&&&&&&&&&&&&&&&&&&&&&&&&&&&&&&&&&&&&&&&&&&         C
*$ CARD  1 DEMANDS THE FOLLOWING VARIABLES:
*$ ITH ISCT ISN IGM IM IBL IBR IEVT ISTART IQOPT IGEOM IQUAD
    0    0   8   25   4  0   0   0      0     -4     3     1               CARD 1
*$ CARD  2 DEMANDS THE FOLLOWING VARIABLES:
*$ MT MTP MCR MS IHT IHS IHM IDEN IQAN IQL IQR IACC
   2  -2   0  0  -5   6   30   0    0   0   0   0                           CARD 2
*$ CARD  3 DEMANDS THE FOLLOWING VARIABLES:
*$ OITM IITL IITM IFISS IPVT IEDOPT IPLOT I1I2I3I4I5I6 ITLIM IFO IANG
   10   100   150   1    0     0      0    1 0 0 1 0 1   0    0  -1       CARD 3
*$ CARD  4 DEMANDS THE FOLLOWING VARIABLES:
*$ EV EVM PV XLAL XLAH XLAX
```

```
  0.0  0. 0.  0.   0.   0.                                                CARD 4
*$ CARD  5 DEMANDS THE FOLLOWING VARIABLES:
*$ EPSI NORM POD NBUC 0 0
  1.0E-2 1.0  0.  0   0 0                                                 CARD 5
*$ CARD  6 DEMANDS THE FOLLOWING VARIABLES:
*$ BHGT BWTH
   0.   0.                                                                CARD 6
*$ IHR(IM)  10  MESHPOINTS                                                    .
0 0  3  0 0  2  0 0  3  0 0 2                                                 .
3*3                                                                           .
*$ IUPS IDOWS NTRANS                                                        P
    0     0     0                                                         R
*$ MATTAB(MTP)                                                              O
    1     2                                                               B
*$ INPUT SOURCES ( IQOPT=-4) UNIT SOURCE IN GROUP NR.1                      L
0 0 1.  1 24 0.          3*3                                               E
*$ INPUT SOURCE RADIAL DISTRIBUTION 2*IT ENTRIES (IT IS THE NUMBER          M
*$ OF FINE MESHES)
1 10 1.  1  10 0.   3*3                                                     D
*$ RAD(IM+1)                                                                E
0 0 0.  0 0  3.    0 0  5.  0 0  8.  0 0  10.                               P
3*3                                                                         E
*$ IDC(IM)                                                                  N
*$ VAKUUM   BERYLLIUM                                                       D
*$   1       2     3         4                                            E
0 0  1     0 0  0  0 0  2  0 0  0                                           N
3*3                                                                         T
*$*$
*KSIOX DBN=ANTRA1      IDDX,IND=1,TYP=CARD,PMN=PRDUM                        D
*$ IDDX(IM)                                                                 A
*$ VACUUM-PL  VACUUM-I* BERYLLIUM-PL BERYLIUM-I*                            T
*$    1          2                                                        A
 0  1  0  2                                                                 .
*$*$                                                                        .
*$                                                                          .
*KSIOX DBN=GANTRAS DDX     ,IND=1,TYP=ARCI,SPEC=FT12A001                 I.ANTRA1
*KSIOX DBN=GANTRAS DATP    ,IND=1,TYP=ARCI,SPEC=FT12A002                 I.ANTRA1
*GO SM=GRUCAL
*GO SM=ANTRA1
/*
//
```

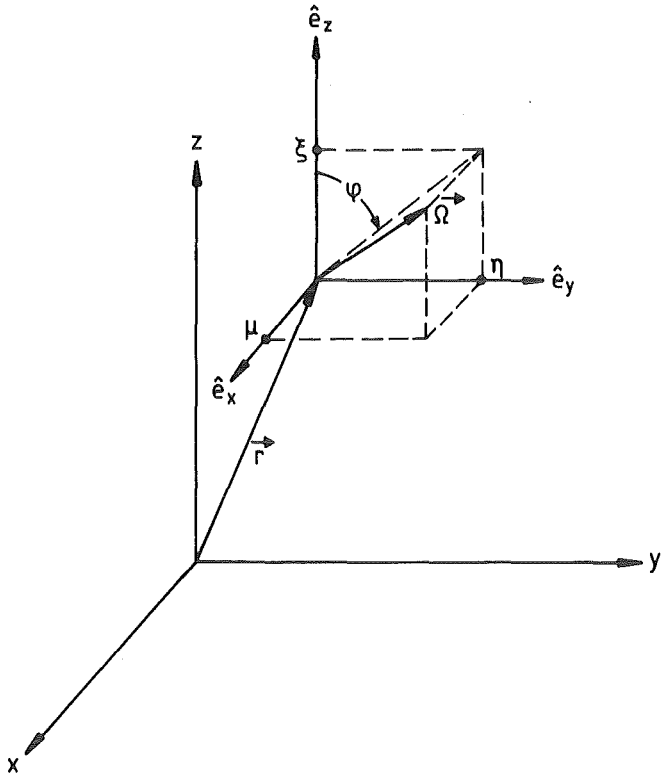

Fig.1 Cartesian space-angle coordinate system in three-dimensions.

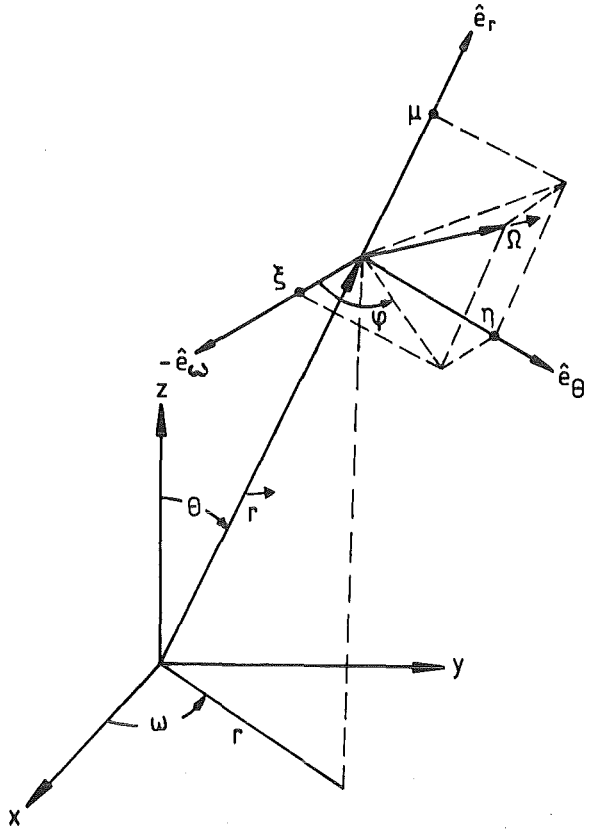

Fig.2 Spherical space-angle coordinate system in three-dimensions.

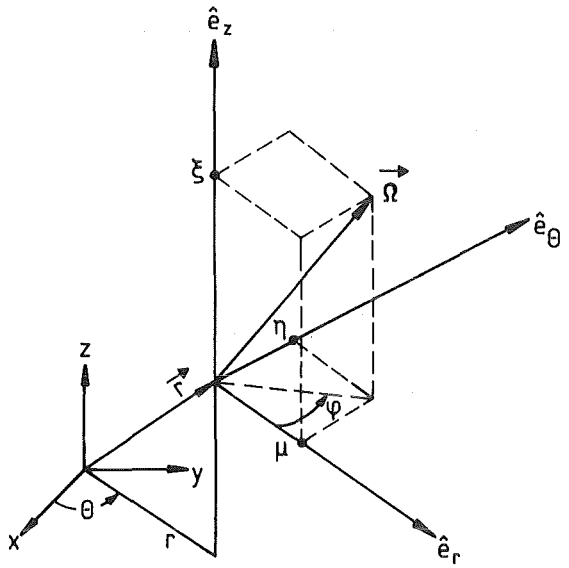

Fig.3 Cylindrical space-angle coordinate system in three-dimensions.

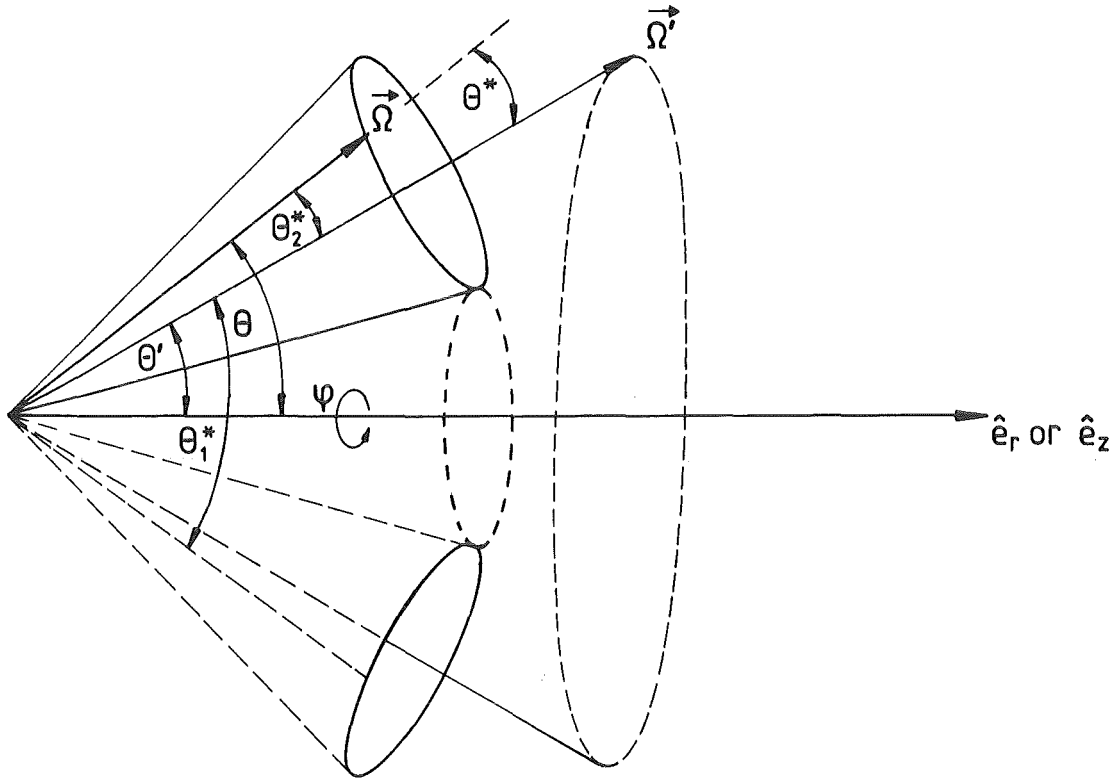

Incident: $\mu' = \cos\theta', \varphi'$

Outgoing: $\mu = \cos\theta, \varphi$

Scattering: $\mu^* = \cos\theta^*, \Delta\varphi = \varphi - \varphi'$

$$\theta^* = \cos^{-1}(\vec{\Omega}\cdot\vec{\Omega}')$$

allowed θ^*-region:

$$\beta_1^* = \cos\theta_1^* = \mu'\mu - \sqrt{1-\mu^2}\ \sqrt{1-\mu'^2}$$

$$\beta_2^* = \cos\theta_2^* = \mu'\mu + \sqrt{1-\mu^2}\ \sqrt{1-\mu'^2}$$

Fig. 4 Definitions of angles in the laboratory system.

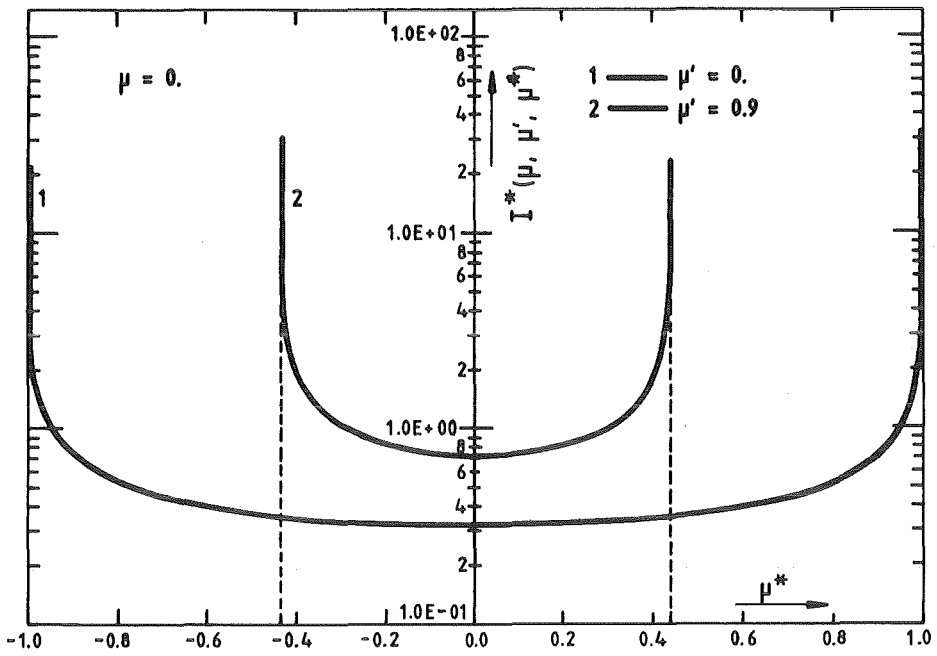

Fig. 5a

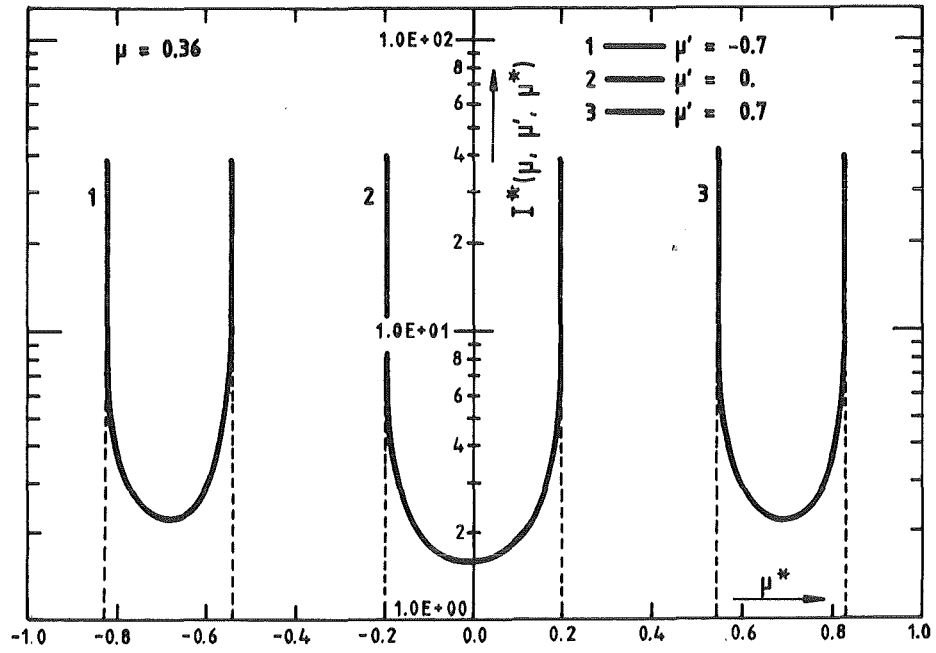

Fig. 5b

Figs. 5a-b Representative examples of the generalized transfer probability function I^* (Eq. 22a).

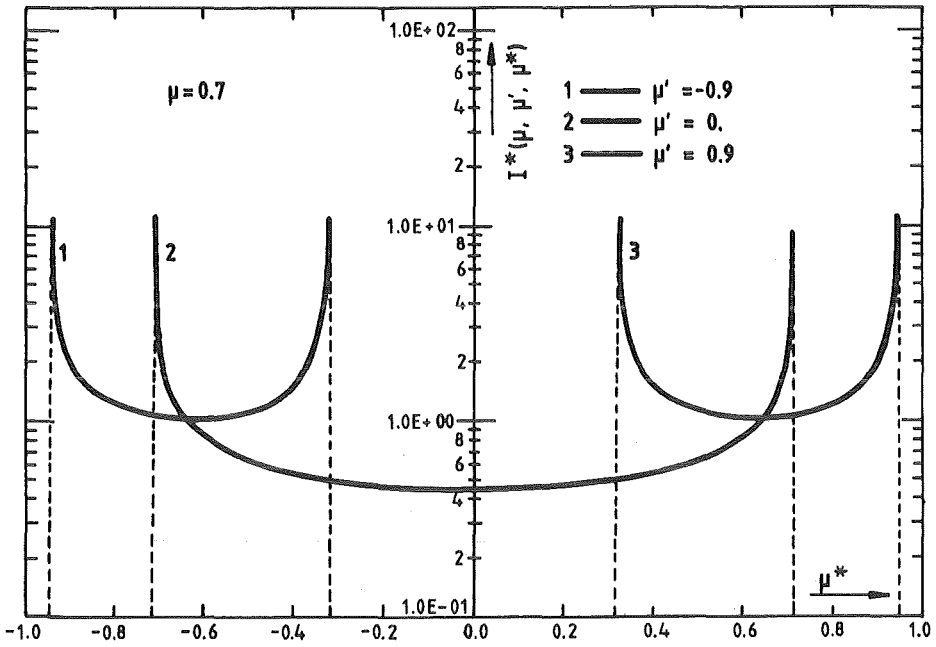

Fig. 5c

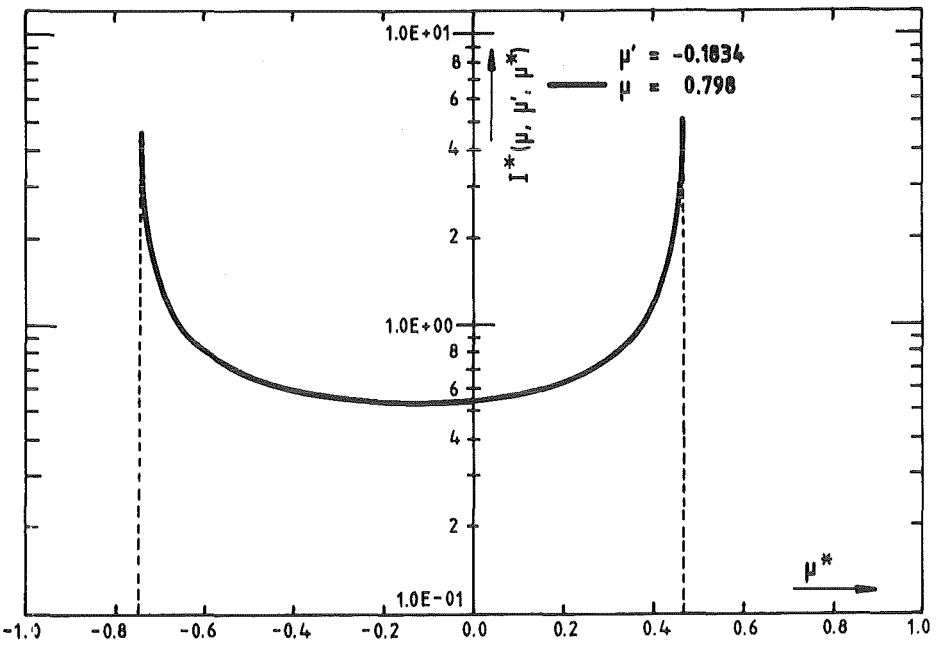

Fig. 5d

Figs. 5c-d Representative examples of the generalized transfer probability function I^* (Eq. 22a).

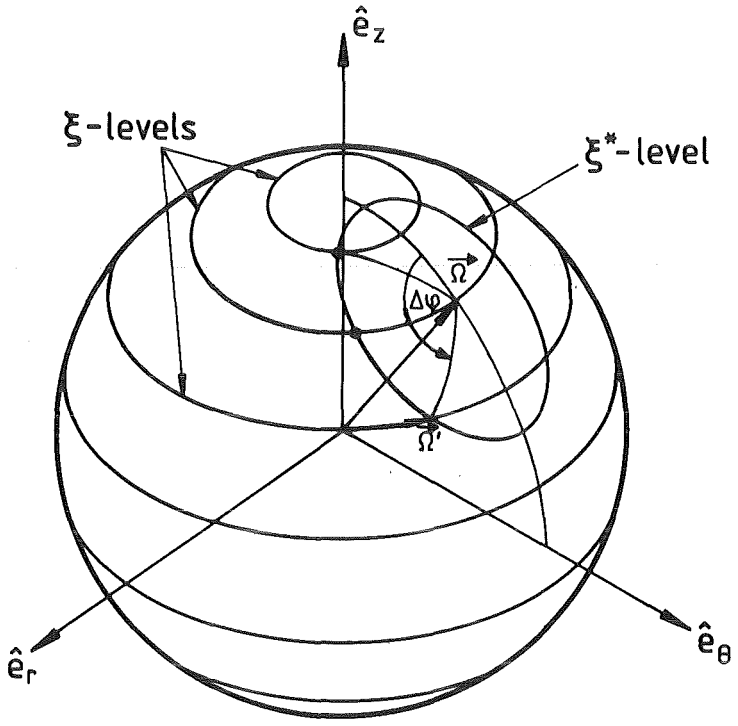

Fig. 6 Unit sphere of directions in cylindrical geometry. Ordering of ξ- and ξ^*-levels.

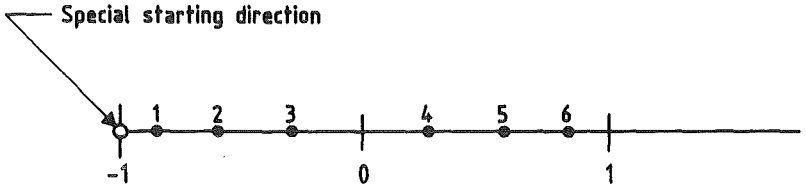

Fig. 7a Ordering of S_6 directions in plane and spherical geometries. The starting direction only applies to spherical geometry.

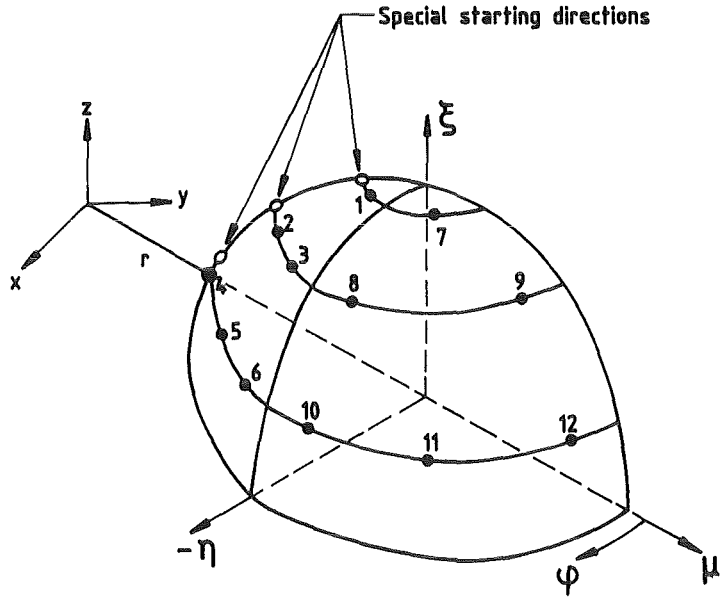

Fig. 7b Ordering of S_6 directions in cylindrical geometry.

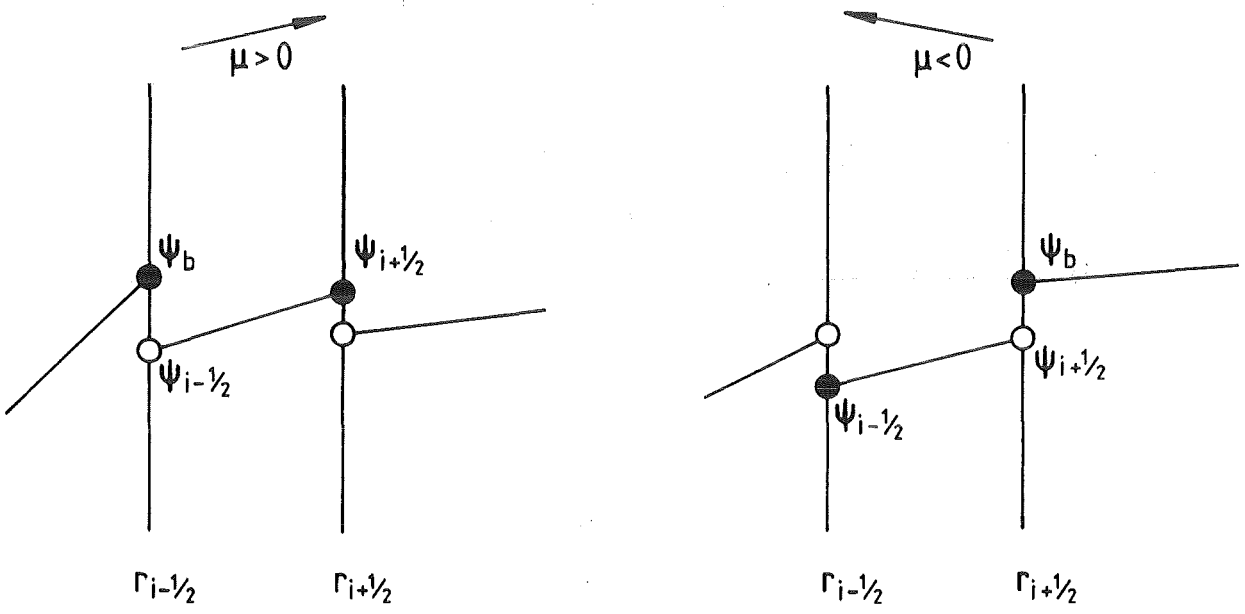

Fig. 8 Linear discontinuous representation of the angular flux in the i^{th} mesh cell. The angular flux from the previous mesh-cell boundary is denoted by ψ_b.

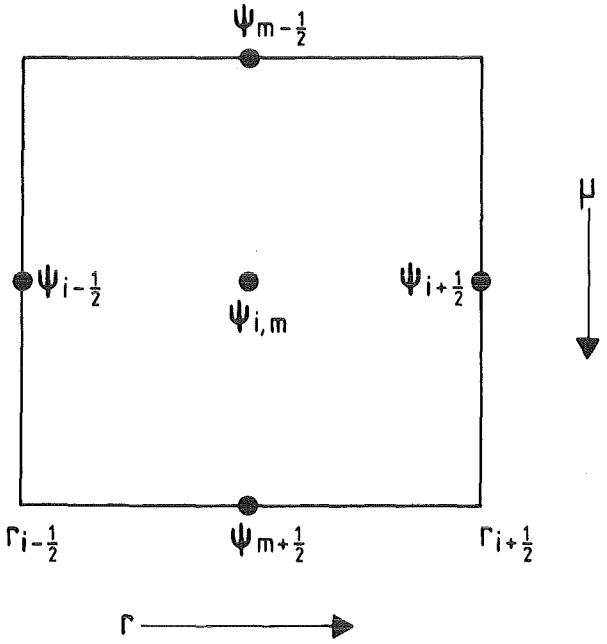

Fig.9 Nodal values for the angular flux in the i, m (space, angle) mesh cell.

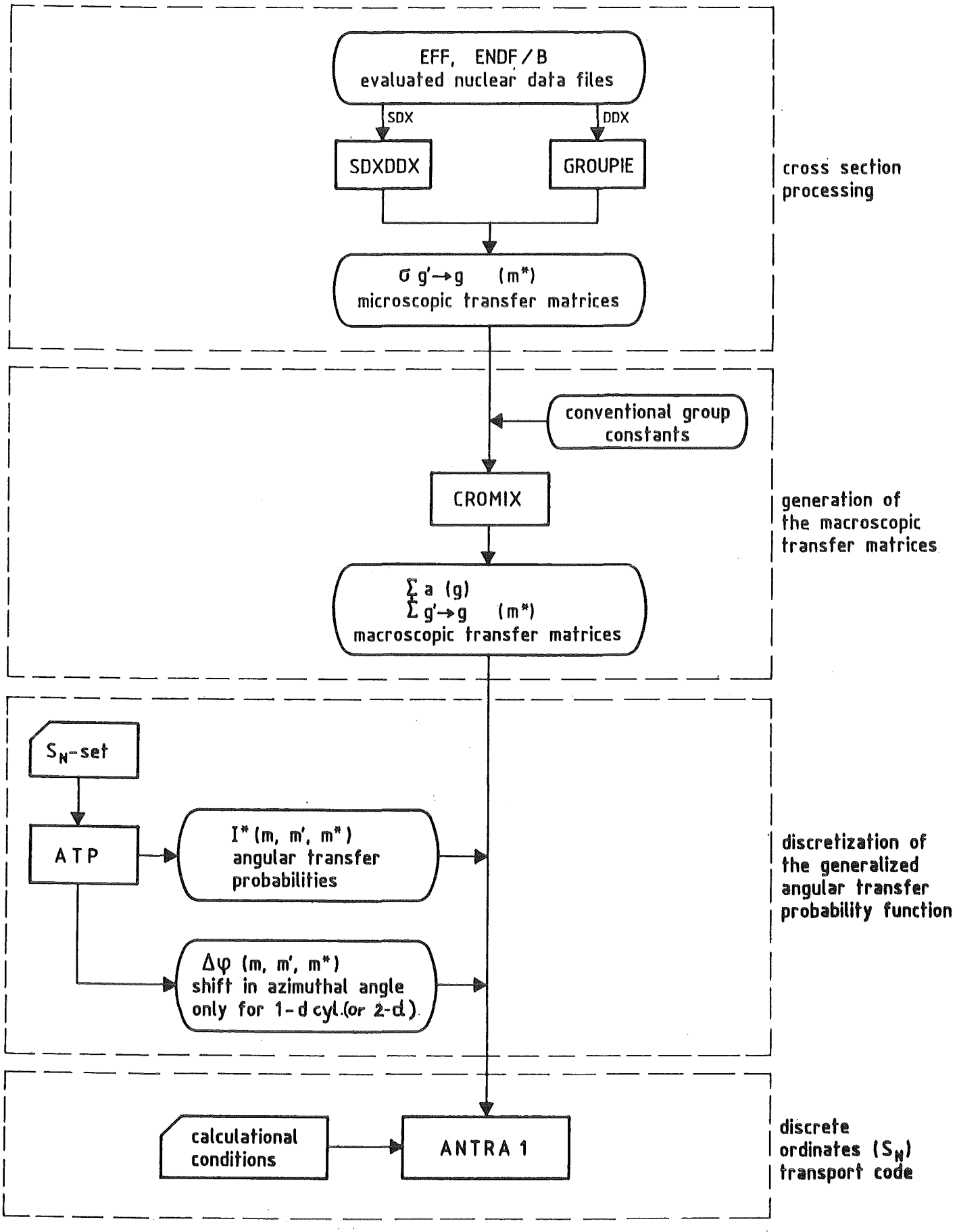

Fig. 10 Schematic flow chart of the GANTRAS code.

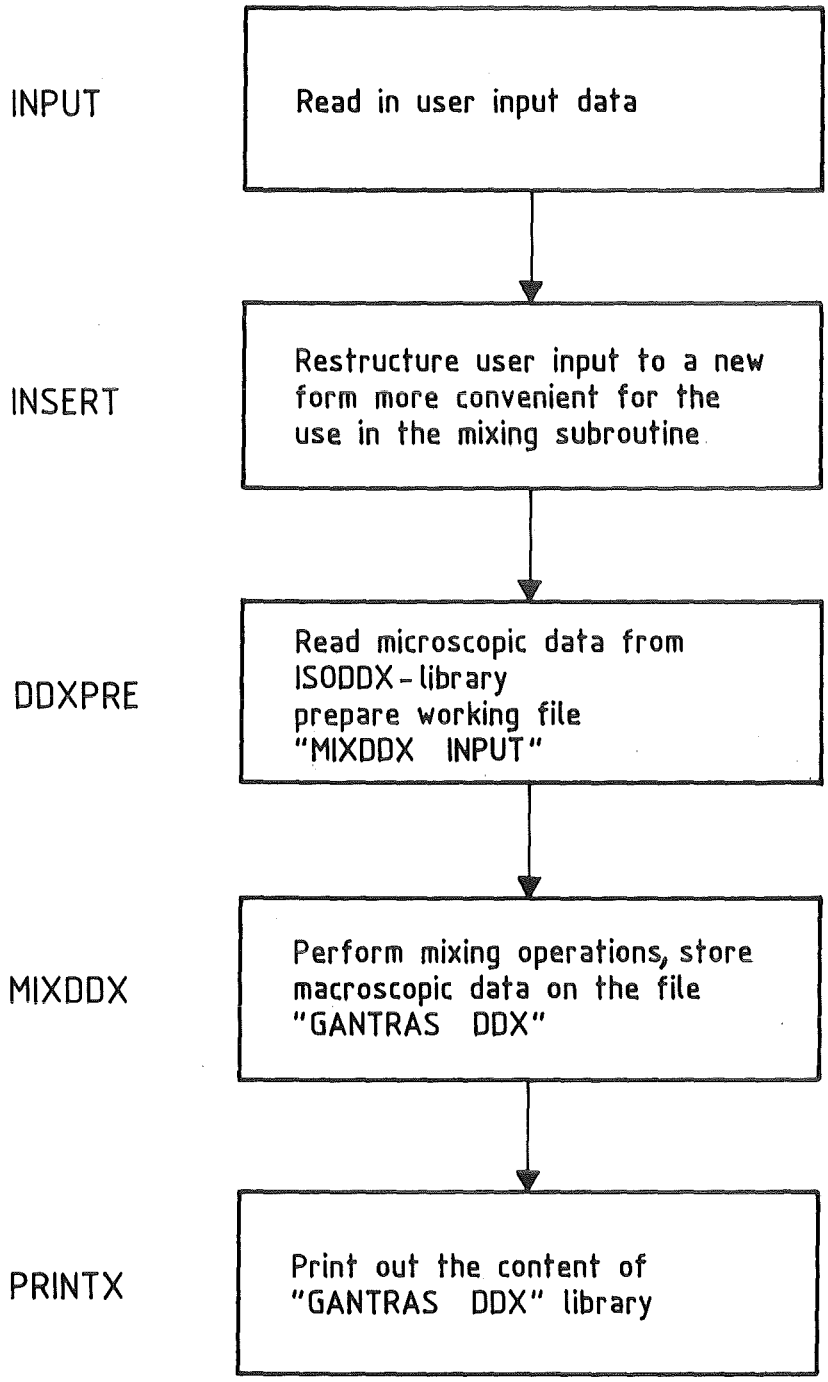

Fig. 11 Logical flow diagram for CROMIX. The subroutine name in which that computation is performed is indicated beside each block.

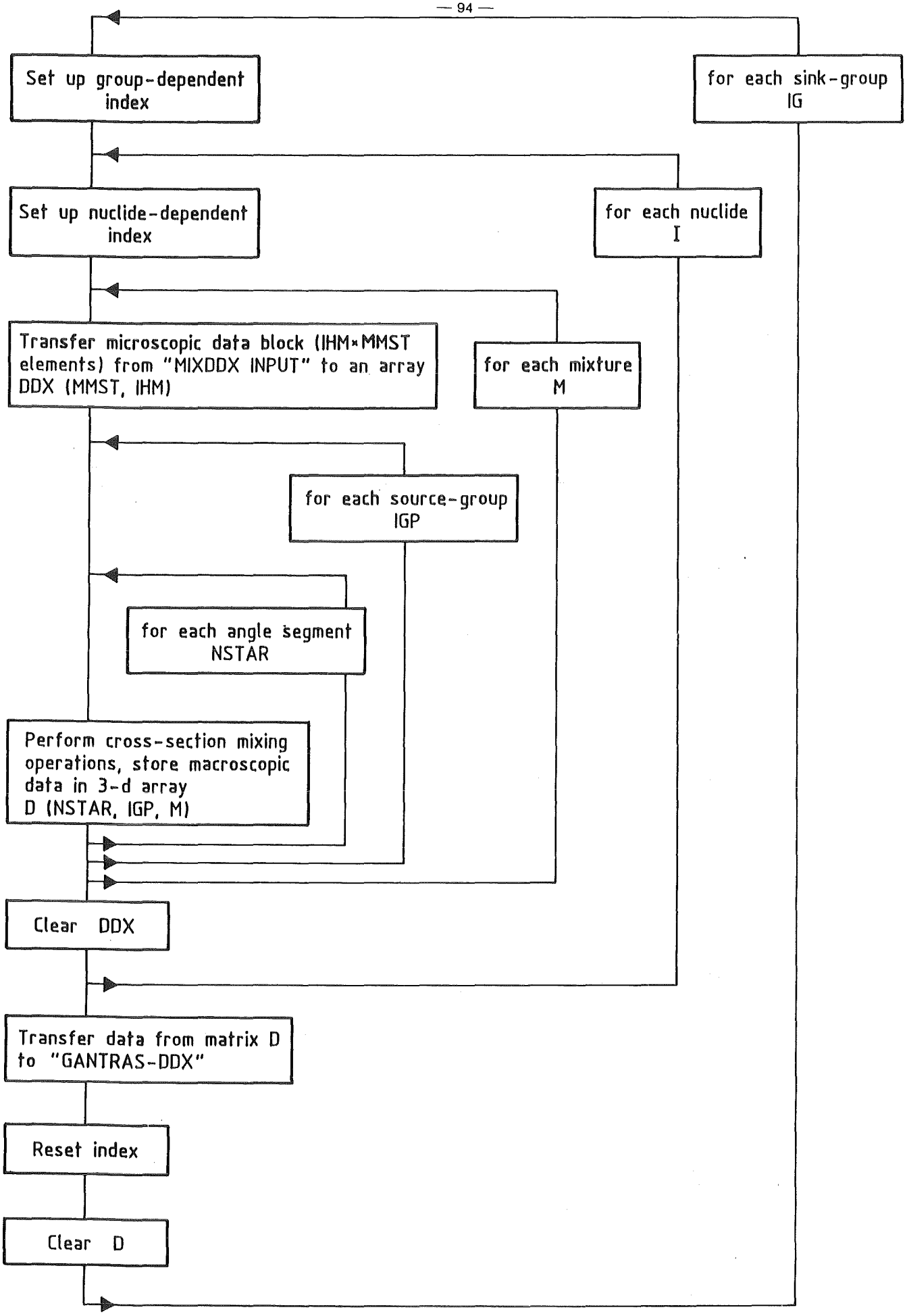

Fig. 12 Simplified flow diagram of the MIXDDX subroutine.

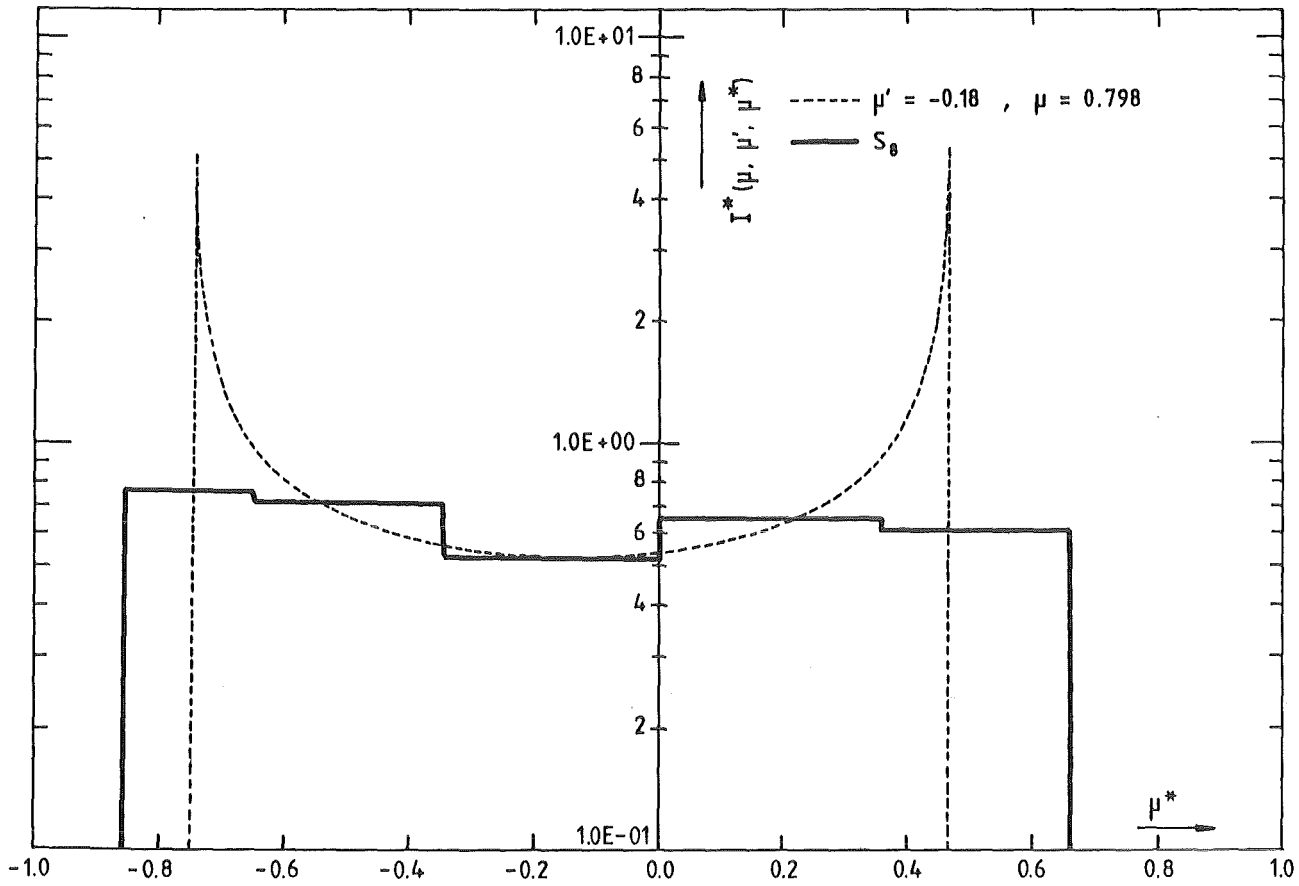

Fig. 13 Generalized angular transfer probability function before and after discretization (S_8 approximation).

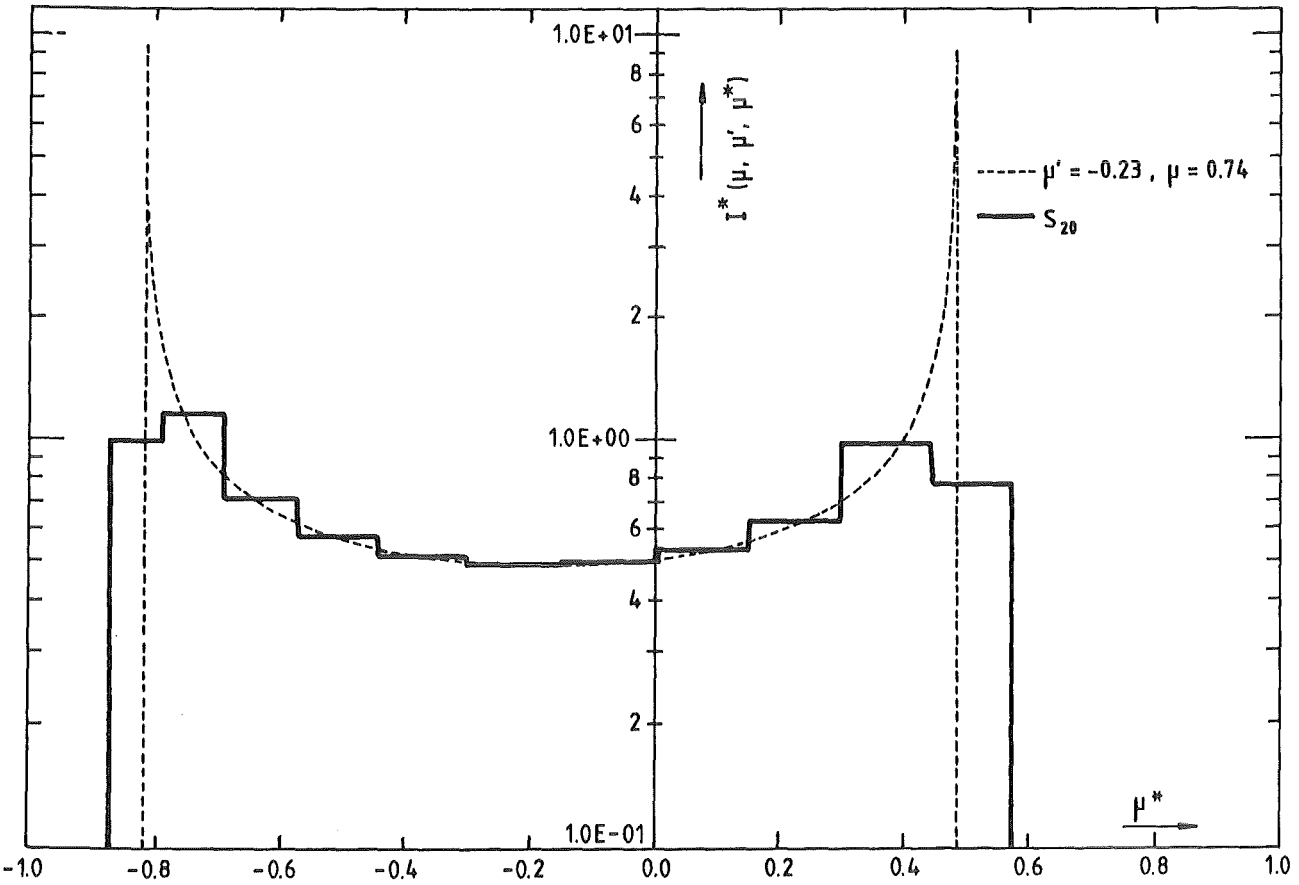

Fig. 14 Generalized angular transfer probability function before and after discretization (S_{20} approximation).

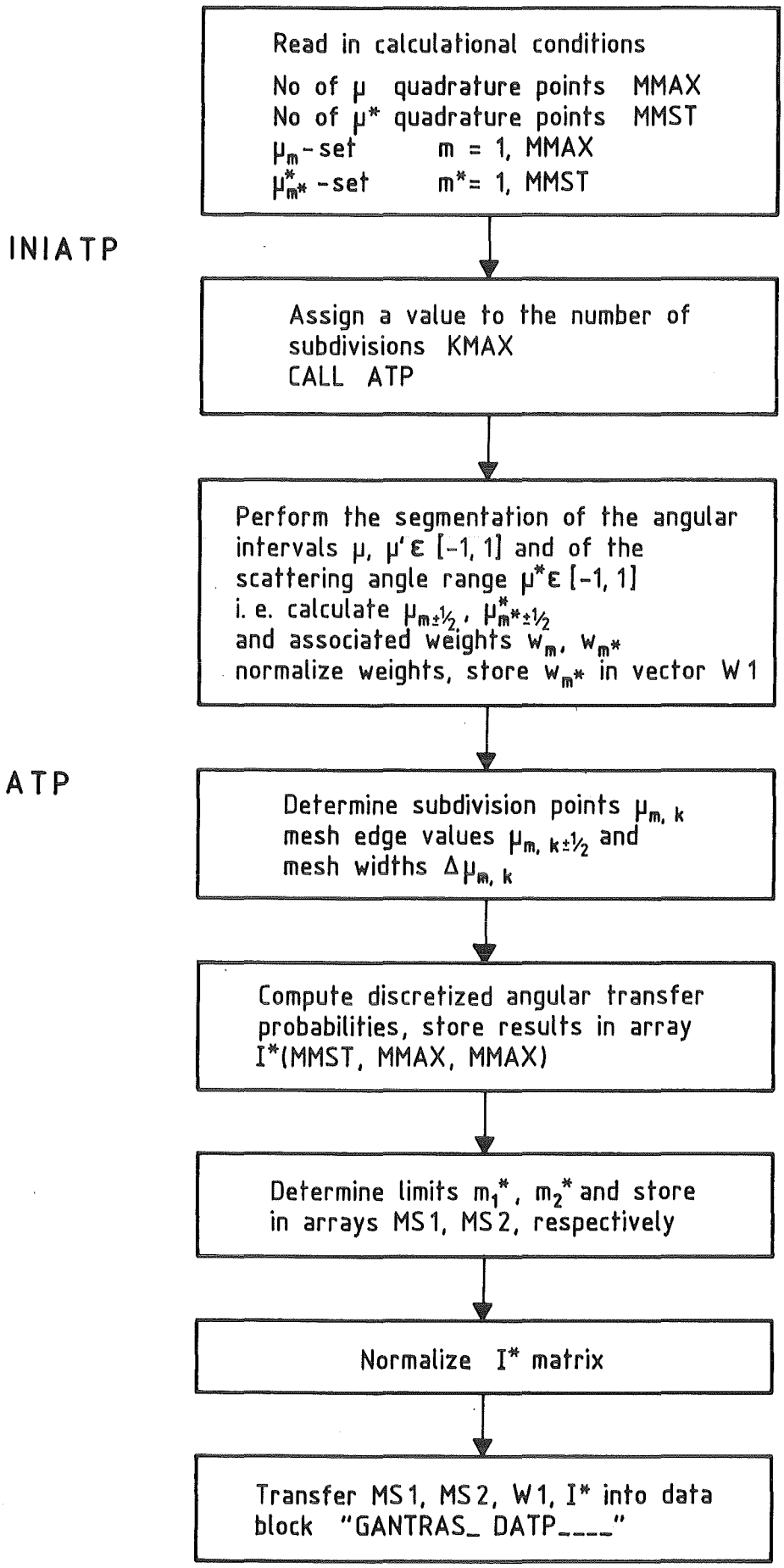

Fig. 15 Schematic flow chart for INIATP and ATP.

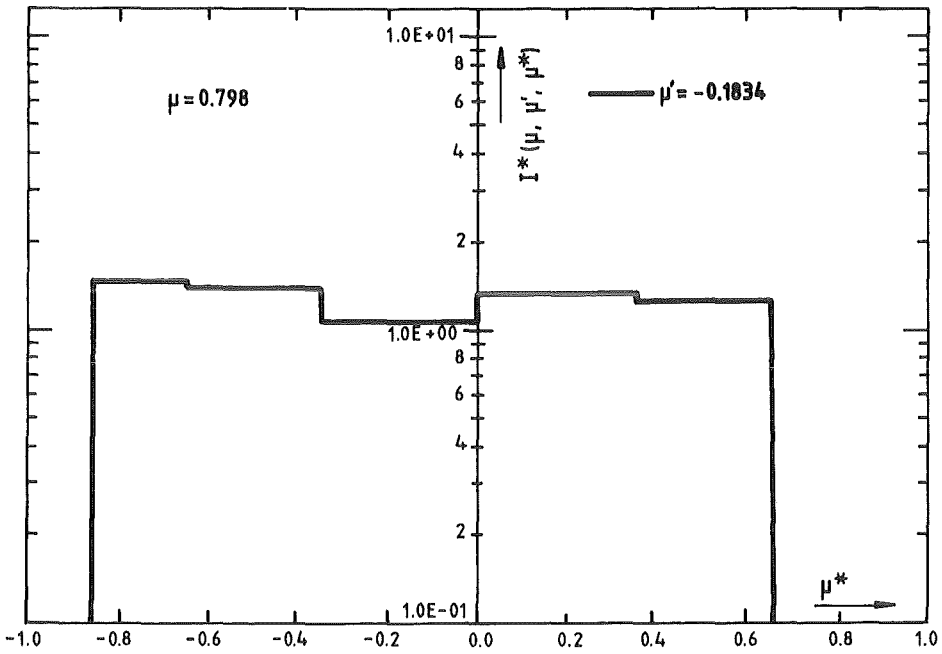

Fig. 16 Discretized angular transfer probability (S_8).

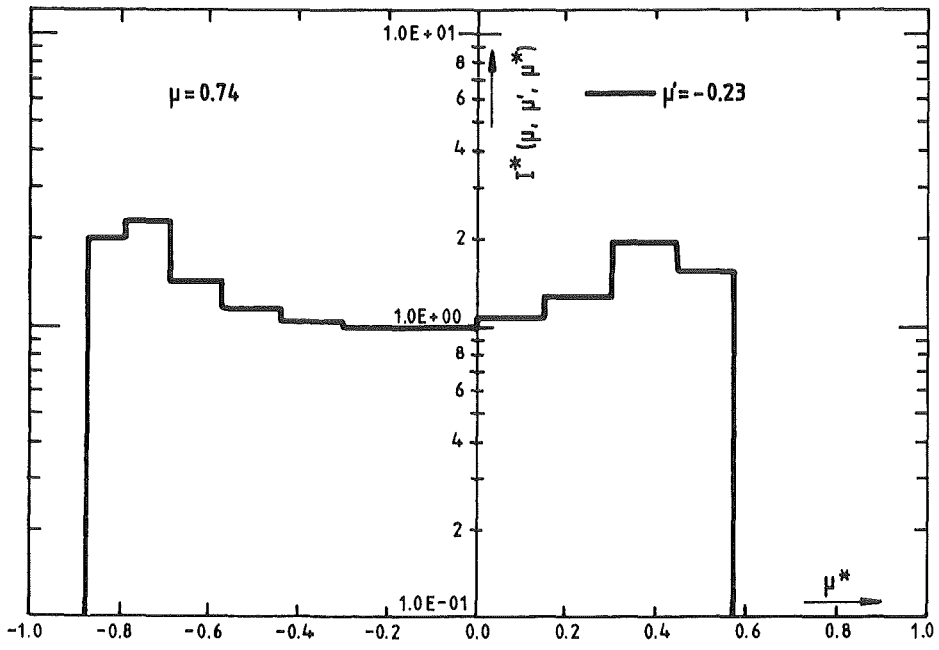

Fig. 17 Discretized angular transfer probability (S_{20}).

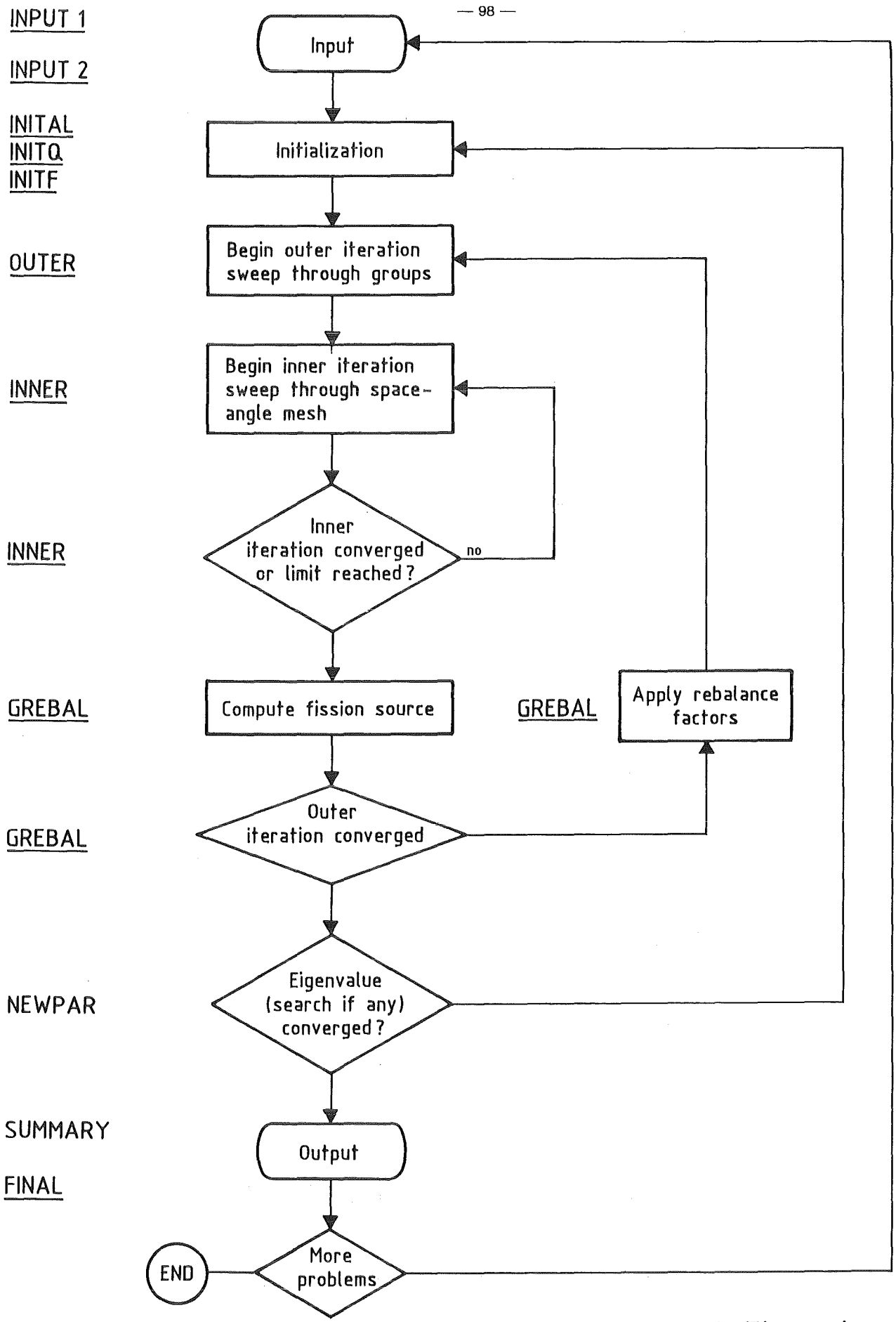

Fig. 18 Simplified logical flow diagram for ANTRA 1. The subroutine name in which that computation is performed is indicated beside each block.

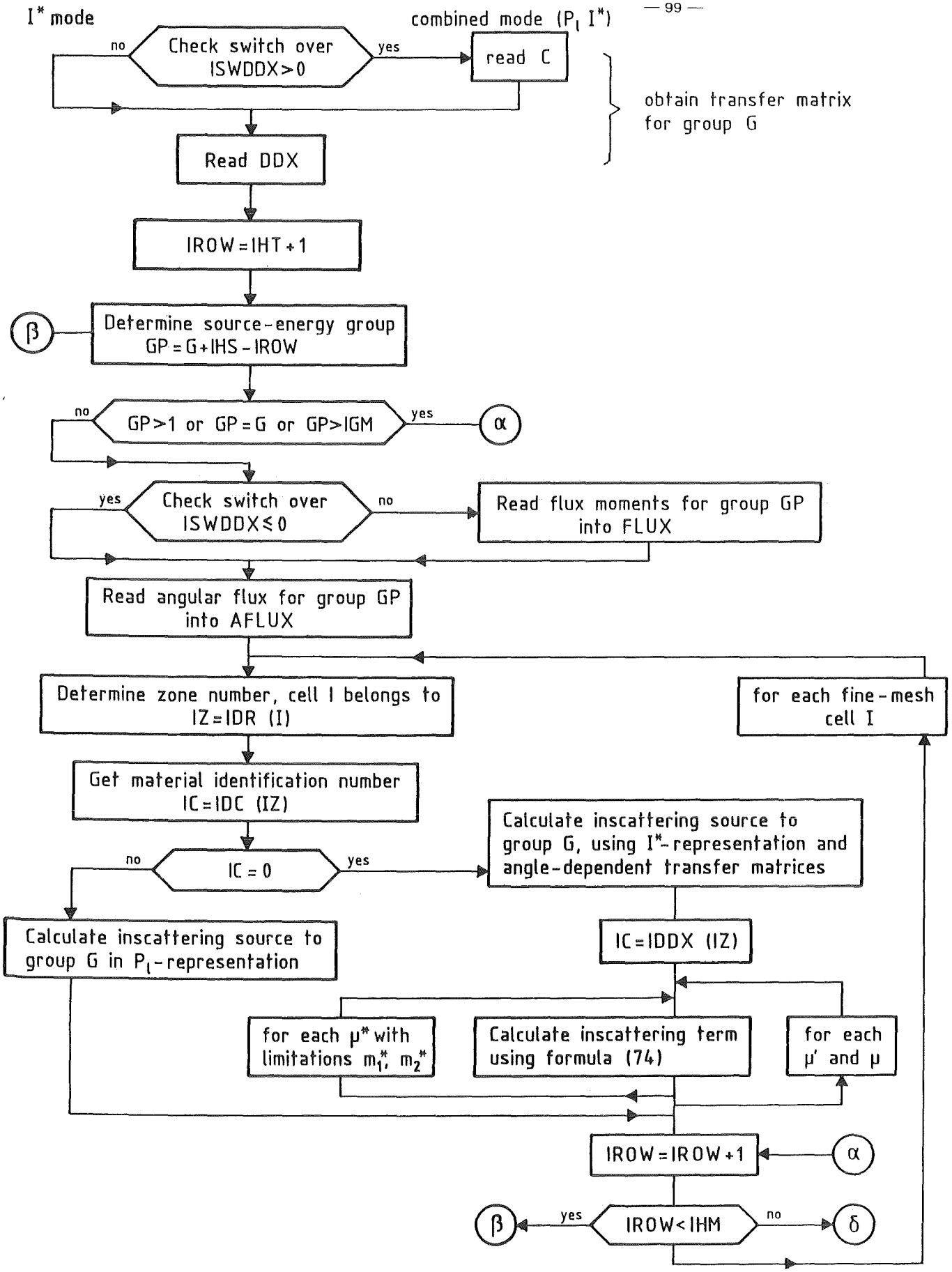

Fig. 19 Simplified flow chart for the modified computational scheme of the group inscattering term in SUBROUTINE SOURCE.

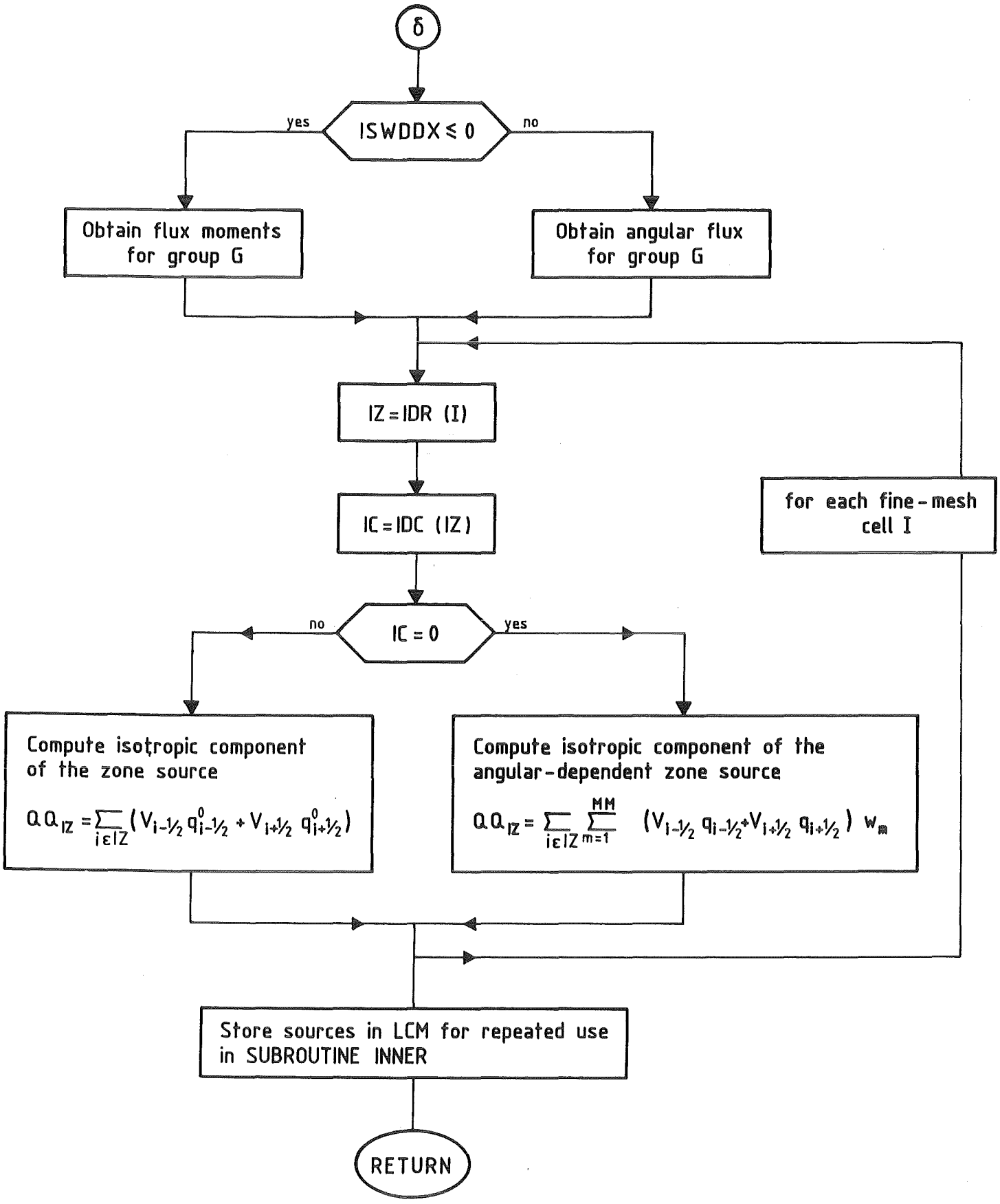

Fig. 19 Continuation.

APPENDIX

Forms of Expansion Coefficients in the Representation of the Scattering Kernel by Truncated Series of Legendre Polynomials

The expansion coefficients are defined by:

$$\Sigma_s^l(\vec{r},E',E) = 2\pi \int_{-1}^{1} \Sigma_s(\vec{r},E',E,\mu_L)P_l(\mu_L)d\mu_L \qquad (A1)$$

where $\mu_L = \vec{\Omega}\cdot\vec{\Omega}'$

To simplify the notation the spatial variable $\vec{r}$ will be omitted. For a single isotope, the Legendre moments of the scattering kernel in the laboratory system (LAB) (as used in the Boltzmann equation) are calculated for elastic and level model inelastic scattering from angular distributions in the center-of-mass system (CM) (as they are given on the nuclear data files). A transformation formula from CM to LAB has the form /3/

$$\sigma_{s,i}^l(E',E) = \begin{cases} \frac{(A+1)^2}{4\gamma(E')E'}\,\sigma_{s,i}(E')P_l(\mu_L)f_i(E',\mu_c) & \text{if } \Gamma(E,1) \le E' \le \Gamma(E,-1) \\ 0 & \text{otherwise} \end{cases} \qquad (A2)$$

where

$$\gamma(E') = A\left(1 + \frac{A+1}{A}\frac{Q_i}{E'}\right)^{1/2}, \qquad (A3)$$

P_l is the Legendre polynomial of order l,

A denotes the ratio of the mass of the nucleus to that of the neutron,

Q_i (i=1,2,...,N) is the excitation energy of the considered level i (for the elastic scattering it is assumed that i=0, Q_0=0),

μ_L expresses the cosine of the scattering angle in the laboratory system and μ_c is the cosine of the scattering angle in the center-of-mass system.

$f_i(E',\mu_c)$ is the angular distribution function of the scattered neutron in the center-of-mass system

$$f_i(E',\mu_c) = 2\pi \frac{\sigma_{s,i}(E',\mu_c)}{\sigma_{s,i}(E)} \qquad (A4)$$

Here $\sigma_{s,i}(E',\mu_c)$ is a differential cross-section for elastic (i=0) or level inelastic scattering and $\sigma_{s,i}(E')$ is the corresponding integrated cross-section

$$\Gamma(E,\mu_L) = \frac{E}{(A-1)^2} \times \left\{ \frac{A^2-1-A(A-1)Q_i/E}{[A^2-1-A(A-1)Q_i/E+\mu_L^2]^{1/2}+\mu_L} \right\}^2 \qquad (A5)$$

In the case of <u>inelastic scattering with continuum excitation</u> the transformation is more complicated therefore LAB quantities are usually given on the file. The Legendre moments are calculated by the equation:

$$\sigma^l_{s,con}(E',E) = \sigma_{con}(E')p_{con}(E'\to E)\int_{-1}^{1} f_{con}(E',\mu_L)p_l(\mu_L)d\mu_L \qquad (A6)$$

where

$\sigma_{con}(E')$ is the inelastic cross-section to the continuum,

$p_{con}(E'\to E)$ is the normalized energy distribution of the scattered neutron,

$f(E',\mu_L)$ is the angular distribution of secondary neutrons.

The <u>(n,2n), (n,3n), (n,n'x) and other reactions</u> which result in emission of more than one neutron are handled in the same way as the neutron scattering with continuum excitation.

Acknowledgements

I wish to acknowledge Dr. H. Küsters, U. Fischer, C. Ferrero and W. Höbel for thought-provoking discussions and C. Broeders for an introduction into KAPROS.

I feel very indebted to the International Atomic Energy Agency in Vienna for the sponsorship of my research and to the Kernforschungszentrum Karlsruhe for further financial support.

References

/1/ Goldfeld A., Tsechanski A. and Shari G., "A Comparison of Different Concepts of Integral Experiments for Fusion Reactor Blanket Design", Nucl. Sci. Eng. 90, 330, (1985)

/2/ Takahashi A., Rusch D., "Fast Rigorous Numerical Method for the Solution of the Anisotropic Neutron Transport Problem and the NITRAN System for Fusion Neutronics Application", Part I, KfK Report 2832/I, Part II KfK Report 2832/II, Kernforschungszentrum Karlsruhe (1979)

/3/ Brockmann H., "Treatment of Anisotropic Scattering in Numerical Neutron Transport Theory", Nucl. Sci. Eng., 77, 377 (1981)

/4/ Odom J., Shultis J., "Anisotropic Neutron Transport Without Legendre Expansions", Nucl. Sci. Eng., 59, 278 (1976)

/5/ Bell G., Hansen G. and Sandmeier A., "Multitable Treatments of Anisotropic Scattering in S_N Multigroup Transport Calculations", Nucl. Sci. Eng., 28, 376 (1967)

/6/ Yamamoto A., Takahashi A. et al., "Neutron Transport Calculations by Using Double Differential Cross-Sections", Journal of Nucl. Sci. Techn. 19, 4, 276 (1982)

/7/ Fischer U., Private Communication, Kernforschungszentrum Karlsruhe

/8/ Mac Farlane R., Muir D., Boicourt M., "The NJOY Nuclear Data Processing System, Volume I: User's Manual", LA-9303-M, Vol. I (ENDF-324), Los Alamos National Lab. (May 1982)

/9/ Fischer U., Wiegner E., "A Processing System for Double-Differential Cross-Sections in Angular Representation", to be published

/10/ Bell G., Glasstone S., "Nuclear Reactor Theory", Van Nostrad Reinhold Company, New York (1970)

/11/ Lewis E., Miller W., "Computational Methods of Neutron Transport", John Wiley & Sons, New York (1983)

/12/ Hill T., "ONETRAN: A Discrete Ordinates Finite Element Code for the Solution of the One-Dimensional Multigroup Transport Equation", LA-5990-MS, Los Alamos National Lab. (June 1975)

/13/ Bachmann H., Kleinheins S., "The Karlsruhe KAPROS Program System", Part Ia, Short KAPROS-Manual, KfK 2317, Kernforschungszentrum Karlsruhe (August 1976), in German

/14/ Harwell Subroutine Library, A Catalogue of Subroutines (1984), AERE-R9185 (March 1984)

/15/ Perry R. T., Moses G. A., "A Combined P_3, VITAMIN-C, MACK-IV, Coupled 25 Neutron - 21 Gamma Group Cross-Section Library - the UW Cross-Section Library", UWFDM-390, University of Wisconsin (1980)

/16/ Hong K-J., Shultis J. K., "Accurate Evaluation of Multigroup Transfer Cross-Sections and their Legendre Coefficients", Nucl. Sci. & Eng., 80, 570-578, (1982)

/17/ Gruppelaar H., Nicrop D., Akkermans J. M., "Processing of Double-Differential Cross-Sections in the new ENDF-VI Format - GROUPXS Code Description and User's Manual", ECN-Report (in press), Netherlands Energy Research Foundation

/18/ Küfner K., "READKØ, A Subroutine Package for Centralized Input and Output Operations in KAPROS (Version 1.8)", KfK Report 3333, Kernforschungszentrum Karlsruhe (1982)

/19/ Brandl V., Private Communication, Kernforschungszentrum Karlsruhe (1980)